UNIVERSITY OF CATANIA

DEPARTMENT OF MATHEMATICS AND COMPUTER SCIENCE

DOCTORAL THESIS

SSD: MAT/07

Dynamics of Classical Systems in the Operator Algebra of Quantum Mechanics

Author:
Rosa DI SALVO

Supervisor:
Prof. Francesco OLIVERI

Head of Ph.D. School:
Prof. Giovanni RUSSO

A thesis submitted in fulfillment of the requirements for the degree of Doctor of Philosophy

in the Partner Institution

UNIVERSITY OF MESSINA

DEPARTMENT OF MATHEMATICS AND COMPUTER SCIENCE, PHYSICS AND EARTH SCIENCES

Declaration of Authorship

I, Rosa DI SALVO, declare that this thesis titled "Dynamics of classical systems in the operator algebra of quantum mechanics" and the work presented in it are my own. Where I have consulted the published work of others, this is always clearly attributed.

ὁ δὲ ἀνεξέταστος βὶος οὐ βιωτός ἀνθρώπῳ.

"The unexamined life is not worth living."

Plato (*Dialogues, Apology of Socrates, 38a*)

*"And I feel that I am a man. And I feel that a man is a very important thing– maybe more important than a star. This is not theology. I have no bent toward gods. But I have a new love for that glittering instrument, the human soul. It is a lovely and unique thing in the universe. It is always attacked and never destroyed– because '**Thou mayest**'."*

John Steinbeck (*East of Eden*)

UNIVERSITY OF CATANIA

Abstract

University of Messina (Partner Institution)
Department of Mathematics and Computer Science,
Physics and Earth Sciences

Doctor of Philosophy

**Dynamics of Classical Systems
in the Operator Algebra
of Quantum Mechanics**

by Rosa DI SALVO

The use of the formalism and the operatorial techniques typical of quantum mechanics proved in recent years to be an effective approach for the description of even macroscopic systems characterized by complex interactions in several contexts with interesting applications both in the bioecological and in the socioeconomic area. The operatorial approach, based on raising and lowering operators, especially using the number representation, provides useful tools for modeling collective dynamics of spatially distributed physical systems in a completely general and precise way. *Quantum–like* models (not necessarily related to the microscopic approach) offer an interesting mathematical insight into phenomena and processes even at macroscopic scales in several situations in which some quantities changing discontinuously are well described in terms of the integer eigenvalues of certain self–adjoint operators useful for a complete description of the system under consideration (the so–called observables of the system itself). Moreover, according to the innovative approach called rule–induced dynamics, the derivation of the dynamics in the operator algebra of quantum mechanics from a time–independent Hamiltonian operator may be enriched by means of the repeated application of specific "rules" including in the dynamics meaningful effects occurring during the time evolution of the system and, therefore, producing an adjustment of the model itself as a consequence of its evolution. This method is of great interest to describe systems for which a nontrivial and sufficiently regular asymptotic behavior is expected.

The original contributions of this thesis, besides the construction and the numerical investigation of operatorial models to describe complex systems of interest in many areas (mathematics, physics, ecology, social sciences), are concerned with the introduction and exploitation of the so called (H, ρ)–induced dynamics. The combined action of the Hamiltonian and of some rules allowed to take into account in the model relevant effects that can not be described by a time independent self–adjoint Hamiltonian. This strategy, which provides a powerful strategy to simulate the effect of using a time–dependent Hamiltonian, revealed capable of greatly enriching the dynamics of the considered models still with simple quadratic Hamiltonians without additional computational costs.

Acknowledgements

The work leading to this thesis has been supported by remarkable individuals who I wish to acknowledge.

Special mention goes to my enthusiastic supervisor, Prof. Francesco Oliveri. I am deeply indebted to him, not only for his tremendous research assistantship, but also for providing me an invaluable moral support through the rough road that led to the drawing up of this thesis. It has been a honor to have been mentored by him. He has taught me, both consciously and unconsciously, how good mathematics may be done. The joy and enthusiasm he has for the research was contagious and motivational for me, even during tough times in the Ph.D. pursuit. With great dedication, he always encouraged my research and gave me the freedom I needed to move on and to grow as a research scientist. His advice on both research as well as on my career has been invaluable.

I am also hugely appreciative to Prof. Fabio Bagarello, especially for sharing his great expertise so willingly, and for the support and inspiration that he together with Dr. Francesco Gargano provided to me. I really enjoyed the pleasant days working together in Palermo.

I wish to acknowledge the referees who reviewed this manuscript, Prof. Vito Antonio Cimmelli and Prof. Emmanuel Haven, for their brilliant comments and suggestions. I am committed to treasure their valuable hints.

Profound gratitude goes to one's nearest and dearest that have contributed immensely to my personal and professional growing.

A special thanks to my family for all their love and encouragement. For my parents who raised me with a love of science and supported me in all my pursuits. Thanks go to Francesca, Paolo, Caterina, Andrea, the little Sebi and Franci, Geppa, and Pino. I am glad to have had the opportunity to carry through with a path that my father would have wanted to embark on. I dedicate this thesis to him, confident that he will be proud of sharing with me this result.

Prof. Luigia Puccio and my close colleagues have been a source of friendships as well as good advice and collaboration. In particular, I found in Maria Vittoria Cuzzupè and Matteo Gorgone good friends ever since we began to share the office, and in Prof. Marilena Crupi an everlasting spring of kindness and respect. Thanks to them I have felt at home at MIFT Department. I have very fond memories of my time there and of many nice leisure experiences. A heartfelt thanks to Matteo for the several moments shared during this Ph.D. course and for becoming a lifelong friend.

I have a special friend I would like to mention here: thank you to Luca Amata. I consider him a true friend and a talented mathematician since my first hesitant steps on the path of mathematics. His unconditional support has been essential all these years and I hope it will continue for decades to come!

Most of all I wish to thank my beloved husband, Ettore, who has been a source of love and energy and encouraged me through good and bad times. He cherished with me every great moment and stood beside me whenever I needed it. Its faithful support is so appreciated. Thank you.

Contents

List of Figures

To my Father

Introduction

The description of the dynamics of classical complex systems may be profitably carried out with an operatorial approach, typical in quantum mechanics, even when dealing with several macroscopic systems related to real case studies (Bagarello, 2012). The key to this approach lies in the consideration that the operatorial framework provides useful tools for describing the interactions occurring within appropriate physical systems in a completely general and precise way.

Without expecting to describe any quantum phenomena or stochastic dynamics, the operatorial approach, based on *raising* and *lowering* operators, especially using the number representation, proved to be useful to set up a natural description of systems in rather different areas. This happens in several situations in which some quantities changing discontinuously are well described in terms of the integer eigenvalues of certain self–adjoint operators useful for a complete description of the system under consideration (the so–called *observables* of the system itself); possible areas of applicability of this idea are, among others, stock markets, love affairs, population migration phenomena, escape strategies of crowds, desertification processes, microbial ecology, cellular automata, or politics. The assumption that specific techniques borrowed from quantum mechanics turn out to be well suited to successfully analyze the dynamical aspects of complex classical systems too is indeed confirmed by a series of recent papers (see Bagarello, 2007; Bagarello and Oliveri, 2010; Bagarello and Oliveri, 2013; Bagarello and Oliveri, 2014; Bagarello, Gargano, and Oliveri, 2015; Bagarello, Cherubini, and Oliveri, 2016; Bagarello and Haven, 2016; Di Salvo and Oliveri, 2016a; Di Salvo and Oliveri, 2016b; Di Salvo and Oliveri, 2016c; Bagarello et al., 2016, and references therein).

The theoretical framework for the analysis of the dynamics of classical systems in the operator algebra of quantum mechanics is built basically as follows: we sketch out a model of the macroscopic system $\mathcal{S}$ under consideration, assume that the variables we are interested in are expressed as *number–like* operators, and then we deduce the dynamics of $\mathcal{S}$ in the Schrödinger or in the Heisenberg representation, once a suitable Hermitian operator $H = H^\dagger$, called the *Hamiltonian* of $\mathcal{S}$ (which, in standard quantum mechanics, corresponds to the total energy of the considered system) has been defined. Thus, we have that the Hamiltonian H, which embeds the main phenomena appearing relevant for a satisfactory characterization of the system $\mathcal{S}$ under consideration, has the property of governing the time evolution of any observable of $\mathcal{S}$ by means of the equation

$$X(t) = \exp(iHt)X\exp(-iHt),$$

or, rather, that H rules the evolution of the *wave function* $\Psi(t)$ describing $\mathcal{S}$ at time t according to the law

$$i\dot{\Psi}(t) = H\Psi(t),$$

where $\Psi(0) = \Psi_0$ describes the initial status of $\mathcal{S}$.

Despite of the fact that this method has been applied to very different situations, it can not give completely general results, at least in its simplest formulation. In particular, if $\mathcal{S}$ is required to have a finite number of degrees of freedom, and H is time independent self–adjoint and quadratic, then we have that the only possible dynamics is periodic or quasi–periodic, which means that such a strategy needs to be varied or enriched in order to produce a more powerful description, working even in the case that the system decays asymptotically to some final state. This motivates the definition of an extended version of the quantum dynamics which allows us to take into account other effects which may occur during the time evolution of the system. In particular, the dynamics may be thought of as driven by a Hermitian time independent Hamiltonian operator H, but with the innovation that, during the time evolution, a check on the system occurs periodically and, in principle, determines a change on certain ingredients of the model. Such a kind of control on the state of $\mathcal{S}$ is called *rule* (and indicated by ρ), and the combined effect of H and ρ produces what in the following is called the (H, ρ)–*induced dynamics*. In this new kind of approach the model preserves its structure, whereas the rule accounts for a sort of dependence of the model itself on the current state of the system by repeatedly modifying, at specific times, the state of the system itself or the value of some of parameters entering H (without modifying the functional form of the Hamiltonian). In some sense, the model adjusts itself as a consequence of its evolution; this feature mimics the changes in the interactions among the actors of the system under different environmental conditions. The combined action of the Hamiltonian operator and a rule, that is really not a mere mathematical trick, but rather an additional ingredient physically justified by what we are deducing from the dynamics, can be efficiently used to describe systems going to some equilibrium, even when H is thought to be Hermitian (see Bagarello and Gargano, 2016a; Bagarello et al., 2017; Di Salvo and Oliveri, 2016a; Di Salvo and Oliveri, 2016c; Bagarello et al., 2016).

The plan of the thesis is the following one.

In Chapter 1, as a start, and in order to fix the formalism, very few tools and aspects related to the theory of quantum mechanics, useful for the subsequent development, are briefly discussed. Some hints on the quantum–mechanical apparatus, with respect to the operator algebra, and particularly to the number operator (used for the definition of the conceptual setting for the applications) are also given.

In Chapter 2, the theoretical framework derived from quantum mechanics for the description of the dynamical properties of classical systems by means of operatorial methods is introduced. The related theoretical and applicative aspects are addressed in completely general terms, leaving aside the concrete interpretation that can be attributed to the involved models.

In Chapter 3, different fermionic models of bacterial populations are presented. In particular, by using a conveniently defined operatorial scheme,

and by adopting the Heisenberg representation of the dynamics, some features of the long–term survival of bacterial populations are investigated, and the colony morphology in stressed/aged bacterial populations of *Pseudomonas aeruginosa* constrained in a closed environment is described. Both linear and nonlinear models are considered (the first of which also in a spatial version); moreover, some effective dissipative mechanisms, phenomenologically introduced, are taken into account.

Chapter 4 deals with the discussion of an operatorial model based on fermionic operators for the description of the dynamics of political parties affected by turncoat–like behaviors of part of their members. The model is built by assuming that the various subgroups of the political parties are described by time dependent number–like operators, and that the dynamics is ruled, in the Heisenberg representation, only by a strictly quadratic Hamiltonian describing the main effects deriving from the interactions among disloyal politicians. In this context, a study of the influence of the parameters entering the model on the dynamics of the political system is discussed.

Chapter 5 is devoted to the introduction of the notion of rule–induced dynamics, intended as a strategy to upgrade the description of the dynamics of a macroscopic system by means of the combined effect of quantum tools and some external or internal action periodically adjusting the model, which is not easy to include in any Hamiltonian.

In Chapter 6, the approach of the (H, ρ)–induced dynamics (in the case in which suitable sets of conditions acts on the state of the system) is applied in the field of cellular automata in order to extend the classical Game of Life, and several aspects of this extension are analyzed.

Finally, Chapter 7 and Chapter 8 deal with the extension of the conservative models of bacterial populations and political party systems (already introduced in Chapter 3 and Chapter 4, respectively) obtained by combining the standard operatorial approach with the additional introduction of specific rules changing periodically the values of certain parameters entering the respective quadratic Hamiltonian operators.

It is worth of being remarked that all the models presented in this thesis, even if built with tools typically used in quantum mechanics, are fully deterministic.

The original contributions of this thesis, besides the construction and the numerical investigation of operatorial models to describe complex systems of interest in many areas (mathematics, physics, ecology, social sciences), are concerned with the introduction and exploitation of the so called (H, ρ)–induced dynamics. The combined action of the Hamiltonian and of some *rules* allowed to take into account in the model relevant effects that can not be described by a time independent self–adjoint Hamiltonian. This strategy revealed capable of greatly enriching the dynamics of the considered models still with simple quadratic Hamiltonians without additional computational costs.

Some of the original results presented in this thesis are contained in the published papers Di Salvo and Oliveri, 2016b; Di Salvo and Oliveri, 2016c; Bagarello et al., 2017, as well as in the papers Di Salvo and Oliveri, 2016a; Bagarello et al., 2016; Di Salvo, Gorgone, and Oliveri, 2016b; Di Salvo, Gorgone, and Oliveri, 2016a that have been submitted for publication; other results will be the object of some papers in progress.

1 On the quantum–mechanical apparatus

In this Chapter, to fix the language, the basic formalism of quantum mechanics, essential for the subsequent developments, is presented, and some aspects of the theory are briefly illustrated.

Certain quantum tools, in particular the number operator, used for the definition of the theoretical framework that provides in a logically satisfying way the conceptual setting for the various applications analyzed in the following, are also introduced.

The aspects here discussed are widely analyzed in any textbook about quantum mechanics (see, for instance, Roman, 1965; Merzbacher, 1998).

1.1 Background and preliminaries

Toward the end of the nineteenth century it seemed quite apparent that the general concepts of what is now called the "classical physics" were adequate to describe all physical phenomena. The macroscopic world evidently appeared intelligible first in the framework of classical mechanics, formalized by I. Newton in the late seventeenth century, and providing a valid treatment of the dynamics of material bodies, and lastly in the context of the classical electrodynamics, finalized by J. C. Maxwell in the latter half of the nineteenth century to describe all the properties of the electromagnetic field.

During the first quarter of the twentieth century, the scientists turned their attention to the microscopic world, and a number of unforeseen difficulties arose concerning the discovery of instances in nature in which certain physical variables assumed only *quantized* or *discrete* values (in contrast to the continuum of values expected on the basis of classical physics) as well as the distinction between *waves* and *particles*. Instances of quantum effects were uncovered in the early part of the last century, among others, by M. Planck, who examined the so–called "black body radiation", N. Bohr, in regard to the spectrum of radiation emitted by excited hydrogen atoms, and A. Einstein, with his theory of the photoelectric effect concerning the nature of light (later supported by A. H. Compton). *Ad hoc* hypotheses about the microscopic world, relating to the quantization of physical variables and the wave–particle duality in nature, were introduced thanks to the contribution of several physicists; by 1930, through the efforts of W. Heisenberg, E. Schrödinger, M. Born, N. Bohr, P. A. M. Dirac, and many others, the system of "quantum mechanics" had been devised (the name derives from Plank's radical suggestion that the photon energy could change only in discrete steps, or *quanta*).

Certainly it would be presumptuous to assert absolutely that quantum mechanics, whose basic tenets are in many respects quite foreign to the concepts and attitudes of classical physics, is the only or even the best possible way of understanding physical phenomena. However, it is not possible to deny the fact that quantum mechanics, in its present form, has been successful in predicting experimental observations (Gillespie, 1974).

The structure of quantum mechanics differs startlingly from that of the classical theory. In particular, the algebra of observables is no longer commutative, but, instead, position and momentum (q and p) satisfy the *canonical commutation relations*

$$[q, p] := qp - pq = i\hbar, \tag{1.1}$$

where i is the imaginary unit, and $\hbar$ is the reduced Planck's constant: $\hbar \equiv h/2\pi = 1.054 \times 10^{-34}$joule $\cdot$ sec.

The equation of Schrödinger treats p and q as differentiation and multiplication operators acting on the Schrödinger *wave–function* Ψ, which has the interpretation of a *probability amplitude*: it is complex–valued, and $|\Psi|^2$ is the probability distribution in the state specified by Ψ. Superposition of the solutions of the equation causes probability interference effects, a phenomenon that, an interference being between events that from a classical view are mutually exclusive, can not be understood classically at all. Later, Ψ was characterized axiomatically as a vector in a Hilbert space, but the peculiar fact remained that one worked with a complex Hilbert space and came up with real probabilities.

Since any state is required to be represented as a positive linear functional, where positivity means that the expectation value $\langle a^2 \rangle$ of the square of any real observable a must always be nonnegative, it turns out that to each state there corresponds a representation of the observables as linear operators on some Hilbert space. As a consequence of the fact that the scheme of quantum theory omits the postulate that the algebra is commutative, quantum mechanically there are no states for which the expectation values of all products are equal to the products of the expectation values. Such a state would provide an algebraic isomorphism to the ordinary numbers, which is possible only for very special noncommutative algebras (Thirring, 1997). The occurrence of nonzero fluctuations $(\Delta a)^2 \equiv \langle a^2 \rangle - \langle a \rangle^2$ is in general unavoidable, and gives rise to the indeterministic features of the theory.

Moreover, quantum mechanics do not conform to classical logic, and the logical maxim *tertium non datur* is not valid in quantum theory. The idea of a "logic of quantum mechanics", or quantum logic, was originally suggested by Birkhoff and von Neumann in their pioneering paper (Birkhoff and Neumann, 1936), and attained notoriety within the last years for its relevant role in the fields of cognitive science and quantum information theory, suggesting quantum theory to be the dominant fundamental logic in the natural world. Quantum logic contests the validity of the only and mutually exclusive possibilities by pointing to the irreparable change caused in the state by preparing the system to test the new propositions. Recent research areas recognize quantum logic in studies of: the subconscious, decisions involving unknown interconnected variables, memory, and question sequencing (Larson, 2015).

1.2 Certain aspects of the formalism

The general framework of the models we will discuss in this thesis relies on the so–called *number representation*. Here, few important facts will be given, paying not much attention to mathematical problems arising from the fact that the operators involved might be unbounded, since this class of operators is not relevant for the applications proposed in this thesis. A detailed reference covering the following topics is Bagarello, 2012.

In this Section, some fundamentals of quantum states and operators, starting with the usual definitions and properties, are briefly considered and the derivation of the time evolution of a system is addressed.

1.2.1 Stationary states

Let us consider a system $\mathcal{S}$ of L identical particles, which means that they can not be distinguished by measuring their properties, *i.e.*, a permutation P of the particles can not be measured. In classical mechanics, particles are always distinguishable in the sense that, at least formally, we can always follow the trajectory through the phase space of each individual particle and disclose its identity. In quantum mechanics, instead, the concept of trajectory does not exist, due to the intrinsic uncertainty in position, embodied in Heisenberg's principle, and identical particles are indistinguishable. One way to describe the state of a system composed of L particles is the wave function $\Psi(x_1, \ldots, x_L)$, where the variable x_i of the i–th particle represents its position and spin: $x_i = (\vec{r}_i, s_i)$. According to the literature, $|\Psi(x_1, \ldots, x_L)|^2$ is interpreted as the probability to find the system $\mathcal{S}$ in the state $(x_1, \ldots, x_L)$ when an actual measurement is performed. There is a number of rules with which measurement processes are represented in quantum mechanics (Buhler, 2006). Basically, any *observable* of $\mathcal{S}$ that can be measured (such as the switch state, or maybe energy or momentum) has the following defining property. To each observable O we associate a self–adjoint operator $\hat{O}$ (with matrix entries O_{ij}) such that the eigenvalues of $\hat{O}$ precisely correspond to all possible measurement outcomes. The corresponding eigenstates of $\hat{O}$ are the quantum states in which the measurement yields a definite outcome equal to the eigenvalue. The eigenvalues of the self–adjoint operator $\hat{O}$ are necessarily real, and the eigenvectors are orthogonal, so that they can be used to form an orthonormal set of base vectors for the system.

It is known that elementary particles (electrons, neutrons, etc.) all have a special degree of freedom called *spin*, which can be regarded as a form of angular momentum.

Definition 1.3 *All particles with integer spin* $(0, 1, 2, \ldots)$ *are bosons, and particles with half–odd–integer spin* $(\frac{1}{2}, \frac{3}{2}, \ldots)$ *are fermions.*

The wave function can exhibit two (and, generically, only two) possible symmetries under exchange; the law governing such behaviors, which distinguishes all particles as either bosons or fermions, was discovered by W. Pauli and is supported by experimental evidence.

Theorem 1.4 (Spin–Statistics Theorem) *Systems of identical bosons have wave functions which are symmetric under interchange of any pair of particle labels.*

The wave function is said to obey Bose–Einstein statistics. Systems of identical fermions have wave functions which are antisymmetric under interchange of any pair of particle labels. The wave function is said to obey Fermi–Dirac statistics.

Theorem 1.4 rules out the additional general result, known as *Pauli Exclusion Principle*, stating that no two identical fermions can be in the same quantum state. On the contrary, no such restriction applies to identical bosons, that is any number of identical bosons can occupy the same quantum state. A systematic exploration of Theorem 1.4 can be found in Duck and Sudarshan, 1998.

1.4.1 Canonical relations and number representation

The formalism of Second Quantization (Paar, 2010) starts by postulating the *Canonical Commutation Relations* (CCR)

$$[a_j, a_k] = 0, \quad [a_j^\dagger, a_k^\dagger] = 0, \quad [a_j, a_k^\dagger] = \delta_{j,k}\mathbb{1}, \tag{1.2}$$

where $j, k = 1, \ldots, L$ (in case of a system with L independent bosonic modes), $\mathbb{1}$ is the identity operator on $\mathcal{H}$, and we have used the definition of the so–called *commutator* $[A, B] := AB - BA$ between A and B. The properties in Equation (1.2) involve the operators $a_\ell^\dagger$, and their adjoints a_ℓ, which create and annihilate the bosons, respectively (in analogy with the similar operators for the treatment of the harmonic oscillator in terms of lowering and raising the energy of the system one quantum at a time).

Of special interest are the self–adjoint operators called *occupation number operators* which can be constructed from the operators $a_\ell^\dagger$ and a_ℓ as follows:

$$\hat{n}_\ell = a_\ell^\dagger a_\ell, \tag{1.3}$$

with $\ell = 1, \ldots, L$, whose eigenvalues are the *occupation numbers* n_ℓ for the L modes of the system. The related self–adjoint operator

$$\hat{N} = \sum_{\ell=1}^{L} \hat{n}_\ell \tag{1.4}$$

is called the *particle number operator* for $\mathcal{S}$.

The creation operators $a_j^\dagger$ allow to construct bosonic states $\varphi_{n_1,\ldots,n_L}$ from the *vacuum* or *ground state* φ_0, that is the vector annihilated by all the a_j's: $a_j\varphi_0 = 0$ for all $j = 1, \ldots, L$. In particular, the Hilbert space $\mathcal{H}$ where a system with L independent bosonic modes lives is constructed as the linear span of the vectors generated by acting on φ_0 with the operators $a_j^\dagger$ and their powers, and then normalizing the obtained vectors, say

$$\varphi_{n_1,\ldots,n_L} := \frac{1}{\sqrt{n_1! \ldots n_L!}} (a_1^\dagger)^{n_1} \cdots (a_L^\dagger)^{n_L} \varphi_{\mathbf{0}}, \tag{1.5}$$

$n_\ell = 0, 1, \ldots$, for all ℓ. The set of vectors defined in (1.5) forms a complete and orthonormal set in $\mathcal{H}$; these vectors are eigenstates of both $\hat{n}_\ell$ and $\hat{N}$:

$$\hat{n}_\ell \varphi_{n_1,\ldots,n_L} = n_\ell \varphi_{n_1,\ldots,n_L}$$

and

$$\hat{N}\varphi_{n_1,\dots,n_L} = N\varphi_{n_1,\dots,n_L},$$

where $N = \sum_{\ell=1}^{L} n_\ell$. Hence, n_ℓ and N are eigenvalues of $\hat{n}_\ell$ and $\hat{N}$, respectively. Moreover, using the CCR we deduce that

$$\hat{n}_\ell(a_\ell\varphi_{n_1,\dots,n_L}) = (n_\ell - 1)(a_\ell\varphi_{n_1,\dots,n_L}),$$

for $n_\ell \geq 1$, whereas, if $n_\ell = 0$, a_ℓ annihilates the vector, and

$$\hat{n}_\ell\left(a_\ell^\dagger\varphi_{n_1,\dots,n_L}\right) = (n_\ell + 1)\left(a_\ell^\dagger\varphi_{n_1,\dots,n_L}\right),$$

for all ℓ and for all n_ℓ.

Thus, the operator $\hat{n}_\ell$ acts on $\varphi_{n_1,\dots,n_L}$, and returns n_ℓ, which is exactly the number of bosons in the ℓ–th mode. The operator $\hat{N}$ counts the total number of bosons. Moreover, the operator a_ℓ destroys a boson in the ℓ–th mode, whereas $a_\ell^\dagger$ creates a boson in the same mode. This is why in the physical literature a_ℓ and $a_\ell^\dagger$ are usually called the *annihilation* and the *creation* operators, respectively. Notice that, due to the fact that $\mathcal{H}$ is infinite–dimensional, the operators introduced so far, a_ℓ, $a_\ell^\dagger$, $\hat{n}_\ell^\dagger$, and $\hat{N}$, are all unbounded.

In using the bosonic creation and annihilation operators, in general, one needs to apply only the commutation relations (1.2) and the property $a_\ell\varphi_0 = 0$. As long as one starts from a wave function with the proper bosonic symmetry, one does not need to worry ever about proper symmetries of wave functions, since they are induced through the algebra of $a_\ell^\dagger$ and a_ℓ.

The vector $\varphi_{n_1,\dots,n_L}$ has to be intended as a describer of the L different modes of bosons of $\mathcal{S}$ in the sense that n_1 bosons are in the first mode, n_2 in the second mode, and so on. Another possibility consists in thinking of $\varphi_{n_1,\dots,n_L}$ as the state of L independent one–dimensional harmonic oscillators, each with a frequency ω_j, such that the first oscillator has energy $\hbar\omega_1\left(n_1 + \frac{1}{2}\right)$, the energy of the second oscillator is $\hbar\omega_2\left(n_2 + \frac{1}{2}\right)$, and so on. This interpretation, however, is not considered in this thesis since it is not interesting for the aims of the proposed approach.

Analogously to the case of bosons, fermions are annihilated and created by similar operators, b_ℓ and $b_\ell^\dagger$, with the difference that these latter operators satisfy other rules, called the *Canonical Anti–commutation Relations* (CAR)

$$\{b_j, b_k\} = 0, \quad \{b_j^\dagger, b_k^\dagger\} = 0, \quad \{b_j, b_k^\dagger\} = \delta_{j,k}\mathbb{1}, \tag{1.6}$$

where $j, k = 1, \dots, L$ (in case of a system with L independent fermionic modes), $\mathbb{1}$ is the identity operator on $\mathcal{H}$, and we have used the definition of the so–called *anti–commutator* $\{A, B\} := AB + BA$ between A and B. The properties in equation (1.6) provide that creation and annihilation operators for fermions alter the occupancy of the wave function without affecting the fermionic symmetry. The immediate difference between the commutation rules (1.2) and the anti–commutation rules (1.6) is that, while the operator a_ℓ^2 is different from 0, the square of b_ℓ is automatically 0, together with all its higher powers. This is indeed an evidence of the Pauli principle: if we

try to construct a system with two fermions with the same quantum numbers (labeled by ℓ) using the language of second quantization, we should act twice with $b_\ell^\dagger$ on the vacuum φ_0. But, as ${b_\ell^\dagger}^2 = 0$, the resulting vector vanishes, in accordance with the fact that such a state has probability 0 to occur.

As for bosons, from the creation and annihilation operators for fermions we can construct $\hat{n}_\ell = b_\ell^\dagger b_\ell$ and $\hat{N} = \sum_{\ell=1}^{L} \hat{n}_\ell$, which are both self–adjoint. In particular, $\hat{n}_\ell$ is the *number operator* for the ℓ–th mode, while $\hat{N}$ is the *number operator* of $\mathcal{S}$.

The Hilbert space $\mathcal{H}$ of the system $\mathcal{S}$ is constructed as for bosons, with the difference that we can act on the *vacuum* $\varphi_{\mathbf{0}}$ with the operators $b_\ell^\dagger$ but not with higher powers, since these powers are simply zero. This means that we construct the vectors

$$\Phi_{n_1,\dots,n_L} := (b_1^\dagger)^{n_1} \cdots (b_L^\dagger)^{n_L} \Phi_{\mathbf{0}}, \tag{1.7}$$

where $n_\ell = 0, 1$, for all ℓ, and no normalization appears. Again, the vectors defined in (1.7) form an orthonormal set (spanning $\mathcal{H}$) of eigenstates of both $\hat{n}_\ell$ ($\ell = 1, \dots, L$) and $\hat{N}$ with eigenvalues n_ℓ ($\ell = 1, \dots, L$) and $N = \sum_{\ell=1}^{L} n_\ell$, respectively. A major difference with respect to what happens for bosons is the property, following from the idempotence of $\hat{n}_\ell$,

$$\hat{n}_\ell^2 = b_\ell^\dagger b_\ell b_\ell^\dagger b_\ell = b_\ell^\dagger (1 - b_\ell^\dagger b_\ell) b_\ell = b_\ell^\dagger b_\ell - b_\ell^\dagger b_\ell^\dagger b_\ell b_\ell = \hat{n}_\ell, \tag{1.8}$$

that the values that the various n_ℓ can assume are simply 0 and 1, whereas, as for bosons, N can take any integer value larger or equal to 0.

Moreover, using the CAR, we deduce that

$$\hat{n}_\ell \left(b_\ell \Phi_{n_1,\dots,n_L} \right) = \begin{cases} (n_\ell - 1)(b_\ell \Phi_{n_1,\dots,n_L}), & n_\ell = 1, \\ 0, & n_\ell = 0, \end{cases}$$

and

$$\hat{n}_\ell \left(b_\ell^\dagger \Phi_{n_1,\dots,n_L} \right) = \begin{cases} (n_\ell + 1)(b_\ell^\dagger \Phi_{n_1,\dots,n_L}), & n_\ell = 0, \\ 0, & n_\ell = 1, \end{cases}$$

for all $\ell = 1, \dots, L$. The interpretation of the *annihilation* and the *creation* operators for fermions does not differ in principle from the one for bosons, except from the fact that the operator $b_\ell^\dagger$ may also be seen as an annihilation operator since, acting on a state with $n_\ell = 1$, that state is actually destroyed.

Of course, for fermionic systems, $\mathcal{H}$ has a finite dimension. In particular, for just one mode of fermions, $dim(\mathcal{H}) = 2$, and for L modes of fermions $dim(\mathcal{H}) = 2^L$. This also implies that, contrarily to what happens for bosons, the fermionic operators are bounded and can be represented by finite–dimensional matrices.

1.4.2 Time evolution

In this Section, we describe how to find the time evolution of a closed quantum microscopic system not interacting with any external reservoir. More precisely, the two possible equivalent strategies consisting in adopting the

Schrödinger rather than the Heisenberg picture in order to obtain the dependence on time of a given measurable quantity are discussed.

Let $\mathcal{H}$ be an Hilbert space, and $B(\mathcal{H})$ the set of all the bounded operators on $\mathcal{H}$. $B(\mathcal{H})$ is a so–called $C^\star$–algebra, that is, an algebra with involution that is complete under a norm, $\| \cdot \|$, satisfying the $C^\star$–property: $\| A^\star A \| = \| A \|^2$, for all $A \in B(\mathcal{H})$. Let $\mathcal{S}$ be the physical system under consideration, and $\mathcal{A}$ the set of all the operators useful for a complete description of $\mathcal{S}$, which includes the observables of $\mathcal{S}$. For simplicity, it is convenient to assume that $\mathcal{A}$ is a $C^\star$–algebra by itself, possibly coinciding with the original set $B(\mathcal{H})$, or, at least, with some closed subset of $B(\mathcal{H})$. This is not possible when using unbounded operators, which do not belong to any $C^\star$–algebra. However, also in the case that some unbounded operator X appears in the scheme, if it is self–adjoint, then we may consider $\exp(iXt)$, which is unitary and, therefore, bounded, and X may be recovered by taking its time derivative in $t = 0$ and multiplying the result by $-i$.

The description of the time evolution of $\mathcal{S}$ is related to a self–adjoint (bounded or unbounded) operator $H = H^\dagger$, the *Hamiltonian* of $\mathcal{S}$, which in standard quantum mechanics is the observable operator corresponding to the total energy of the system. Hence, H possesses a complete, orthonormal set of eigenvectors $\{\eta_k(x)\}$ and a corresponding set of real eigenvalues $\{E_k\}$,

$$H\eta_k(x) = E_k\eta_k(x), \quad k = 1, 2, \ldots$$

where the numbers $\{E_k\}$ are the allowed values of the total energy of the system. Thus, the quantum–mechanical Hamiltonian generates the time–evolution, as in classical mechanics, except that the influence of the non-commutativity must now be taken into account.

Provided $\mathcal{S}$ is not disturbed (such as by being measured), the Hamiltonian operator H determines the time evolution of the wave function $\Psi(t)$ describing the system at time t through the differential equation, known as the Schrödinger equation,

$$i\hbar\frac{d\Psi(t)}{dt} = H\Psi(t). \tag{1.9}$$

According to this postulate, so long as the system is not disturbed[1], Ψ evolves with time in a completely deterministic way, that is, if Ψ_0 is the wave function describing $\mathcal{S}$ at time $t = 0$; then (in absence of external agents intruding upon the system) as t assumes further values $t_1, t_2, \ldots$, the wave function successively coincides with the $\mathcal{H}$–vectors $\Psi(t_1), \Psi(t_2), \ldots$ which are solutions to (1.9) satisfying the initial condition $\Psi(0) \equiv \Psi_0$.

Since H does not depend explicitly on t, the formal solution of the Schrödinger equation is $\Psi(t) = \exp(-iHt)\Psi(0) = \exp(-iHt)\Psi_0$. As the time increases, the evolution of the wave function is completely specified by the differential equation (1.9), and we can then compute the mean value of each operator $Z \in \mathcal{A}$ in the state $\Psi(t)$, say

$$z(t) = \langle \Psi(t), Z\Psi(t) \rangle . \tag{1.10}$$

[1] An example of such a disturbance is given by the measurement process, which alters in a sudden, random way the otherwise orderly time development of the wave function.

Notice that, in general, the explicit form of the solution $\exp(-iHt)\Psi_0$ may be actually unknown, at least if there is no easy way to compute the action of the unitary operator $\exp(-iHt)$ on the vector Ψ_0, which is not granted at all.

The second point of view considered in this thesis in order to look at the time evolution of $\mathcal{S}$, which is completely equivalent to the previous picture (Bagarello, 2012), consists in adopting the *Heisenberg representation*, in which the wave function does not evolve in time, while each operator $X \in \mathcal{A}$ does, and its time evolution is given by the Heisenberg equation

$$X(t) = \exp(iHt)X\exp(-iHt), \tag{1.11}$$

or, equivalently, by the solution of the differential equation

$$\frac{dX(t)}{dt} = i\exp(iHt)[H, X]\exp(-iHt) = i[H, X(t)]. \tag{1.12}$$

The time evolution defined in this way is a one–parameter group of automorphisms of $\mathcal{A}$.

An operator $Y \in \mathcal{A}$ is a *constant of motion* if it commutes with H. Indeed, in this case, equation (1.12) implies that $\dfrac{dY(t)}{dt} = 0$, so that $Y(t) = Y$ for all t.

The vector $\varphi_{n_1,\ldots,n_L}$ in (1.5) (or the vector $\Phi_{n_1,\ldots,n_L}$ in (1.7) depending on the fact that the system involves bosonic or fermionic modes, respectively) defines the expectation value of any operator $Z \in \mathcal{A}$ changing with time as

$$z(t) = \langle \varphi_{n_1,\ldots,n_L}, Z(t)\varphi_{n_1,\ldots,n_L}\rangle, \tag{1.13}$$

where $\langle\ ,\ \rangle$ is the scalar product in $\mathcal{H}$.

2 Theoretical operatorial models of classical problems

In this Chapter, we present the theoretical framework for the description of the dynamic properties of different systems by means of operatorial methods of quantum mechanics. The disquisition is carried out in very general terms, leaving aside the interpretation that can be attributed to the various models, and is intended to cover the theoretical and applicative aspects of interest for the developments considered later.

2.1 Background

Operatorial techniques borrowed from quantum mechanics even provide a valuable tool for the analysis and the description of the dynamical aspects of different macroscopic classical systems related to real case studies.

The main motivations which suggest the use of tools, like operator algebras and, in particular, the number representation, originally developed in a quantum context to describe classical situations, have been widely discussed along the years (see Bagarello, 2012, and the references therein). Indeed, in many situations several quantities changing discontinuously are well described in terms of the integer eigenvalues of certain relevant self–adjoint operators, the observables of the system, and the dynamics may be ruled by an energy–like operator called the Hamiltonian of the system.

In the following, the systems that we shall describe are thought of as *compartmental models*, *i.e.*, systems that can be viewed as divided into *compartments* among which some fluxes occur. A sketch of such models is pictured by representing the compartments by boxes and the connections between them by arrows, each box having a number of connections leading to itself (inflows) and a number of arrows leading from itself (outflows).

The theoretical framework adopted hereafter for the description of a macroscopic system consists of a model involving fermionic annihilation and creation operators, and the number operators associated to the involved compartments. In particular, we shall use fermionic operators due to two main reasons. The first one is of technical nature, since the Hilbert space of a model involving a finite number of fermionic modes has a finite dimension (in other words, fermionic operators are bounded), whereas the use of bosonic operators always entails, even for very simple systems, the introduction of an infinite–dimensional Hilbert space. As it is widely discussed in the literature (see Roman, 1965 for instance), this means that the fermionic operators, in case of a model involving N different compartments, can be represented as matrices acting on a 2^N–dimensional Hilbert space, and hence they are $2^N \times 2^N$ matrices. This reflects also in the fact that, while the eigenvalues of a bosonic number operator are all the positive integers (and therefore can take very high values), one has that 0 and

1 are the only allowed eigenvalues of a fermionic number operator. This latter consideration leads to the second justification, which concerns the interpretation given to the model in all those situations, as in the case of ecosystems, in which for each compartment only two possible non–trivial situations are admitted: a first one (the *ground state*), having a very low density, or a second one (the *excited state*), in which the density is very high. In such contexts, trying to increase the density of the excited state, as well as to decrease the density of the ground state, simply annihilates that compartment. This fact simply means that there exist upper and lower bounds to the densities of the compartments which can not be overcome for obvious reasons. Fermionic operators have been successfully used in the definition of local densities of observables in different macroscopic systems, for instance closed ecological systems (Bagarello and Oliveri, 2014), desertification models (Bagarello, Cherubini, and Oliveri, 2016), or decision making mechanisms (Bagarello and Haven, 2014; Bagarello and Haven, 2015; Bagarello, 2015).

According to the operatorial approach, the dynamics of a system $\mathcal{S}$ is therefore governed by the Hermitian Hamiltonian operator $H = H^\dagger$, which, in standard quantum mechanics, is the observable operator corresponding to the total energy of the system and, besides describing the main effects which are observed in $\mathcal{S}$, has the property of determining the time evolution of the system. The way in which H may be constructed is described in Bagarello, 2014 and in Bagarello, 2012.

The models adopted in this framework are built by expressing the variables we are interested in as number–like operators, *i.e.*, self–adjoint operators like $\hat{n} = a^\dagger a$, with a and $a^\dagger$ the annihilation and creation operator, respectively, since this choice turns out to be the most convenient in all those cases in which the mean values of $\hat{n}$ corresponding to an assigned initial condition can be interpreted as a density attached to a compartment of the macroscopic system.

Without expecting to describe any quantum effect or stochastic dynamics, this perspective allows us to build a deterministic system, evolving with time in a completely deterministic way, just as position and momentum do in classical mechanics.

Two equivalent viewpoints in order to look at the time evolution of a system $\mathcal{S}$ consist, on the one hand, in considering the wave function $\Psi(t)$ describing $\mathcal{S}$ at time t evolving according to the Schrödinger equation $i\dot{\Psi}(t) = H\Psi(t)$, where $\Psi(0) = \Psi_0$ describes the initial status of the system, or, on the other hand, in adopting the Heisenberg representation, according to which the wave function does not evolve in time, while each operator $X(t)$ acting on the Hilbert space where $\mathcal{S}$ lives at time t do, according to the Heisenberg equation $\dot{X}(t) = i[H, X(t)]$, whereupon it is $X(t) = \exp(iHt)X(0)\exp(-iHt)$. The formal solution of the Schrödinger equation is, since H is assumed independent explicitly of t, $\Psi(t) = \exp(-iHt)\Psi(0) = \exp(-iHt)\Psi_0$.

Both in the Schrödinger and in the Heisenberg representation the formal solution is not, in general, explicitly known (an easy way to compute the required operations is not granted at all). However, for quadratic Hamiltonians, the dynamic equations are linear and it is possible to drastically reduce the computational complexity of the problem. On the contrary, the methods for the numerical resolution of the nonlinear equations (arising when

one uses a non quadratic Hamiltonian) encounter major obstacles due to the remarkable growth of the size of the problem as the number N of the involved compartments increases, even in the case of models not too much complicated. Of course, this results in a strong limitation on the kind of systems that can be analyzed in practice, and makes the operatorial approach computationally unmanageable without large supercomputing resources in case of models describing nonlinear interactions between compartments or spatially nonhomogeneous models on a lattice. This increase in the computational cost may be avoided without a loss in quality with the introduction of the notion of rule–induced dynamics.

From now on we will use mainly the Heisenberg picture for the mathematical formulation of the dynamics of the contemplated systems, so that the wave function is stationary. Although the Schrödinger and the Heisenberg formulations are formally equivalent, the latter, in the light of the applications we shall consider, provides a physically more appealing picture.

2.2 Systems modeled by quadratic Hamiltonians

Let us consider at first a simple linear model describing the dynamics of a certain physical system $\mathcal{S}$ in terms of N different fermionic modes a_j, $j = 1, 2, \ldots, N$. Of course, these operators satisfy the Canonical Anti–commutation Rules (no more than one particle can ever be in the same state), respectively. Moreover, we assume that the general Hamiltonian containing the essential features of the system $\mathcal{S}$ is given by

$$\begin{aligned} H &= H_0 + H_I, \qquad \text{with} \\ H_0 &= \sum_{j=1}^{N} \omega_j \, a_j^\dagger \, a_j, \\ H_I &= \sum_{1 \le j < k \le N} \lambda_{j,k} \left(a_j \, a_k^\dagger + a_k \, a_j^\dagger \right) + \sum_{1 \le j < k \le N} \mu_{j,k} \left(a_j^\dagger \, a_k^\dagger + a_k \, a_j \right), \end{aligned} \tag{2.1}$$

where ω_i $(i = 1, \ldots, N)$, $\lambda_{j,k}$, and $\mu_{j,k}$ $(j = 1, \ldots, N-1, k = j+1, \ldots, N)$ are real parameters. The operator in (2.1) is made up of a free standard part, H_0, and a contribution, H_I, related to the interactions among the components. In particular, the parameters in H_0, which, in agreement with the quantum mechanical literature, are called the frequencies, measure the inertia of the different compartments (Bagarello, 2012): the higher the value of a certain ω_j, the higher the tendency of the density of the j–th degree of freedom to stay constant in time (that is to say, the smaller the amplitudes of the oscillations of the related densities). On the other hand, the interaction Hamiltonian H_I, which is quadratic in the raising and lowering operators, describes the effects of the simultaneous increasing and/or decreasing of the densities of the various fermionic modes. In particular, the term $a_j a_k^\dagger$ makes the density of the k–th compartment of $\mathcal{S}$ to increase and that of the j–th one to decrease, while the adjoint contribution, $a_k a_j^\dagger$, is responsible for the opposite phenomenon. Similarly, the terms like $a_j^\dagger a_k^\dagger$ or $a_k a_j$ are intended to produce a simultaneous increase or decrease of both the j–th and the k–th compartment of $\mathcal{S}$. Notice that the presence of the adjoint contributions in H_I ensures the fact that the Hamiltonian H is self–adjoint, *i.e.*,

$H = H^\dagger$. The parameters $\lambda_{j,k}$ measure a sort of *competition* (*mors tua vita mea*) between the j–th and the k–th compartment, whereas the parameters $\mu_{j,k}$ a sort of *cooperation* (*unita vincimus*). Of course, $\lambda_{j,k}$ ($\mu_{j,k}$, respectively) must be taken to be 0 when between the j–th and the k–th component of the system there is no competition (cooperation, respectively). When $H_I = 0$, $[H, \hat{n}_j] = [H_0, \hat{n}_j] = 0, j = 1, 2, \ldots, N$, *i.e.*, H describes a somehow static situation, in which the densities of the compartments of $\mathcal{S}$, described by the number operators $\hat{n}_j$, stay constant even if the operators a_j and $a_j^\dagger$ have a non trivial time dependence.

To look at the time evolution of the system $\mathcal{S}$ in accordance with the Heisenberg scheme, we should consider the evolution in time of any operator X acting on $\mathcal{S}$ according to the Heisenberg equation $\dfrac{dX(t)}{dt} = i[H, X(t)]$. The dynamical equations deduced in correspondence of each operator a_j ($j = 1, \ldots, N$) thus have the form:

$$\begin{aligned} \dot{a}_j = i\Bigg(& -\omega_j a_j + \sum_{1\le\ell<j} \lambda_{\ell,j} a_\ell + \sum_{j<k\le N} \lambda_{j,k} a_k \\ & + \sum_{1\le\ell<j} \mu_{\ell,j} a_\ell^\dagger - \sum_{j<k\le N} \mu_{j,k} a_k^\dagger \Bigg). \end{aligned} \tag{2.2}$$

In order to close the system, in general, the Hermitian conjugates of these equations, say

$$\begin{aligned} \dot{a}_j^\dagger = i\Bigg(& \omega_j a_j^\dagger - \sum_{1\le\ell<j} \lambda_{\ell,j} a_\ell^\dagger - \sum_{j<k\le N} \lambda_{j,k} a_k^\dagger \\ & - \sum_{1\le\ell<j} \mu_{\ell,j} a_\ell + \sum_{j<k\le N} \mu_{j,k} a_k \Bigg), \end{aligned} \tag{2.3}$$

have to be considered too. Since H is a quadratic operator, the equations (2.2) and (2.3) turn out to be linear. By introducing the vector

$$A = \left(a_1, \ldots, a_N, a_1^\dagger, \ldots, a_N^\dagger\right)^T, \tag{2.4}$$

the system of the equations of motion can be rewritten as

$$\dot{A} = UA, \tag{2.5}$$

where U is the symmetric matrix deduced from the equations (2.2) and (2.3). The solution is clearly

$$A(t) = V(t)A(0), \tag{2.6}$$

with $V(t) = \exp(Ut)$. Therefore, the computation of the densities of the various compartments of the system, described by the number operators $\hat{n}_j, j = 1, \ldots, N$, is immediately obtained, and the only numerical difficulty consists in finding, given U, the matrix $\exp(Ut)$. Calling $V_{j,k}(t)$ the generic time–dependent matrix entry of $V(t)$, and $n_j(t) = \left\langle \varphi_{\mathbf{n}}, a_j^\dagger(t) a_j(t) \varphi_{\mathbf{n}} \right\rangle$, where $\mathbf{n} = (n_1, \ldots, n_N)$ contains the initial densities of the compartments, and $\varphi_{\mathbf{n}}$

is an eigenstate of all the number operators $\hat{n}_j$ with eigenvalue n_j, it is

$$n_j(t) = \sum_{k=1}^{N} \left(|V_{j,k}(t)|^2 + |V_{j,k+N}(t)|^2 \right) n_k, \quad j = 1, \dots, N. \tag{2.7}$$

These are the required functions describing the densities of each compartment of $\mathcal{S}$, with initial conditions fixed by the vector $\varphi_{\mathbf{n}}$. Thus, for quadratic Hamiltonians, since we know the solution to (2.2), we do not need to consider the dynamic equations for each entry of the operators a_j, but simply the global equations for the fermionic operators.

As we will show in Section 2.3, the simplification expressed by (2.7) is no longer applicable when the dynamic equations are nonlinear, since in this case we do not have explicitly the solution.

2.3 Models with general cubic Hamiltonians

Here, we deal with the case of systems whose dynamics is driven by differential equations which are no longer linear.

The interaction among the N compartments of the same system $\mathcal{S}$ introduced in Subsection 2.2 can be represented in a more complex way by considering in the full Hamiltonian H, rather than just quadratic terms, also contributions of order greater than two. For simplicity, we consider a Hamiltonian operator containing cubic contributions:

$$\begin{aligned} H &= H_0 + H_I, \qquad \text{with} \\ H_0 &= \sum_{j=1}^{N} \omega_j \, a_j^\dagger \, a_j, \\ H_I &= \sum_{1 \le j < k \le N} \lambda_{j,k} \left(a_j \, a_k^\dagger + a_k \, a_j^\dagger \right) + \sum_{1 \le j < k \le N} \mu_{j,k} \left(a_j^\dagger \, a_k^\dagger + a_k \, a_j \right) \\ &\quad + \sum_{1 \le j,k,\ell \le N} \nu_{j,k,\ell} \left(a_j^\dagger a_k^\dagger a_\ell + a_\ell^\dagger a_k a_j \right). \end{aligned} \tag{2.8}$$

The interpretation of the terms in the last sum in H_I is prompted by the fact that the expressions $a_j^\dagger a_k^\dagger a_\ell$ ($j, k, \ell = 1, \dots, N$) model the fact that whenever a particle of type ℓ is annihilated, one of type j and another one of type k are created, expressing in such a way the simultaneous increase of the densities of both the j–th and the k–th compartments of the system associated with the decrease of the ℓ–th one. The adjoint term in H, which is needed in order to render the operator H Hermitian, describes the specular phenomenon: a type–ℓ particle is created and two type–j and type–k ones are annihilated; certainly, the total number of particles is not preserved. Notice that, in order to make the formulation of the model completely general, one might consider further terms of the form $a_j^\dagger a_k a_\ell^\dagger$ or $a_j a_k^\dagger a_\ell^\dagger$. However, the description of the dynamics would not differ due to the presence of such contributions (expressing mechanisms similar to those described just above).

The Heisenberg equations of motion extend those in (2.2) and (2.3):

$$\begin{aligned}
\dot{a}_j = i\Bigg(& -\omega_j a_j + \sum_{1\le\ell<j} \lambda_{\ell,j} a_\ell + \sum_{j<k\le N} \lambda_{j,k} a_k + \sum_{1\le\ell<j} \mu_{\ell,j} a_\ell^\dagger - \sum_{j<k\le N} \mu_{j,k} a_k^\dagger \\
& + \sum_{k,\ell\in\{1,\dots,N\}\setminus\{j\}} \nu_{j,k,\ell} \left(2a_j^\dagger a_j - \mathbb{1}\right)\left(a_k^\dagger a_\ell + a_k a_\ell\right)\Bigg), \\
\dot{a}_j^\dagger = i\Bigg(& \omega_j a_j^\dagger - \sum_{1\le\ell<j} \lambda_{\ell,j} a_\ell^\dagger - \sum_{j<k\le N} \lambda_{j,k} a_k^\dagger - \sum_{1\le\ell<j} \mu_{\ell,j} a_\ell + \sum_{j<k\le N} \mu_{j,k} a_k \\
& - \sum_{k,\ell\in\{1,\dots,N\}\setminus\{j\}} \nu_{j,k,\ell} \left(a_\ell^\dagger a_k + a_\ell^\dagger a_k^\dagger\right)\left(2a_j^\dagger a_j - \mathbb{1}\right)\Bigg),
\end{aligned} \tag{2.9}$$

with $j = 1, \dots, N$. The solutions of the nonlinear system (2.9) are to be found by means of numerical methods (as an example by Runge–Kutta methods). Analyzing this problem in terms of size, in accordance with the classical representation of the fermionic operators, since the operators a_j and $a_j^\dagger$ ($j = 1, \dots, N$) are actually $2^N \times 2^N$ matrices, the number of nonlinear equations to be solved amounts to $2N \cdot 2^{2N}$. Therefore, the calculation of numerical solutions of (2.9) is not readily implementable at all. In fact, a strong limitation of the classical fermionic operatorial approach lies precisely in the exponential rise of size of the nonlinear differential system of the equations of motion as soon as not extremely low values of N are considered or, even further, in case of spatial models. In this latter event the calculation of numerical solutions becomes in practice a computationally intractable problem in absence of huge computing resources.

2.4 Dissipative effects

The problem of a simple description of irreversible processes in quantum mechanics is usually very hard. Perfect isolation of quantum systems is not possible since any realistic system is influenced by the coupling to an environment, which typically has a large number of degrees of freedom. In general, a complete microscopic description of the degrees of freedom of the environment is too complicated. Probably, the simplest choice consists in using a non self–adjoint, effective, Hamiltonian which is properly chosen in order to describe the phenomenon we are interested to. Of course, using such an operator to describe the time evolution of a system usually causes several problems. First of all, it is not evident at all that the dynamics is still driven by a Heisenberg–like equation of motion. Actually, the assumption is that the wave function $\Psi(t)$ of the system still evolves obeying the Schrödinger equation $i\dot{\Psi} = H\Psi$, even if $H \neq H^\dagger$.

As widely discussed in Bagarello, 2012 and references therein, a rigorous way to describe damping in a quantum system is to *open it*, making the system to interact with a suitable reservoir. In this way, the dynamics of the full system remains unitary, even if an exchange between the system and the (infinitely extended) reservoir allows us to describe quantities which are not conserved during the time evolution. In principle, in order to look for some simple description of the dynamics of an open system, one should investigate the unitary dynamics of the total system, *i.e.* system and

environment, to obtain information about the reduced system of interest by averaging the appropriate observables over the degrees of freedom of the environment (Breuer and Petruccione, 2007). Usually, the dynamics of an open quantum system is described in terms of the reduced density operator which is obtained from the density operator of the total system by tracing over the variables of the environment. In order to eliminate the degrees of freedom of the environment, various approximations are needed which lead to a closed equation of motion for the density matrix of the open system. A possible choice to that effect is the Markov approximation, which may lead to a so–called quantum master equation that, in turn, generates a quantum dynamical semigroup in the space of reduced density matrices. Prominent representants of such equations are the quantum optical master equation, and, derived under slightly different assumptions, the quantum Brownian motion master equation, with applications in condensed matter physics. In general, the validity of the master equation approach is guaranteed in a Markovian setting, where the master equation takes the famous Gorini–Kossakowski–Sudarshan–Lindblad (GKSL) form and is a generator of a dynamical semigroup.

Also, quite often, an *effective approach* can be used, *i.e.*, that of replacing self–adjoint with non self–adjoint Hamiltonians, keeping unchanged the other rules of the game. This kind of procedure is used in branches of quantum physics, like quantum optics, to describe simply (though not rigorously) decay processes (see Ben-Aryeh, Mann, and Yaakov (2004) and Cherbal et al. (2007), and references therein). In particular, in order to describe a damping effect, it is sufficient, even if not rigorous, to replace some real parameters involved in the Hamiltonian operator with complex numbers. In particular, it results that it is enough to add an even small negative imaginary part to just a single parameter of H_0 in (2.1) and (2.8) to induce a damping for all the compartments of the considered system (Bagarello and Oliveri, 2014; Bagarello, Cherubini, and Oliveri, 2016; Di Salvo and Oliveri, 2016c).

Consider, therefore, the time evolution of the observable X still given by the equation

$$X(t) = \exp(iHt)X\exp(-iHt),$$

even if $H \neq H^\dagger$ (the consequences of this position on the choice of the natural scalar product of the Hilbert space of the theory are not addressed here).

In order to find conditions which produce damping, let us consider the following simple interacting model deduced from the one introduced in Bagarello and Oliveri, 2010:

$$H = \omega_1 a_1^\dagger a_1 + \omega_2 a_2^\dagger a_2 + \lambda(a_1^\dagger a_2 + a_2^\dagger a_1),$$

where $[a_i, a_j^\dagger] = \delta_{i,j}\,\mathbb{1}$, $i, j = 1, 2$, and $\omega_j, \lambda \in \mathbb{R}$. The time evolution of $a_j(t)$, and of $\hat{n}_j(t) = a_j^\dagger(t)a_j(t)$ as a consequence, can be deduced analytically, and the mean values of $\hat{n}_j(t)$ can also be found:

$$\begin{cases} n_1(t) = \langle \hat{n}_1(t)\rangle = n_1|\Phi_{1,1}(t)|^2 + n_2|\Phi_{1,2}(t)|^2, \\ n_2(t) = \langle \hat{n}_2(t)\rangle = n_1|\Phi_{2,1}(t)|^2 + n_2|\Phi_{2,2}(t)|^2. \end{cases}$$

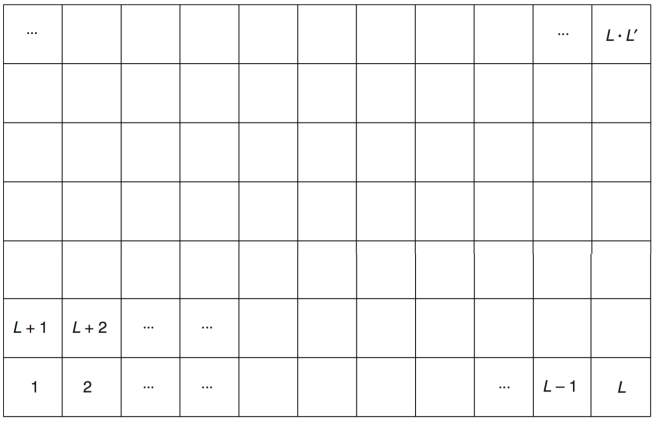

FIGURE 2.1: A representation of 2–D lattice for the spatial model.

Here $n_j = \langle \hat{n}_j(0) \rangle$ are fixed by the initial conditions for the system, while the various functions $|\Phi_{k,l}(t)|$ all share the same general analytic expression:

$$|\Phi_{k,l}(t)|^2 = a_{11} \exp(it(\overline{\alpha}_1 - \alpha_1)) + a_{12} \exp(it(\overline{\alpha}_2 - \alpha_2)) + a_{21} \exp(it(\overline{\alpha}_2 - \alpha_1)) + a_{22} \exp(it(\overline{\alpha}_1 - \alpha_2)),$$

where a_{ij} are constants, while

$$\alpha_1 = \frac{1}{2}(\omega_1 + \omega_2 + \Omega), \qquad \alpha_2 = \frac{1}{2}(\omega_1 + \omega_2 - \Omega),$$

where $\Omega = \sqrt{(\omega_1 + \omega_2)^2 + 4\lambda^2}$. It is clear that, as far as ω_j and λ are real, $n_1(t)$ and $n_2(t)$ can only oscillate. On the other hand, let us consider the possibility of having these parameters complex–valued: $\omega_j = \omega_{j,re} + i\omega_{j,im}$, $\lambda = \lambda_{re} + i\lambda_{im}$, with $\omega_{j,re}$, $\omega_{j,im}$, λ_{re} and λ_{im} real. A simple analysis suggests that, in order to get $n_j(t) \to 0$ for $t \to \infty$, it is enough to add a negative imaginary part to ω_1 or to ω_2. More precisely, if we take $\lambda_{im} = 0$ and $\omega_{1,im} = \omega_{2,im} < 0$, both $n_1(t)$ and $n_2(t)$ goes to zero asymptotically. On the other hand, it is easy to check that, if $\omega_{1,im} = \omega_{2,im} = 0$, there is no possible choice of λ_{re} and λ_{im} which produces damping.

This simple model suggests that, for a phenomenological description of damping, it is sufficient to add a (small) negative imaginary part to the parameters of the free Hamiltonian, leaving unchanged the (real) interaction parameter.

2.5 Spatial models of diffusion processes

This Section deals with the description of operatorial models also including spatial interactions. These models have an important role in modeling different biological and/or sociological systems (Bagarello, 2012). Possible applications of the operatorial approach on a lattice include the study of migration phenomena (Bagarello and Oliveri, 2013), in which a population moves from a poor place to a richer region already occupied by a second group of people, desertification processes (Bagarello, Cherubini, and Oliveri, 2016), ecosystem modeling (Di Salvo and Oliveri, 2016b), escape strategies (Bagarello, Gargano, and Oliveri, 2015), and general features connected

to competitions between species.

Spatial versions of operatorial models are achieved considering extra diffusion terms in the Hamiltonian operator H. The large number of modes for such models forces us to consider systems ruled by quadratic Hamiltonians in order to have acceptable computational costs.

Start considering a two–dimensional rectangular (or square) region $\mathcal{R}$ divided into cells, labeled by $\alpha = 1, \ldots, L \cdot L'$, as depicted in fig. 2.1. With $\alpha = 1$ we label the first cell down to the left, while $L \cdot L'$ labels the last cell up to the right. In principle, in each cell α, a certain number N of compartments, represented by suitable operators $a_{j,\alpha}$, $j = 1, \ldots, N$, $\alpha = 1, \ldots, L \cdot L'$, are distributed. The rules that these operators satisfy extend the CAR relations:

$$\{a_{i,\alpha}, a^\dagger_{j,\beta}\} = \delta_{i,j}\delta_{\alpha,\beta}\mathbb{1}, \quad \{a_{i,\alpha}, a_{j,\beta}\} = \{a^\dagger_{i,\alpha}, a^\dagger_{j,\beta}\} = 0, \tag{2.10}$$

where $i, j = 1, \ldots, N$, $\alpha, \beta = 1, \ldots, L \cdot L'$. The main idea to build up a spatial model of the system under consideration is to extend what we have discussed in Section 2.2 by assuming the dynamics governed by a quadratic Hamiltonian operator H_S for the full system consisting of a sum of all the terms composing the first standard part H_0 and the contribution H_I related to the interactions among the parts (see Equation (2.1)) in each cell α plus another contribution, H_M, responsible for the migration or diffusion of the compartments all around the lattice. A natural choice for H_M is the following one:

$$H_M = \sum_{i=1}^{N} \sum_{\alpha=1}^{L\cdot L'} \gamma_{i,\alpha} \sum_{\beta=1}^{L\cdot L'} p_{\alpha,\beta} \, (a_{i,\alpha}\, a^\dagger_{i,\beta} + a_{i,\beta}\, a^\dagger_{i,\alpha}), \tag{2.11}$$

where $\gamma_{i,\alpha}$ and $p_{\alpha,\beta}$ ($i = 1, \ldots, N$, $\alpha, \beta = 1, \ldots, L \cdot L'$) are real quantities, to keep H_M self–adjoint. All the parameters entering the spatial model are, in general, assumed to be cell dependent to allow for the description of an anisotropic situation. In particular, $p_{\alpha,\beta}$ can only be 0 or 1 depending on the possibility of the actors of the model to move from the cell α to cell β, or vice versa, and the parameters $\gamma_{i,\alpha}$ are the mobilities. In fact, if $p_{\alpha,\beta} = 1$, the term $a_{i,\alpha}\, a^\dagger_{i,\beta}$ produces a lowering in the density of the i–th compartment in the cell α with a related raising of its density in the cell β, which means that some member of this compartment is moving from α to β. For this reason, $p_{\alpha,\beta}$'s, together with the parameters $\gamma_{i,\alpha}$, measure the *diffusion coefficients*. Indeed, if, for instance, $\gamma_{i,\alpha} = 0$, $\forall \alpha \in \{1, \ldots, L \cdot L'\}$, and $\exists \beta \in \{1, \ldots, L \cdot L'\}$ such that $\gamma_{j,\beta} > 0$, then no diffusion is possible for the i–th compartment, while the j–th compartment can move between certain cells of $\mathcal{R}$. However, we stress that, also when $\gamma_{i,\alpha} = 0$, $\forall \alpha \in \{1, \ldots, L \cdot L'\}$, there exists still the possibility of increasing, after some time, the density of the i–th compartment in a part of $\mathcal{R}$ where this density was initially very small due to the presence of the contributions

$$\sum_{\substack{j=1 \\ j\neq i}}^{N} \left(\lambda_{j,\alpha}(a_{i,\alpha}\, a^\dagger_{j,\alpha} + a_{j,\alpha}\, a^\dagger_{i,\alpha}) + \mu_{j,\alpha}(a^\dagger_{i,\alpha}\, a^\dagger_{j,\alpha} + a_{j,\alpha}\, a_{i,\alpha}) \right), \tag{2.12}$$

which allows the density of i–th compartment to increase just as a consequence of its interaction with the other compartments of the model in the

cell α. These are of course effects of *competition* and/or *cooperation* among the actors of the system which are localized in a single cell of $\mathcal{R}$.

Moreover, to account for other possible spatial interactions related to the migration which may be naturally expected between some couple of actors of the system, a contribution like

$$\sum_{1\leq i<j\leq N}\sum_{\xi\in\Xi_\alpha}\left(\lambda_{i,\xi}(a_{i,\alpha}\,a^\dagger_{j,\xi}+a_{j,\xi}\,a^\dagger_{i,\alpha})+\mu_{i,\xi}(a^\dagger_{i,\alpha}\,a^\dagger_{j,\xi}+a_{j,\xi}\,a_{i,\alpha})\right) \tag{2.13}$$

can be introduced in H_I, Ξ_α being the set of the indices referring to the cells which are adjacent to α in the chosen topology (*e.g.*, the cells belonging to the so called Moore neighborhood).

Since the Hamiltonian H has a quadratic form, the differential equations for the annihilation operators, and possibly for the creation operators, keep linear and, therefore, are not, in principle, particularly difficult to solve (provided that the computations on the total amount of operators involved in the spatial model, *i.e.*, the number of compartments times the number of cells of the lattice, are computationally manageable).

2.6 Computational complexity

In this Section, we discuss some considerations related to the computational cost of the operatorial linear method described in Section 2.2 in the particular case where the model representing the system is defined by using fermionic operators.

According to eq. (2.7), in order to obtain the mean values of the number operators at each instant t (which represent the quantities of interest in the described approach, at least as regards the applications proposed in this thesis), we need the computation of the exponential of the $2N\times 2N$ matrix Ut (we have an $N\times N$ matrix when there are no cooperation terms so that we do not need to consider the creation operators as additional unknowns). There are various methods in the literature, based on different grounds (see Moler and Van Loan, 2003 and the references therein for a survey on this topic), for carrying out the exponential of even large matrices. The best general algorithms use matrix decomposition methods; they start with the Schur decomposition and include some sort of eigenvalue clustering. There are also variants which involve a further reduction to a block form. In all cases, for an $N\times N$ matrix, the initial decomposition costs $O(N^3)$. Therefore, roughly speaking, the computational complexity for the exponential of a matrix of order N can be considered as $O(N^3)$.

System (2.5) is made of $2N$ first order linear differential equations, and a good numerical solution (for instance by a Runge–Kutta method) at the cost $O(N^2)$ ($O(N)$ if U is a sparse matrix) could be looked for. Nevertheless, this is not completely true since a numerical approach requires the use of $A(0)$, and, according to the classical representation of N–mode fermionic operators, each component of the latter is a matrix of order 2^N; therefore, the linear system (2.5) actually involves $2N\cdot 2^{2N}$ differential equations.

It is easily ascertained that for quadratic Hamiltonians the system experiences time evolutions which are periodic or quasi–periodic. To describe some kind of "more interesting" dynamics, without adding extra ingredients to the operatorial approach described in the previous Sections, we need

to change something in the form of H. A natural choice consists in assuming a Hamiltonian with terms of order greater than two; however, in such a case, adopting the Heisenberg representation, to obtain the time evolution of the system, we have to compute at each instant of time the exponential of a $2^N \times 2^N$ matrix, or, equivalently, to compute the numerical solution of a system of $2N \cdot 2^{2N}$ nonlinear differential equations. This approach becomes almost intractable from a computational point of view if one wants to consider models with a large number of fermionic modes, or, even more, spatial models.

An interesting possibility to enrich the description of the dynamics without increasing the computational complexity of the problem is given by the (H, ρ)–induced dynamics (described in Chapter 5), where the evolution is driven, besides the Hamiltonian operator, by certain conditions, which may, in particular, change periodically the values assigned to the parameters of the Hamiltonian. For reasons that we will explain later, the implementation of the rule–induced dynamics in the case in which the rule is a map in the space of the parameters of H requires the need to follow the evolution of all the entries, according to the standard representation, of the fermionic operators building the model (see Subsection 5.3.1).

We now discuss a different point of view for the problem of deducing the time evolution of the operators that bypasses both the need of directly computing the exponential of the matrix Ut, and the huge amount of computation to obtain a numerical solution of (2.5).

Let us reconsider the system (2.5) but assuming that each component $A_j(t)$ of A is an $2N$–component row vector whose value at $t = 0$ is the j–th element of the canonical orthonormal basis of $\mathbb{R}^{2N}$. As a consequence, (2.5) now represents a linear differential equation for the $2N \times 2N$ matrix A to be solved with the initial condition $A(0) = \mathbb{1}$, and now the solution reads

$$A(t) = \exp(Ut). \tag{2.14}$$

We can compute this solution by numerically solving a system of $4N^2$ linear differential equations, with computational cost $O(N^3)$ that reduces to $O(N^2)$ if the matrix U is sparse (this usually occurs in operatorial models on a lattice (Bagarello and Oliveri, 2013; Bagarello, Cherubini, and Oliveri, 2016; Di Salvo and Oliveri, 2016b)).

The expression $\left(|A_{j,k}(t)|^2 + |A_{j,k+N}(t)|^2\right)$ provides the mean value $n_j(t)$ corresponding to the initial values $n_\ell(0) = \delta_{k\ell}$ $(\ell = 1, \ldots, N)$. Therefore, in correspondence to the general initial values $(n_1, \ldots, n_N)$, the mean values are obtained by means of the formula

$$n_\ell(t) = \sum_{k=1}^{N} \left(|A_{\ell,k}(t)|^2 + |A_{\ell,k+N}(t)|^2\right) n_k. \tag{2.15}$$

We point out that this approach in the case where U is not a sparse matrix does not lead to a relevant lowering of computation complexity. Nevertheless, as it will appear clear in Chapter 5, this strategy provides useful if we consider modified modelizations where the evolution is ruled by some Hamiltonian operator together with the periodic application of a rule that modifies the value of some of the parameters involved in the Hamiltonian on the basis of the current state of the system.

2.7 An application: the dynamics of a closed ecosystem

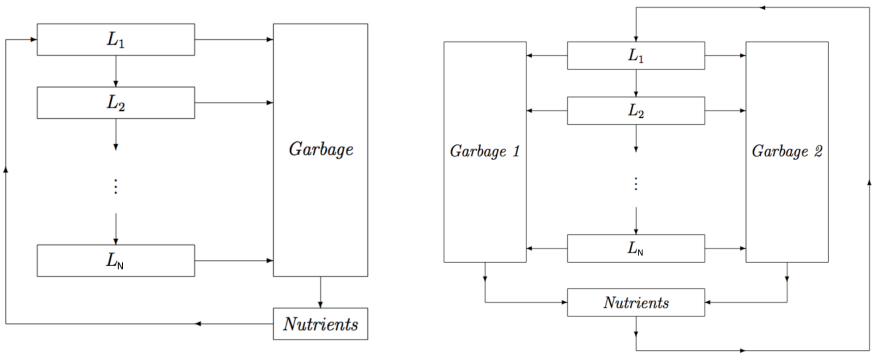

(a) (b)

FIGURE 2.2: A schematic view to the N–compartment models of closed ecosystem with a single kind of garbage, (a), or two different garbages, (b).

In this Section, we deal with the application of operatorial techniques of quantum physics to the very simple theoretical models of closed ecosystem made of N levels of organisms interacting with some external compartments for the nutrients and one or two kinds of garbage (both the situations are schematized in fig. 2.2). The models considered here, which have been described in Bagarello and Oliveri, 2014, are built by adopting raising and lowering fermionic operators (since these mimic quite well densities, or local densities, of species) whose evolution is ruled by a self–adjoint Hamiltonian operator, which can be either quadratic or can contain higher order terms.

Closed ecological systems are ecosystems that do not rely on matter exchange with any part outside the system. They are often used to describe small artificial systems designed and controlled by humans (*e.g.*, agricultural systems and activated sludge plants, or aquaria, or fish ponds). Mathematical models of such systems, besides being useful in describing the real earth's ecosystems, may help in making predictions of how the system may change under certain circumstances. For artificial systems, models may help to optimize their design too.

In a closed ecological system, any waste product produced by one species must be used by at least one other species and converted into nutrients: to do this, an energy supply from outside the system is needed. Therefore, a closed ecological system must contain at least one autotrophic — chemotrophic or phototrophic — organism. Small closed ecosystems may serve as useful models for the analysis of ecosystem properties in general, due to their relatively simple trophic structure and the high intensity of the biotic material and energy transformations. The most widely used mathematical models are compartment models whose time evolution is governed by a system of ordinary differential equations.

The models described below, which are thought of as a first simplified version of what a realistic closed ecological system should be, have a common structure: they are all made by N different internal compartments (the *levels*), interacting with a certain number of external compartments playing the role of the nutrients needed to feed the organisms in level 1 (autotroph organisms), and the garbage produced by all the elements occupying the various levels. Part of the garbage turns into nutrients after some time. The organisms of levels greatest than 1 (heterotroph organisms) are fed by those of the immediately preceding level. In fig. 2.2, a schematic view to the possible interrelations among the various compartments gives a visual clarification of the structure of the models. Each system considered here is closed, meaning with this that the only dynamical degrees of freedom are those of the levels, the garbage(s) and the nutrients: there is nothing else, and only these quantities can interact between them. The simplest model is the one where one has only a level of heterotroph organisms.

Two linear models. The first closed ecosystem which is taken into account is the simplest one, made of N levels of organisms interacting with a compartment for the nutrients and a single compartment for the garbage (see fig. 2.2 (a)). Since we are interested in the densities of these compartments, we adopt fermionic operators.

The dynamics of the ecosystem is described by a Hamiltonian operator containing the essential features one wants to model. For the first linear model the following Hamiltonian is used:

$$\begin{cases} H = H_0 + H_I, & \text{with} \\ H_0 = \displaystyle\sum_{j=0}^{N+1} \omega_j \, a_j^\dagger \, a_j, & \\ H_I = \displaystyle\sum_{j=0}^{N} \lambda_j \left(a_j \, a_{N+1}^\dagger + a_{N+1} a_j^\dagger \right) + \sum_{j=0}^{N-1} \nu_j \left(a_j \, a_{j+1}^\dagger + a_{j+1} a_j^\dagger \right), & \end{cases} \tag{2.16}$$

where a_j ($j = 0, 1, \ldots, N+1$) is a fermionic operator, and ω_j, ν_j and λ_j are real constants. The zero-th mode is related to the nutrients, the $(N+1)$-th mode to the garbage, while all the remaining modes describe the organisms of the various trophic levels. The Hamiltonian (2.16), which is quadratic in the raising and the lowering operators, has the form discussed for the general case in Section 2.2 except for the terms of simultaneous increase or decrease of the densities of the different fermionic modes, that are not considered in this case. The meaning of the various parts forming H is to be intended as previously clarified: the free standard part H_0 is related to the inertia of the different compartments, while H_I describes the effects due to the presence of interaction. In particular, the contributions $\lambda_j \, a_j \, a_{N+1}^\dagger$ ($j = 1, \ldots, N$) describe an increasing of garbage and a simultaneous decreasing of the densities of the levels (metabolic waste and death organisms become garbage), whereas, for $j = 0$, the contribution $\lambda_j a_{N+1} a_j^\dagger$ describes the fact that the garbage is recycled by decomposers and transformed into nutrients. Furthermore, the terms $\nu_j \, a_j \, a_{j+1}^\dagger$ ($j = 1, \ldots, N-1$) express the fact that the nutrients are used by the organisms of level 1, and that the organisms of level j feed those of the level $j+1$.

The equations of motion, deduced by $\dot{X} = i[H, X]$, are:

$$\begin{cases} \dot{a}_0 = i\left(-\omega_0 a_0 + \lambda_0 a_{N+1} + \nu_0 a_1\right), \\ \dot{a}_l = i\left(-\omega_l a_l + \lambda_l a_{N+1} + \nu_{l-1} a_{l-1} + \nu_l a_{l+1}\right), \\ \dot{a}_N = i\left(-\omega_N a_N + \lambda_N a_{N+1} + \nu_{N-1} a_{N-1}\right), \\ \dot{a}_{N+1} = i\left(-\omega_{N+1} a_{N+1} + \sum_{j=0}^{N} \lambda_j a_j\right), \end{cases} \tag{2.17}$$

where $l = 1, \ldots, N-1$. Recall that a_0 and a_{N+1} are not organisms but the nutrients and the garbage, respectively. It is not surprising, therefore, that the related equations of motion differ from the other ones. Also, the equation for a_N looks slightly different from those for a_l, $l = 1, \ldots, N-1$, since the N–th level has a single outgoing arrow, which goes to the garbage.

Since for quadratic Hamiltonians the dynamic equations are linear, the solution can be found analytically, and it is possible to drastically reduce the computational complexity of the problem (Bagarello, 2012). System (2.17) can effectively be rewritten as $\dot{A} = UA$, where

$$A = \begin{pmatrix} a_0 \\ a_1 \\ \vdots \\ \vdots \\ a_N \\ a_{N+1} \end{pmatrix}, \qquad U = \mathrm{i} \begin{pmatrix} -\omega_0 & \nu_0 & 0 & \cdots & \cdots & \lambda_0 \\ \nu_0 & -\omega_1 & \nu_1 & \cdots & \cdots & \lambda_1 \\ \cdots & \cdots & \cdots & \cdots & \cdots & \cdots \\ \cdots & \cdots & \cdots & \cdots & \cdots & \cdots \\ \cdots & \cdots & \cdots & \cdots & -\omega_N & \lambda_N \\ \lambda_0 & \lambda_1 & \lambda_2 & \cdots & \lambda_N & -\omega_{N+1} \end{pmatrix},$$

U being a symmetric matrix, and the solution is $A(t) = V(t)A(0)$, with $V(t) = \exp(Ut)$. Calling $V_{k,l}(t)$ the entries of the matrix $V(t)$, and $n_k(t) = \left\langle \varphi_{\mathbf{n}}, a_k^\dagger(t) a_k(t) \varphi_{\mathbf{n}} \right\rangle$, where $\mathbf{n} = (n_0, n_1, \ldots, n_N, n_{N+1})$ are the initial conditions, it is

$$n_k(t) = \sum_{l=0}^{N+1} |V_{k,l}(t)|^2 \, n_l. \tag{2.18}$$

These are the required densities of the various compartments of the system, $k = 0, 1, \ldots, N+1$, with initial conditions fixed by the vector $\varphi_{\mathbf{n}}$.

The model considered up to now is simply a first approximation of a closed ecosystem. A more realistic approach relies on the idea of modeling the possibility of having garbages of different kind, in particular a soft garbage (mainly coming from autotroph organisms), which easily turns into nutrients, and a hard garbage (mainly coming from heterotroph organisms), which also produces nutrients but only after a much longer period. Therefore, a second linear model obtained by adding a second reservoir to the system is now considered.

The leading idea is that, considering different coupling constants between the garbages G_1 and G_2 with the nutrients, the model is able to reproduce the fact that part of the waste products and dead organisms is turned into nutrients quickly (say, the autotroph detritus), while other parts (say, the heterotroph detritus) are converted into nutrients only after a longer time. The presence of two compartments for the garbages implies the need

to add another degree of freedom and, consequently, an extra fermionic operator a_{N+2}. The other ingredients, as well as their meaning, are those of the previous model. The structure of the ecosystem is depicted in fig. 2.2 (b). The main differences introduced are that two arrows now start from each level L_j, moving towards G_1 and G_2 and that both G_1 and G_2 (with different time scales) contribute to the nutrients.

The Hamiltonian now looks like

$$\begin{cases} H = H_0 + H_I, \qquad \text{with} \\ H_0 = \sum_{j=0}^{N+2} \omega_j \, a_j^\dagger \, a_j, \\ H_I = \sum_{j=0}^{N} \lambda_j^{(1)} \left(a_j \, a_{N+1}^\dagger + a_{N+1} a_j^\dagger \right) + \sum_{j=0}^{N} \lambda_j^{(2)} \left(a_j \, a_{N+2}^\dagger + a_{N+2} a_j^\dagger \right) \\ \quad + \sum_{j=0}^{N-1} \nu_j \left(a_j \, a_{j+1}^\dagger + a_{j+1} a_j^\dagger \right), \end{cases} \tag{2.19}$$

where $\lambda_j^{(1)}$ describes the interaction between the organisms and G_1, while $\lambda_j^{(2)}$ is used to fix the strength of the interaction between the organisms and G_2. The meaning of the various contributions are analogous to those in Section 2.2. The equations of motion extend those in (2.17),

$$\begin{cases} \dot{a}_0 = i \left(-\omega_0 a_0 + \lambda_0^{(1)} a_{N+1} + \lambda_0^{(2)} a_{N+2} + \nu_0 a_1 \right), \\ \dot{a}_l = i \left(-\omega_l a_l + \lambda_l^{(1)} a_{N+1} + \lambda_l^{(2)} a_{N+2} + \nu_{l-1} a_{l-1} + \nu_l a_{l+1} \right), \\ \dot{a}_N = i \left(-\omega_N a_N + \lambda_N^{(1)} a_{N+1} + \lambda_N^{(2)} a_{N+2} + \nu_{N-1} a_{N-1} \right), \\ \dot{a}_{N+1} = i \left(-\omega_{N+1} a_{N+1} + \sum_{l=0}^{N} \lambda_l^{(1)} a_l \right), \\ \dot{a}_{N+2} = i \left(-\omega_{N+2} a_{N+2} + \sum_{l=0}^{N} \lambda_l^{(2)} a_l \right), \end{cases} \tag{2.20}$$

$l = 1, \ldots, N-1$, and can be solved in a similar way. Setting

$$N_{tot} := \sum_{l=0}^{N+2} a_l^\dagger \, a_l, \tag{2.21}$$

it follows that $[H, N_{tot}] = 0$, so that N_{tot} is a conserved quantity: what disappears from the levels appears in the garbages and in the nutrients. Notice that, since no compartment here has an infinite number of degrees of freedom, no damping is allowed within the present scheme.

A nonlinear model. A nonlinear version of the same system schematically described in fig. 2.2 (b) is defined as follows. Instead of considering two different quadratic terms in H to represent the interaction of the various levels with the two garbages, the idea is to consider a single cubic contribution. For instance, $a_j \, a_{N+1}^\dagger \, a_{N+2}^\dagger$ models the fact that the density

of the j–th level decreases while, simultaneously, the densities of both G_1 and G_2 increase: an organism, through its metabolism or dying, produces garbage of two different kinds, soft and hard. The full Hamiltonian of the system is the following one:

$$\begin{cases} H = H_0 + H_I, \qquad \text{with} \\ H_0 = \sum_{j=0}^{N+2} \omega_j \, a_j^\dagger \, a_j, \\ H_I = \sum_{j=1}^{N} \lambda_j \left(a_j \, a_{N+1}^\dagger \, a_{N+2}^\dagger + a_{N+2} \, a_{N+1} \, a_j^\dagger \right) \\ \quad + \sum_{j=1}^{2} \nu^{(j)} \left(a_0 \, a_{N+j}^\dagger + a_{N+j} a_0^\dagger \right) + \sum_{j=0}^{N-1} \nu_j \left(a_j \, a_{j+1}^\dagger + a_{j+1} a_j^\dagger \right). \end{cases} \tag{2.22}$$

The notation is the same as before: for instance, zero refers to the fermionic mode for the nutrients, while $N+1$ and $N+2$ refer to the modes for the two garbages. The physical interpretation of the Hamiltonian is easily found: H_I describes an interaction between the levels and the two garbages (first contribution), the nutrients and the two garbages (second contribution), and a hopping term (third term): the nutrients are used to feed the organisms of level 1, and the organisms of level j feed those of level $j+1$ ($j = 1, \ldots, N-1$). The conjugate term, $a_{j+1} a_j^\dagger$, is needed in order to render the Hamiltonian self–adjoint, since all the parameters are supposed here to be real. The Heisenberg equations of motion look much harder than the previous ones. Indeed, calling $X := \sum_{l=1}^{N} \lambda_l \, a_l$, we have

$$\begin{cases} \dot{a}_0 = i(-\omega_0 a_0 + \nu_0 a_1 + 2X a_0 a_{N+1}^\dagger a_{N+2}^\dagger + 2 a_{N+2} a_{N+1} X^\dagger a_0 \\ \qquad + \nu^{(1)} a_{N+1} + \nu^{(2)} a_{N+2}), \\ \dot{a}_j = i(-\omega_j a_j + \nu_j a_{j+1} + \nu_{j-1} a_{j-1} + 2X a_j a_{N+1}^\dagger a_{N+2}^\dagger \\ \qquad + a_{N+2} a_{N+1} (2X^\dagger a_j - \lambda_j \mathbb{1})), \\ \dot{a}_N = i(-\omega_N a_N + \nu_{N-1} a_{N-1} + 2X a_N a_{N+1}^\dagger a_{N+2}^\dagger \\ \qquad + a_{N+2} a_{N+1} (2X^\dagger a_N - \lambda_N \mathbb{1})), \\ \dot{a}_{N+1} = i(-\omega_{N+1} a_{N+1} + X a_{N+2}^\dagger (\mathbb{1} - 2 a_{N+1}^\dagger a_{N+1}) + \nu^{(1)} a_0), \\ \dot{a}_{N+2} = i(-\omega_{N+2} a_{N+2} + X a_{N+1}^\dagger (2 a_{N+2}^\dagger a_{N+2} - \mathbb{1}) + \nu^{(2)} a_0), \end{cases} \tag{2.23}$$

$l = 1, \ldots, N-1$. It is evident that this system is not closed. In order to close it, the Hermitian conjugates of these equations have to be considered too. This leads to a nonlinear system, whose solution can be found numerically. Notice also that, because of the nonlinearity, the operator N_{tot} introduced in (2.21) does not commute with the Hamiltonian, and it is not evident if any other integral of motion exists at all. Losing the linearity looks like *opening the system* to the outer world: part of N_{tot} could be lost or created, during the time evolution. This could have interesting consequences, since one might expect that a realistic ecosystem is not entirely closed. On a mechanical level, this looks like having a sort of unavoidable friction in the system, friction which can be made small, or even very small, but not zero. However, this feature of a nonlinear model is not enough to produce in the

dynamics of the system a clear damping effect, and in fact this has to be introduced phenomenologically.

A further remark regards the consequences of the fact that the differential equations ruling the dynamics are nonlinear for non quadratic Hamiltonians. The point is that the methods for the numerical solution of the nonlinear equations encounter major obstacles due to the remarkable growth of the size of the problem as the number of the involved compartments increases, even in the case of models not too much complicated. Of course, this results in a strong limitation on the kind of systems that can be analyzed in practice by means of nonlinear models, and, in particular, makes the operatorial approach computationally unmanageable without large supercomputing resources, for instance in the case of spatial models describing nonlinear interactions between compartments on a lattice (Di Salvo and Oliveri, 2016b).

Phenomenological damping. After a sufficiently long time, if the ecosystem is supposed to be unable to recycle completely all the produced garbage, the densities of the species are expected to decrease significantly, and to approach to zero eventually. A damping effect accounting for such a behavior of the system may be added to the model phenomenologically.

Damping can be deduced by adopting a standard Heisenberg-like dynamics, simply by replacing the original real parameters in H with some complex quantities. Moreover, it results that it is not important, or necessary, to replace all the real parameters of H with complex quantities. For instance, all the interaction parameters need not to be changed. In practice, a negative and relatively small imaginary part is added only to ω_{N+1}. The reason for the choice of the sign of the imaginary part is forced owing to the fact that taking a positive imaginary part for ω_{N+1} produces a blow up of the solution. As a matter of fact, this could also be deduced directly from the equations of motion. To illustrate this, consider the differential equation $\dot{x} = -i\omega x$, where $\omega = \omega_r + i\omega_i$, $\omega_r, \omega_i \in \mathbb{R}$, $x \in \mathbb{C}$. It is clear that $x(t) = \exp(-i\omega t)x(0) = \exp(-i\omega_r t)\exp(\omega_i t)x(0)$, which is decaying only if $\omega_i < 0$.

The damping obtained by means of this trick is evident (especially in G_1, at a lower rate in the other compartments) both in the linear cases and in the nonlinear one. In such a way the models are made *efficiently decaying*, that is, by allowing only one parameter of the free Hamiltonian H_0 to be complex (with a negative imaginary part), a damping for the densities of all the compartments is reproduced. This is exactly the expected behavior in a realistic closed ecosystem, with high (but not perfect) efficiency.

3 Fermionic models of bacterial populations

The aim of this Chapter is to describe some features of the long–term survival of bacterial populations by using conveniently defined fermionic models. Adopting the Heisenberg–like dynamics, we investigate an operatorial scheme derived from the general one presented in Section 2.7 for the description of the colony morphology in stressed/aged bacterial populations of *Pseudomonas aeruginosa* constrained in a closed environment (Di Salvo and Oliveri, 2016b). We study the evolution of similar bacterial populations by considering either a linear model or a nonlinear one; some *effective* dissipative mechanisms, phenomenologically introduced, are also considered. In order to better describe the bacterial colony morphology and characteristics of *P. aeruginosa*, the linear model is considered on a square lattice too (Di Salvo and Oliveri, 2016c).

3.1 Preliminaries and general definitions

Bacteria are highly–complex thermodynamic systems, requiring a source of energy for maintaining their structure and functions. Bacterial growth is influenced by several factors: nutrient availability, pH, temperature, oxygen, osmolarity, presence of toxic compounds (heavy metals, hydrogen peroxide, antibiotics, etc.). When one or more environmental conditions become unfavourable, bacteria react in order to survive. Some genera, such as *Bacillus* and *Clostridium*, when under negative stimuli, produce the endospore, *i.e.*, a differentiated cell with no active metabolism, able to survive for an indefinite time in terms of "latent life". When optimal conditions are restored, the endospore germinates, metabolism is activated, and a new vegetative cell appears. Most of bacterial genera, however, are not able to produce

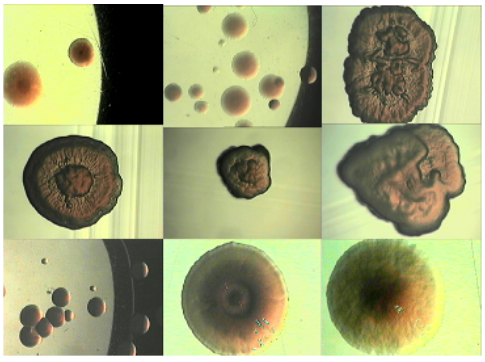

FIGURE 3.1: Variations in the colony morphology of a population of *P. aeruginosa* after 1 month of incubation.

endospores; nonetheless, they can trigger efficient resistance mechanisms. In the last 30 years, the survival of non–sporulating bacteria attracted the attention of many microbiologists with the aim of characterizing the molecular mechanisms underlying the bacterial stress response. In general, when under stress, several phenotypic variations are observed (reduction of cell size, morphological transitions from rod to spherical shape (Reeve, Amy, and Matin, 1984), decrease in metabolic activity (Chapman, Fall, and Atkinson, 1971), synthesis repression of constitutive proteins, synthesis activation of stress–induced proteins required for survival (Givskov, Eberl, and Molin, 1994)); parallely, increased resistance against external challenges (*e.g.*, H_2O_2, antibiotics, disinfecting solutions) and improved ability to persist in their habitat are displayed (Van Overbeek et al., 1995).

Among others, *P. aeruginosa* is an ubiquitous bacterium which can be found in marine and estuarine environments, in soils, etc. It is able to use more than one hundred of chemical compounds as carbon and energy sources, and, due to its wide metabolic versatility, is able to persist for prolonged periods of time without external sources of nutrients. Moreover, it is the ethiological agent of cystic fibrosis, a fatal chronic disease, and can be involved in urinary infections, conjunctivitis, otitis and pneumonia. Actually, it represents an emergence in nosocomial infections, because of its high degree of resistance against several classes of antibiotics and persistence also in disinfecting solutions. For these features, it is important to develop models able to better comprehend, or at least describe, the observed long–term survival of *P. aeruginosa* (Carnazza et al., 2008).

The model here analyzed takes some ideas from the one proposed in Bagarello and Oliveri, 2014, where, as described in detail in Section 2.7, the dynamics of the various trophic levels in a closed ecosystem has been proposed and investigated. In particular, we consider a spatial model in a finite, closed, two–dimensional square region, made by L^2 cells, involving four compartments in each cell, say the nutrients, the bacteria and two different garbages (the first one made up of the dead cells which are reusable as nutrients, and the second one with the waste material not yet reusable or requiring much more time to become recyclable).

By introducing four time dependent operators representing the relevant actors of the system, and a self–adjoint Hamiltonian describing the interactions among them, the dynamics is deduced, as in quantum mechanics, using the *Heisenberg–like* representation.

The formulation here proposed is based on the assumption that the compartments entering the model are described by the fermionic annihilation operators a_j, together with the creation operators $a_j^\dagger$, and their associated number operators $\hat{n}_j = a_j^\dagger a_j$ ($j = 1, \ldots, 4$).

In the following, the mean value of each number operator has the meaning of a measure of the density of the associated compartment. For each compartment, we will have two only possible nontrivial situations: the ground state, corresponding to a very low density, and the excited state, where the density is very high. Hence, increasing the density of the excited state, or decreasing the density of the ground state, annihilates that compartment.

The model is inspired by the considerations made in Section 2.7, and by the observation of the biological dynamics of some bacterial colonies

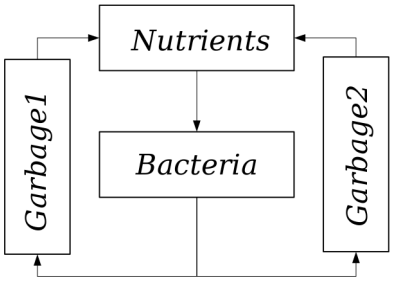

FIGURE 3.2: A schematic view to the 4–compartment model of a bacterial population in a batch culture as a closed ecosystem.

where the living bacteria, as the nutrients disappear, besides reducing their metabolism, use as a source of energy either dead cells or part of their components (Carnazza et al., 2008). This seems to be one of the working mechanisms in the observed long–term survival of bacteria like *P. aeruginosa* constrained in a closed environment (see fig. 3.1). In particular, only a part of the chemical compounds produced by the metabolism is easily reusable; moreover, some of the products of metabolic activity contribute to degrade the environmental conditions, and, therefore, may act as a stress factor.

A diagram of the interactions among the above–mentioned compartments is illustrated in fig. 3.2.

3.2 The linear dynamical model

The dynamics of the 4–compartment linear model of a closed ecosystem is defined by means of the self–adjoint quadratic Hamiltonian operator

$$\begin{cases} H = H_0 + H_I, \qquad \text{with} \\ H_0 = \sum_{j=1}^{4} \omega_j \, a_j^\dagger \, a_j, \\ H_I = \lambda \left(a_1 \, a_2^\dagger + a_2 a_1^\dagger \right) + \sum_{j=1}^{2} \nu_j^{(1)} \left(a_j \, a_3^\dagger + a_3 a_j^\dagger \right) + \sum_{j=1}^{2} \nu_j^{(2)} \left(a_j \, a_4^\dagger + a_4 a_j^\dagger \right), \end{cases} \tag{3.1}$$

where the first mode is related to the nutrients, the second one to the bacteria, and the last two to the garbages. The real constants ω_j appearing in the first standard part H_0 are related to the tendency of each degree of freedom to stay constant in time; the larger their values, the smaller the amplitudes of the oscillations of the related densities (Bagarello, 2012), whereas the real parameters λ, $\nu_j^{(1)}$ and $\nu_j^{(2)}$ in H_I are concerned to the interactions among the bacteria, the nutrients, and the garbages. In more detail, the term $\lambda a_1 a_2^\dagger$ describes an increasing of bacteria and a simultaneous decreasing of the density of nutrients, and the terms involving the parameters $\nu_j^{(1)}$ ($\nu_j^{(2)}$, respectively) describe the analogous interactions between the nutrients (the bacteria, respectively) and the two garbages: the garbages are recycled and

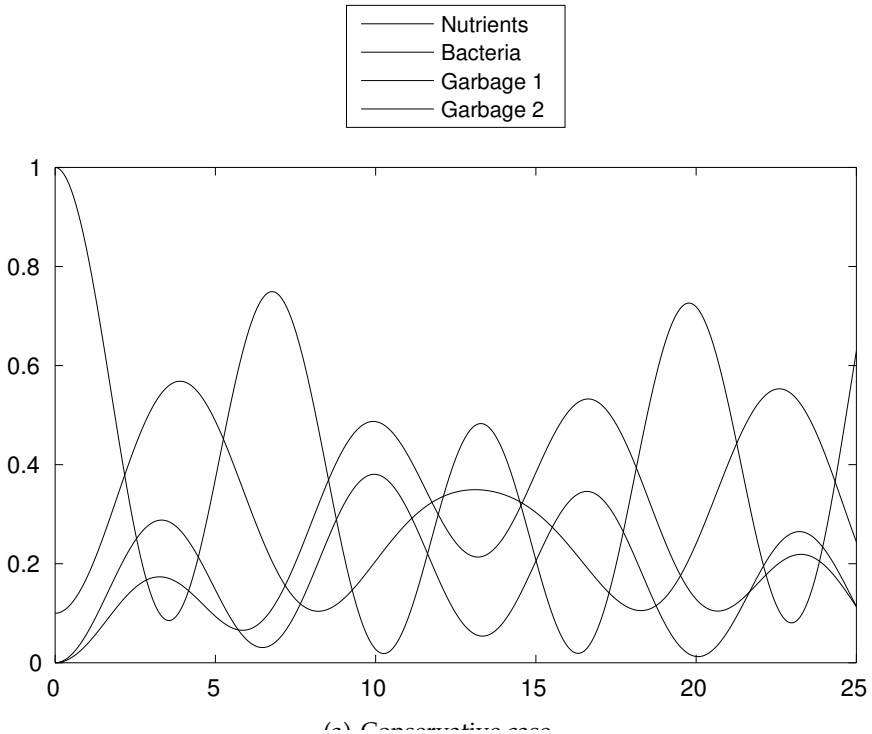

(a) Conservative case

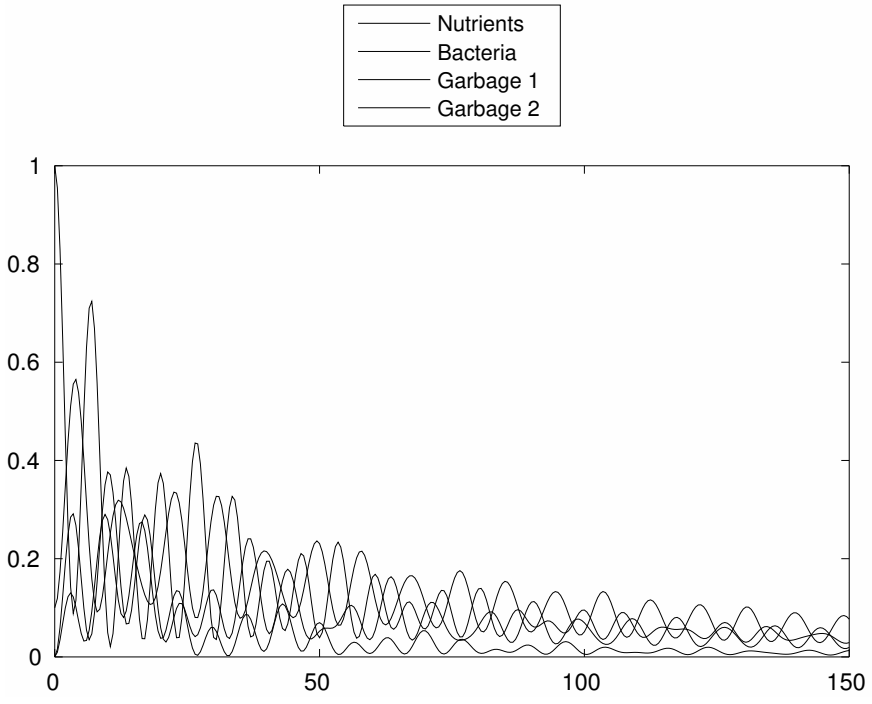

(b) Non–conservative case

FIGURE 3.3: Linear model: time evolution of the densities of the compartments both in the case of a purely conservative system, (a), and in the case in which a dissipative effect is phenomenologically introduced, (b).

transformed into nutrients, and the bacteria, because of their metabolic activity, produce garbage. Of course, the adjoint contributions are added in order to make the Hamiltonian self–adjoint.

The linear dynamic equations deduced for each observable of the system in accordance with the Heisenberg scheme read

$$\begin{cases} \dot{a}_1 = i\left(-\omega_1 a_1 + \lambda a_2 + \nu_1^{(1)} a_3 + \nu_1^{(2)} a_4\right), \\ \dot{a}_2 = i\left(-\omega_2 a_2 + \lambda a_1 + \nu_2^{(1)} a_3 + \nu_2^{(2)} a_4\right), \\ \dot{a}_3 = i\left(-\omega_3 a_3 + \nu_1^{(1)} a_1 + \nu_2^{(1)} a_2\right), \\ \dot{a}_4 = i\left(-\omega_4 a_4 + \nu_1^{(2)} a_1 + \nu_2^{(2)} a_2\right). \end{cases} \tag{3.2}$$

As widely discussed in Bagarello, Cherubini, and Oliveri (2016) and Bagarello and Oliveri (2014), the operatorial approach is suited to cover also dissipative systems, in order to deal with more realistic situations in which one or more compartments can experience stress; in this case, a simple and efficient strategy consisting in giving up the self–adjointness of H (allowing the use of complex–valued parameters) can be adopted. We simply include this effect in the model by adding to some of the inertia parameters a small negative imaginary part. Fig. 3.3(a) shows, as expected, the quasi–periodic oscillating behavior obtained in the conservative linear case; on the contrary, when a small stress factor is introduced only for the second kind of garbage, the amplitude of the oscillations of the densities of all the compartments decays as time increases. Under the assumption that the ecosystem is unable to completely recycle all the produced garbage, as expected, after a sufficiently long time, a significant decay of the densities of all the levels in the model arises, as depicted in fig. 3.3(b). The simulations shown in fig. 3.3 are produced by selecting the following values of the parameters: $\omega_1 = 0.3$, $\omega_2 = 0.2$, $\omega_3 = 0.4$, $\omega_4 = 0.5$ ($\omega_4 = 0.5 - 0.05\mathrm{i}$ in case of stress effects, respectively), $\lambda = 0.3$, $\nu_1^{(1)} = 0.25$, $\nu_1^{(2)} = 0.2$, $\nu_2^{(1)} = 0.15$, $\nu_2^{(2)} = 0.1$, and the following initial densities for the four compartments: $n_1 = 1$, $n_2 = 0.1$, $n_3 = 0$, and $n_4 = 0$.

Since the fermionic operators a_j, $j = 1, \ldots, 4$, are represented by matrices of order 16, the system (3.2) consists of 1024 differential equations to be solved with a suitable set of initial conditions, say:

$$a_1(0) = \begin{pmatrix} 0 & 1 & 0 & 0 & 0 & 0 & 0 & 0 & 0 & 0 & 0 & 0 & 0 & 0 & 0 & 0 \\ 0 & 0 & 0 & 0 & 0 & 0 & 0 & 0 & 0 & 0 & 0 & 0 & 0 & 0 & 0 & 0 \\ 0 & 0 & 0 & 1 & 0 & 0 & 0 & 0 & 0 & 0 & 0 & 0 & 0 & 0 & 0 & 0 \\ 0 & 0 & 0 & 0 & 0 & 0 & 0 & 0 & 0 & 0 & 0 & 0 & 0 & 0 & 0 & 0 \\ 0 & 0 & 0 & 0 & 0 & 1 & 0 & 0 & 0 & 0 & 0 & 0 & 0 & 0 & 0 & 0 \\ 0 & 0 & 0 & 0 & 0 & 0 & 0 & 0 & 0 & 0 & 0 & 0 & 0 & 0 & 0 & 0 \\ 0 & 0 & 0 & 0 & 0 & 0 & 0 & 1 & 0 & 0 & 0 & 0 & 0 & 0 & 0 & 0 \\ 0 & 0 & 0 & 0 & 0 & 0 & 0 & 0 & 0 & 0 & 0 & 0 & 0 & 0 & 0 & 0 \\ 0 & 0 & 0 & 0 & 0 & 0 & 0 & 0 & 0 & 1 & 0 & 0 & 0 & 0 & 0 & 0 \\ 0 & 0 & 0 & 0 & 0 & 0 & 0 & 0 & 0 & 0 & 0 & 0 & 0 & 0 & 0 & 0 \\ 0 & 0 & 0 & 0 & 0 & 0 & 0 & 0 & 0 & 0 & 0 & 1 & 0 & 0 & 0 & 0 \\ 0 & 0 & 0 & 0 & 0 & 0 & 0 & 0 & 0 & 0 & 0 & 0 & 0 & 0 & 0 & 0 \\ 0 & 0 & 0 & 0 & 0 & 0 & 0 & 0 & 0 & 0 & 0 & 0 & 0 & 1 & 0 & 0 \\ 0 & 0 & 0 & 0 & 0 & 0 & 0 & 0 & 0 & 0 & 0 & 0 & 0 & 0 & 0 & 0 \\ 0 & 0 & 0 & 0 & 0 & 0 & 0 & 0 & 0 & 0 & 0 & 0 & 0 & 0 & 0 & 1 \\ 0 & 0 & 0 & 0 & 0 & 0 & 0 & 0 & 0 & 0 & 0 & 0 & 0 & 0 & 0 & 0 \end{pmatrix},$$

$$a_2(0) = \begin{pmatrix}
0&0&1&0&0&0&0&0&0&0&0&0&0&0&0&0\\
0&0&0&-1&0&0&0&0&0&0&0&0&0&0&0&0\\
0&0&0&0&0&0&0&0&0&0&0&0&0&0&0&0\\
0&0&0&0&0&0&0&0&0&0&0&0&0&0&0&0\\
0&0&0&0&0&0&1&0&0&0&0&0&0&0&0&0\\
0&0&0&0&0&0&0&-1&0&0&0&0&0&0&0&0\\
0&0&0&0&0&0&0&0&0&0&0&0&0&0&0&0\\
0&0&0&0&0&0&0&0&0&0&0&0&0&0&0&0\\
0&0&0&0&0&0&0&0&0&0&1&0&0&0&0&0\\
0&0&0&0&0&0&0&0&0&0&0&-1&0&0&0&0\\
0&0&0&0&0&0&0&0&0&0&0&0&0&0&0&0\\
0&0&0&0&0&0&0&0&0&0&0&0&0&0&0&0\\
0&0&0&0&0&0&0&0&0&0&0&0&0&0&1&0\\
0&0&0&0&0&0&0&0&0&0&0&0&0&0&0&-1\\
0&0&0&0&0&0&0&0&0&0&0&0&0&0&0&0\\
0&0&0&0&0&0&0&0&0&0&0&0&0&0&0&0
\end{pmatrix},$$

$$a_3(0) = \begin{pmatrix}
0&0&0&0&1&0&0&0&0&0&0&0&0&0&0&0\\
0&0&0&0&0&-1&0&0&0&0&0&0&0&0&0&0\\
0&0&0&0&0&0&-1&0&0&0&0&0&0&0&0&0\\
0&0&0&0&0&0&0&1&0&0&0&0&0&0&0&0\\
0&0&0&0&0&0&0&0&0&0&0&0&0&0&0&0\\
0&0&0&0&0&0&0&0&0&0&0&0&0&0&0&0\\
0&0&0&0&0&0&0&0&0&0&0&0&0&0&0&0\\
0&0&0&0&0&0&0&0&0&0&0&0&1&0&0&0\\
0&0&0&0&0&0&0&0&0&0&0&0&0&-1&0&0\\
0&0&0&0&0&0&0&0&0&0&0&0&0&0&-1&0\\
0&0&0&0&0&0&0&0&0&0&0&0&0&0&0&1\\
0&0&0&0&0&0&0&0&0&0&0&0&0&0&0&0\\
0&0&0&0&0&0&0&0&0&0&0&0&0&0&0&0\\
0&0&0&0&0&0&0&0&0&0&0&0&0&0&0&0
\end{pmatrix},$$

$$a_4(0) = \begin{pmatrix}
0&0&0&0&0&0&0&0&1&0&0&0&0&0&0&0\\
0&0&0&0&0&0&0&0&0&-1&0&0&0&0&0&0\\
0&0&0&0&0&0&0&0&0&0&-1&0&0&0&0&0\\
0&0&0&0&0&0&0&0&0&0&0&1&0&0&0&0\\
0&0&0&0&0&0&0&0&0&0&0&0&-1&0&0&0\\
0&0&0&0&0&0&0&0&0&0&0&0&0&1&0&0\\
0&0&0&0&0&0&0&0&0&0&0&0&0&0&1&0\\
0&0&0&0&0&0&0&0&0&0&0&0&0&0&0&-1\\
0&0&0&0&0&0&0&0&0&0&0&0&0&0&0&0\\
0&0&0&0&0&0&0&0&0&0&0&0&0&0&0&0\\
0&0&0&0&0&0&0&0&0&0&0&0&0&0&0&0\\
0&0&0&0&0&0&0&0&0&0&0&0&0&0&0&0\\
0&0&0&0&0&0&0&0&0&0&0&0&0&0&0&0\\
0&0&0&0&0&0&0&0&0&0&0&0&0&0&0&0\\
0&0&0&0&0&0&0&0&0&0&0&0&0&0&0&0
\end{pmatrix}.$$

Once we know the entries of the matrices $a_j(t)$ $(j = 1, \ldots, 4)$ at time t, the local densities of the compartments are simply obtained by computing the sum of the squared absolute values of the elements in a row of matrices $a_j(t)$. The 16 rows produce the solutions for all the possible initial states, which are the combinations with repetition of 4 elements chosen in the set $\{0, 1\}$. Due to the linearity of the problem, actually we do not need to know the solutions for all possible initial data; it suffices to have the *fundamental*

solutions corresponding to the initial data $(n_1 = \delta_{i1}, n_2 = \delta_{i2}, n_3 = \delta_{i3}, n_4 = \delta_{i4})$, $i = 1, \ldots, 4$, where δ_{ij} is the Kronecker symbol, to get, through a linear combination, the solutions for all initial states. Also, we are not forced to use initial densities in the set $\{0, 1\}$, but rather we may choose the initial data for all compartments in the whole interval $[0, 1]$.

Furthermore, as widely discussed in Section 2.1, we know that the linearity of equations (3.2) implies the explicit knowledge of their exact solution, so that the computational cost may be drastically reduced by writing (3.2) in compact form as

$$\dot{A}(t) = UA(t), \tag{3.3}$$

with

$$A(t) = \begin{pmatrix} a_1(t) \\ a_2(t) \\ a_3(t) \\ a_4(t) \end{pmatrix}, \quad U = i \begin{pmatrix} -\omega_1 & \lambda & \nu_1^{(1)} & \nu_1^{(2)} \\ \lambda & -\omega_2 & \nu_2^{(1)} & \nu_2^{(2)} \\ \nu_1^{(1)} & \nu_2^{(1)} & -\omega_3 & 0 \\ \nu_1^{(2)} & \nu_2^{(2)} & 0 & -\omega_4 \end{pmatrix}, \tag{3.4}$$

and by expressing the solution as

$$A(t) = V(t)A(0), \tag{3.5}$$

with $V(t) = \exp(Ut)$. So, if we call $V_{jk}(t)$ the generic time–dependent matrix entry of $V(t)$, and n_ℓ the initial density of the ℓ–th compartment of the system, we find that

$$n_j(t) = \sum_{\ell=1}^{4} |V_{j\ell}(t)|^2 \; n_\ell \tag{3.6}$$

at the cost of computing the exponential of the 4×4 matrix Ut.

3.3 The nonlinear dynamical model

In this Section, we consider nonlinear effects in the model by including in the Hamiltonian of the system contributions of order greater than two. In particular, we introduce in the interaction part H_I of the Hamiltonian operator cubic terms, say

$$\begin{cases} H = H_0 + H_I, \qquad \text{with} \\ H_0 = \displaystyle\sum_{j=1}^{4} \omega_j \, a_j^\dagger \, a_j, \\ H_I = \lambda \left(a_2 \, a_3^\dagger \, a_4^\dagger + a_4 \, a_3 \, a_2^\dagger \right) + \mu \left(a_1 \, a_2^\dagger + a_2 a_1^\dagger \right) \\ \qquad + \displaystyle\sum_{k=3}^{4} \nu^{(k)} \left(a_1 \, a_k^\dagger + a_k a_1^\dagger \right); \end{cases} \tag{3.7}$$

the real parameters ω_j $(j = 1, \ldots, 4)$, λ, μ, $\nu^{(k)}$ $(k = 3, 4)$ are to be interpreted once again as being related to the inertia and the strength of the interactions among the compartments (Bagarello and Oliveri, 2014). The

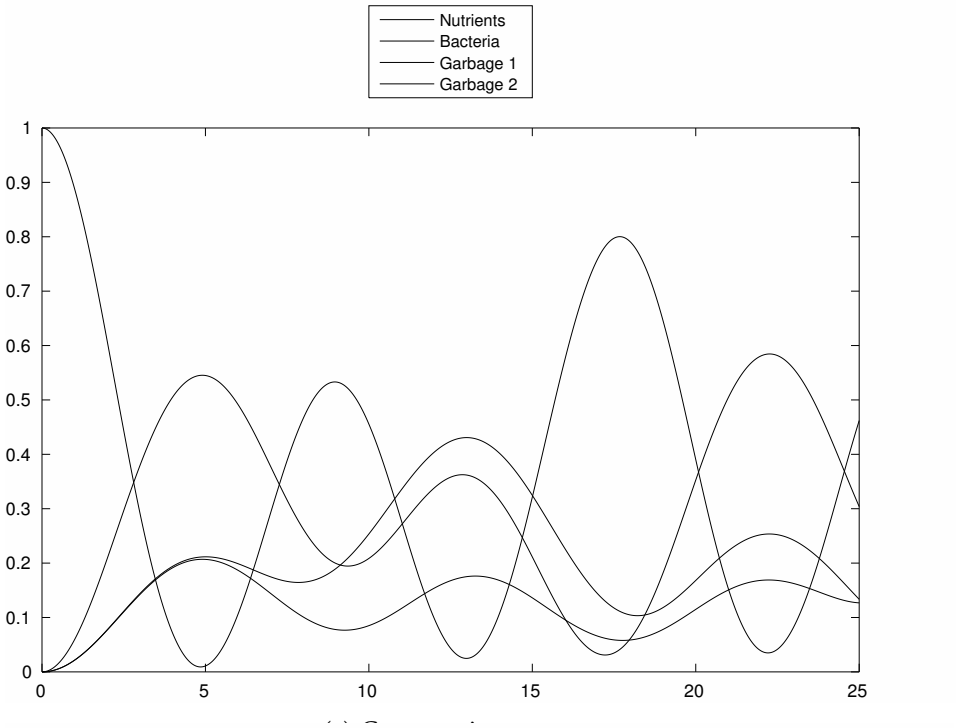

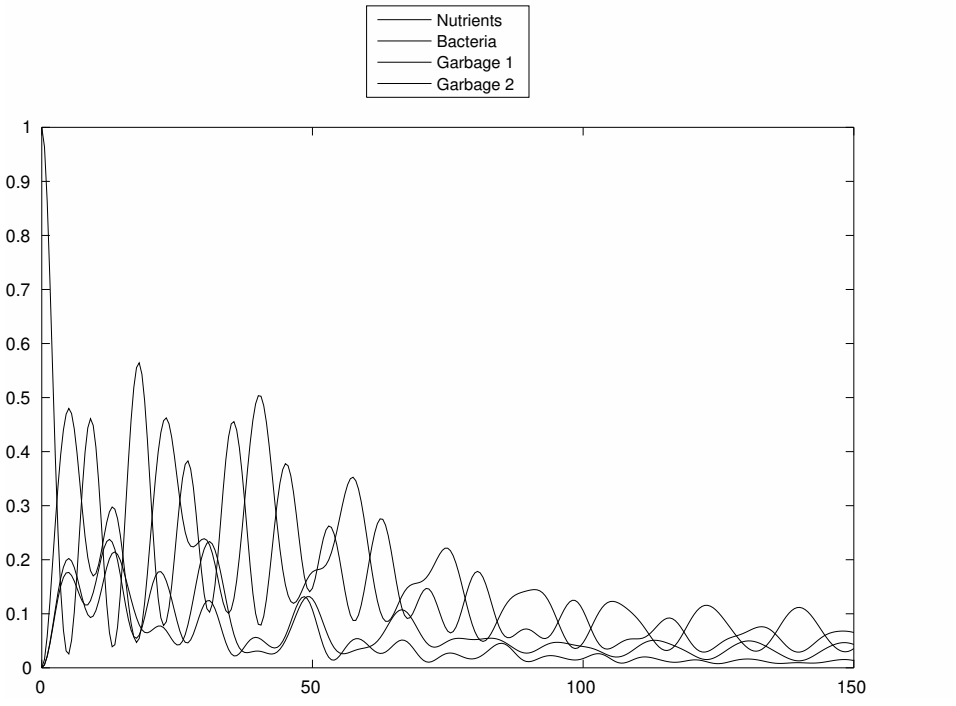

(b) Non–conservative case

FIGURE 3.4: Nonlinear model: time evolution of the densities of the compartments both in the case of a purely conservative system, (a), and in the case in which a dissipative effect is phenomenologically introduced, (b).

differential equations derived from (3.7) take now the following more complicated form:

$$\begin{cases} \dot{a}_1 = i\left(-\omega_1 a_1 + \mu a_2 + 2\lambda a_2 a_1 a_3^\dagger a_4^\dagger + 2\lambda a_4 a_3 a_2^\dagger a_1 + \nu^{(3)} a_3 + \nu^{(4)} a_4\right), \\ \dot{a}_2 = i\left(-\omega_2 a_2 + \mu a_1 + \lambda a_4 a_3 (2a_2^\dagger a_2 - \mathbb{I})\right), \\ \dot{a}_3 = i\left(-\omega_3 a_3 + \lambda a_2 a_4^\dagger (\mathbb{I} - 2a_3^\dagger a_3) + \nu^{(3)} a_1\right), \\ \dot{a}_4 = i\left(-\omega_4 a_4 + \lambda a_2 a_3^\dagger (2a_4^\dagger a_4 - \mathbb{I}) + \nu^{(4)} a_1\right). \end{cases} \tag{3.8}$$

Since the size reduction of the computational cost to compute the evolution of the system produced by the equation (3.8) is not possible for the obtained nonlinear dynamic equations, the solutions of the system (3.8) are to be found numerically, which means that we are forced to numerically solve 1024 nonlinear differential equations, or, according to the formula (1.11), to compute at each time t the exponential of the matrix Ht, which is a $2^4 \times 2^4$ matrix, together with its inverse (conjugate).

Similarly to what was already discussed for the linear model, also in the nonlinear case the effect of some stress factor acting on the system can be taken into account by considering some of the inertia coefficients having a small negative imaginary part. The evolutions drawn in fig. 3.4, obtained using the values of the parameters $\omega_1 = 0.3$, $\omega_2 = 0.2$, $\omega_3 = 0.4$, $\omega_4 = 0.5$ ($\omega_4 = 0.5 - 0.05\mathrm{i}$ in case of stress effects, respectively), $\lambda = 0.1$, $\mu = 0.25$, $\nu_3 = 0.15$, $\nu_4 = 0.15$, and the initial densities for the four compartments $(n_1 = 1, n_2 = n_3 = n_4 = 0)$, show once again irregular oscillatory behaviors for the nonlinear conservative model compared to the decay of the system due to the lack of recycling of part of the garbage produced by the ecosystem in the non–conservative case.

The introduction of terms of order greater than two in H from one hand entails the lack of an exact solution of the Heisenberg equations of motion (so that no less than 1024 nonlinear differential equations need to be solved in order to deduce the evolution of the system) and, on the other one, forces, according to quantum theory, the initial densities of the compartments to be flattened to the integer values 0 (completely empty) or 1 (completely filled). The major limitation of the employment of a nonlinear fermionic model still resides in the fact that numerically solve a system of nonlinear differential equations obviously becomes a huge task as the number of compartments of the system grows, requiring very high computational costs. Moreover, the size of the problem almost immediately exceeds the limit of manageability with ordinary computing resources in the event that the operatorial approach is intended to be generalized to the case of a nonlinear spatial model. This is the reason why for the description of the colony morphology of bacterial populations of *P. aeruginosa* on a lattice we will just consider linear models.

3.4 Spatial linear model on a 2–D square lattice

In this Section, we investigate spatial effects for both *homogeneous* and *non-homogeneous* regions with respect to the parameters of the model represented through regular $L \times L$ square grids (see fig. 3.5). Assume that the

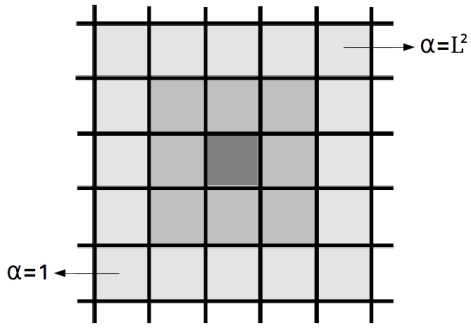

FIGURE 3.5: A two–dimensional square lattice of size L^2.

j–th actor $a_{j,\alpha}$, $j = 1, \ldots, 4$, $\alpha = 1, \ldots, L^2$, of our model occupies the cell α and interacts *locally* with the other actors. Suppose also that some of the actors can diffuse along the L^2 cells of a two–dimensional square lattice. Again, the operators $a_{j,\alpha}$ and their adjoints $a^\dagger_{j,\alpha}$, $j = 1, \ldots, 4$, are chosen as fermionic operators, while the mechanisms of the spatial dynamics of the ecosystem are modeled by the following quadratic Hamiltonian, in which a new part, H_M, related to the migration or diffusion of some of the actors, has been introduced,

$$H = H_0 + H_I + H_M, \tag{3.9}$$

with

$$\begin{cases} H_0 = \displaystyle\sum_{\alpha=1}^{L^2} \sum_{j=1}^{4} \omega_{j,\alpha}\, a^\dagger_{j,\alpha}\, a_{j,\alpha}, \\ H_I = \displaystyle\sum_{\alpha=1}^{L^2} \left(\sum_{j=2}^{4} \lambda_{j,\alpha}(a_{1,\alpha}\, a^\dagger_{j,\alpha} + a_{j,\alpha}\, a^\dagger_{1,\alpha}) \right. \\ \qquad + \displaystyle\sum_{\gamma \in \Gamma_\alpha} \lambda_{2,\gamma}(a_{1,\alpha}\, a^\dagger_{2,\gamma} + a_{2,\gamma}\, a^\dagger_{1,\alpha}) \\ \qquad \left. + \displaystyle\sum_{k=3}^{4} \nu_{k,\alpha}(a_{2,\alpha}\, a^\dagger_{k,\alpha} + a_{k,\alpha}\, a^\dagger_{2,\alpha}) \right), \\ H_M = \displaystyle\sum_{j=1}^{4} \sum_{\alpha=1}^{L^2} \mu_{j,\alpha} \sum_{\beta=1}^{L^2} p_{\alpha,\beta}\, (a_{j,\alpha}\, a^\dagger_{j,\beta} + a_{j,\beta}\, a^\dagger_{j,\alpha}). \end{cases} \tag{3.10}$$

The parameters $\mu_{j,\alpha}$ and $p_{\alpha,\beta}$ are meant as described in Section 2.2; since here we consider only the diffusion of bacteria, it is $\mu_{j,\gamma} = 0$ for $j \neq 2$. The

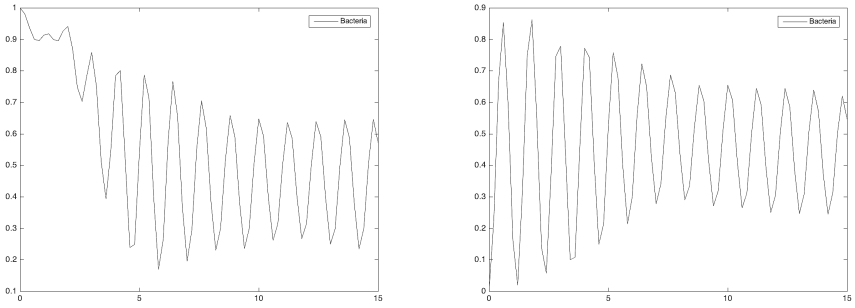

(a) Central cell (b) Peripheral cell

FIGURE 3.6: Homogeneous model: time evolutions of the density of the bacteria on the central cell, (a), and on a peripheral cell, (b), of the lattice.

equations of motion look like

$$\begin{cases} \dot{a}_{1,\alpha} = i\Big(-\omega_{1,\alpha} a_{1,\alpha} + \lambda_{2,\alpha}\, a_{2,\alpha} + \displaystyle\sum_{\gamma\in\Gamma_\alpha} \lambda_{2,\gamma}\, a_{2,\gamma} \\ \qquad + \lambda_{3,\alpha}\, a_{3,\alpha} + \lambda_{4,\alpha}\, a_{4,\alpha}\Big), \\ \dot{a}_{2,\alpha} = i\Big(-\omega_{2,\alpha} a_{2,\alpha} + \lambda_{2,\alpha}\, a_{1,\alpha} + \displaystyle\sum_{\gamma\in\Gamma_\alpha} \lambda_{2,\gamma}\, a_{1,\gamma} \\ \qquad + \nu_{3,\alpha}\, a_{3,\alpha} + \nu_{4,\alpha}\, a_{4,\alpha} + \displaystyle\sum_{\beta=1}^{L^2} (\mu_{2,\alpha} + \mu_{2,\beta})\, p_{\alpha,\beta}\, a_{2,\beta}\Big), \\ \dot{a}_{3,\alpha} = i\Big(-\omega_{3,\alpha} a_{3,\alpha} + \lambda_{3,\alpha}\, a_{1,\alpha} + \nu_{3,\alpha}\, a_{2,\alpha}\Big), \\ \dot{a}_{4,\alpha} = i\Big(-\omega_{4,\alpha} a_{4,\alpha} + \lambda_{4,\alpha}\, a_{1,\alpha} + \nu_{4,\alpha}\, a_{2,\alpha}\Big), \end{cases} \tag{3.11}$$

$\alpha = 1, \ldots, L^2$. Also in this case, in which no term of order greater than two appears in H, the system (3.11) is linear so that the dynamics can be easily deduced by computing the exponential of a $4L^2 \times 4L^2$ square matrix.

Numerical simulations. All the simulations shown below have been obtained by choosing a square lattice of side $L = 27$. We consider either the case where the parameters entering the model are equal all over the lattice, *i.e.*, they are cell–independent, or the one where they are cell–dependent. In both situations we also investigate the noise effects induced in the dynamics by assuming that in about 5% of the cells randomly chosen the values of inertia parameters are significantly higher, and the interaction parameters among the compartments are significantly smaller than those in the remaining cells; in some sense, these are *holes* where the rates of change of all compartments are significantly unfavoured. As far as the initial conditions are concerned, in all cases we choose the nutrients uniformly distributed (with maximum local density) on the entire region, bacteria present with maximum local density only in a restricted central area (made by 9 cells), and the two garbages uniformly empty.

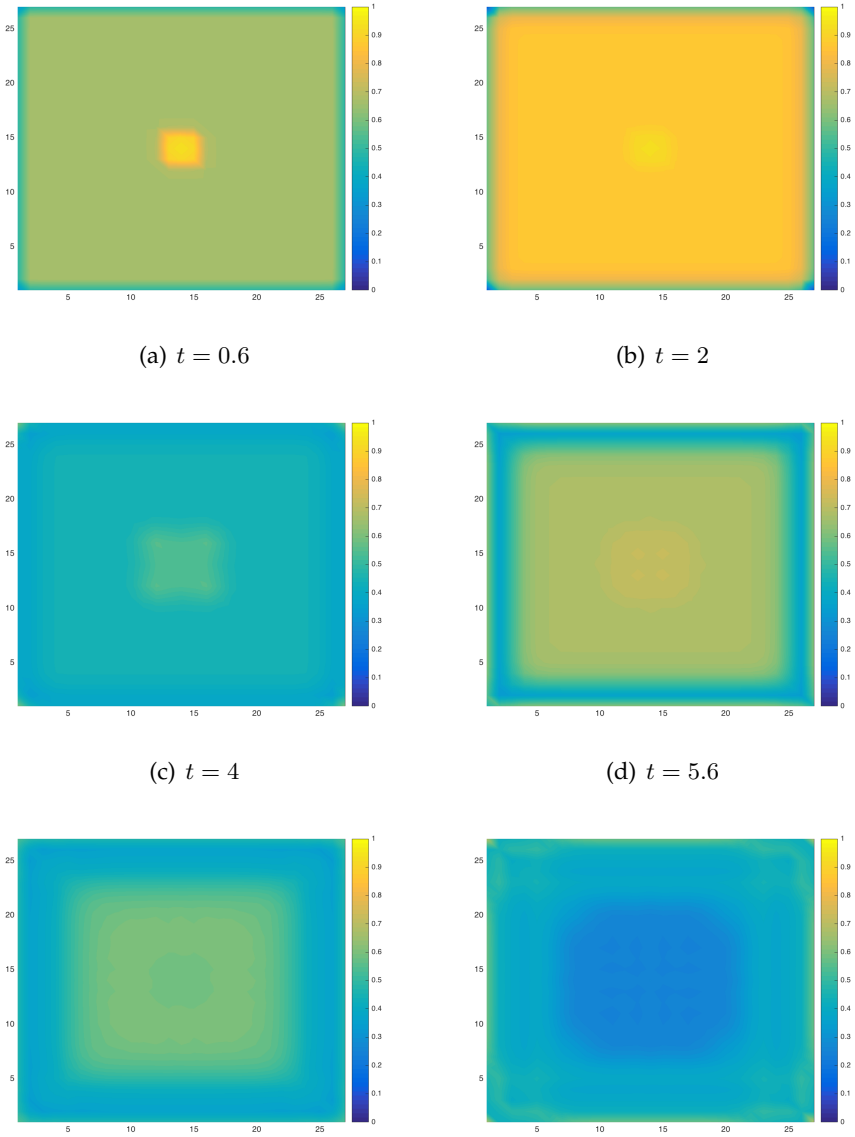

(a) $t = 0.6$ (b) $t = 2$

(c) $t = 4$ (d) $t = 5.6$

(e) $t = 9.2$ (f) $t = 12$

FIGURE 3.7: Homogeneous linear model with diffusion on the lattice. The frames show the density of the bacteria on the region at times 0.6, 2, 4, 5.6, 9.2, 12, respectively.

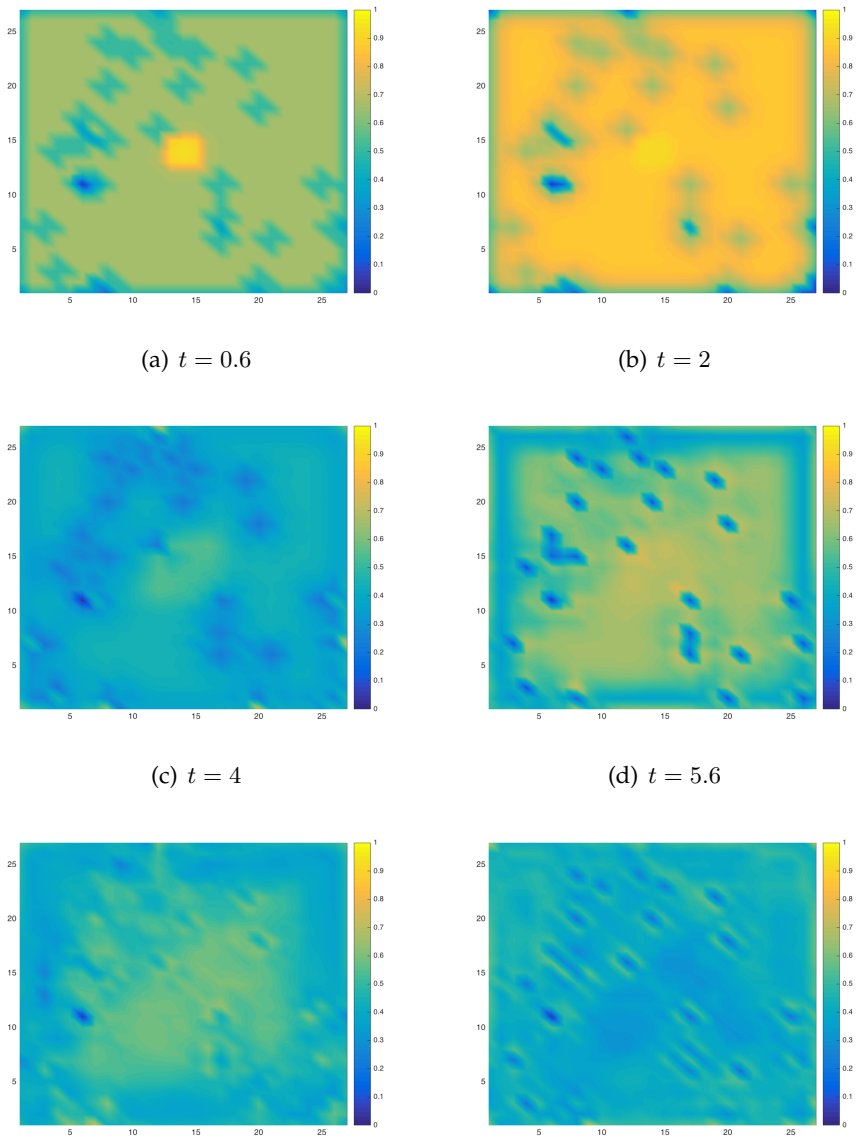

(a) $t = 0.6$ (b) $t = 2$

(c) $t = 4$ (d) $t = 5.6$

(e) $t = 9.2$ (f) $t = 12$

FIGURE 3.8: Homogeneous linear model with spatial diffusion on a lattice where some cells have parameters lowering the rates of change of all compartments. The frames show the density of the bacteria over the region at times 0.6, 2, 4, 5.6, 9.2, 12, respectively.

Assume that all the parameters have the same value in all the cells. More precisely, we choose $\omega_{1,\alpha} = 0.3$, $\omega_{2,\alpha} = 0.1$, $\omega_{3,\alpha} = 0.3$, $\omega_{4,\alpha} = 0.4$, $\lambda_{2,\alpha} = 0.5$, $\lambda_{3,\alpha} = 0.4$, $\lambda_{4,\alpha} = 0.2$, $\nu_{3,\alpha} = 0.6$, $\nu_{4,\alpha} = 0.4$ ($\alpha = 1, \ldots, L^2$).

In fig. 3.6 the densities of bacteria in the central cell and in a peripheral one are plotted. In both situations, the density exhibits an oscillatory behavior even if the amplitudes of the oscillations decrease in time. This is not the effect of a dissipative mechanism (the model is conservative) but it is due to the diffusion along the lattice (as can be seen in fig. 3.7), whereupon for large times the distribution of bacteria tends to be uniform all over the lattice.

In the case in which the lattice has some *holes*, even if the density of bacteria, as t increases, tends to become homogeneous all over the lattice, it is possible to observe (see fig. 3.8) some anisotropy.

We now move on to consider nonhomogeneous regions, which results in using cell–dependent parameters. A reasonable choice in the sense of the biological interpretation of the model (peripheral cells are uncrowded areas with available resources) is to assume that the inertia parameters decrease moving away from the center, while the other parameters moderately grow. To be more precise, we used the following values of the parameters: $\omega_{1,\alpha} = 0.3/(1 + d_\alpha)$, $\omega_{2,\alpha} = 0.1/(1 + d_\alpha)$, $\omega_{3,\alpha} = 0.3/(1 + d_\alpha)$, $\omega_{4,\alpha} = 0.4/(1 + d_\alpha)$, $\lambda_{1,\alpha} = 0.5d_\alpha$, $\lambda_{1,\alpha} = 0.4d_\alpha$, $\lambda_{1,\alpha} = 0.2d_\alpha$, $\nu_{2,\alpha} = 0.6d_\alpha$, $\nu_{3,\alpha} = 0.4d_\alpha$, provided that $d_\alpha \neq 0$, where d_α is the Euclidean distance (normalized to 1) between the cell α and the central one; moreover, $\mu_{2,\alpha} = 0.3$ ($\alpha = 1, \ldots, L^2$), whereas $p_{\alpha,\beta} = p_{\beta,\alpha}$ is vanishing for $\alpha = \beta$, equal to $1/d^2(\alpha, \beta)$, where $d(\alpha, \beta)$ is the Euclidean distance between the adjacent cells α and β, and zero elsewhere; for adjacent cells, $d(\alpha, \beta)$ is 1 or $\sqrt{2}$, depending on the relative positions. Thus, bacteria can only move from a cell to a neighboring one.

Also in this case, it is observed (see fig. 3.9) that the diffusion has the effect of distributing the bacteria all over the lattice, the only difference being that some symmetric patterns appear; this is not surprising since the parameters entering the model change radially. The noise effects due to the holes that disturb the symmetrical patterns are evident in fig. 3.10.

In all the considered settings, the densities of the bacteria in the cells of the lattice tend to become homogeneous, even if some patterns arise when the parameters are cell–dependent. The figs. 3.11 and 3.12 clearly show this phenomenon, even though with some differences related to the fact that, in the case of dynamics with cell–dependent parameters, the density homogenization process occurs more rapidly. Due to its mathematical structure, in each cell the model produces a periodic or at most quasiperiodic behavior, and the main frequencies of oscillations of the densities in the various cells are the same when the parameters do not vary along the cells; therefore, some kind of synchronization may arise, and the oscillations are maintained for longer times until they are killed by the diffusion processes.

The mean values of the densities of all the compartments exhibit an oscillating behavior with decreasing amplitudes, and tend to stabilize, whereas their variances over the entire region tend to become smaller and smaller. The situation is not so much different for the mean values and the variances of the densities of the various compartments that can be observed (see figs. 3.13 and 3.14) in the *holes* of the lattice.

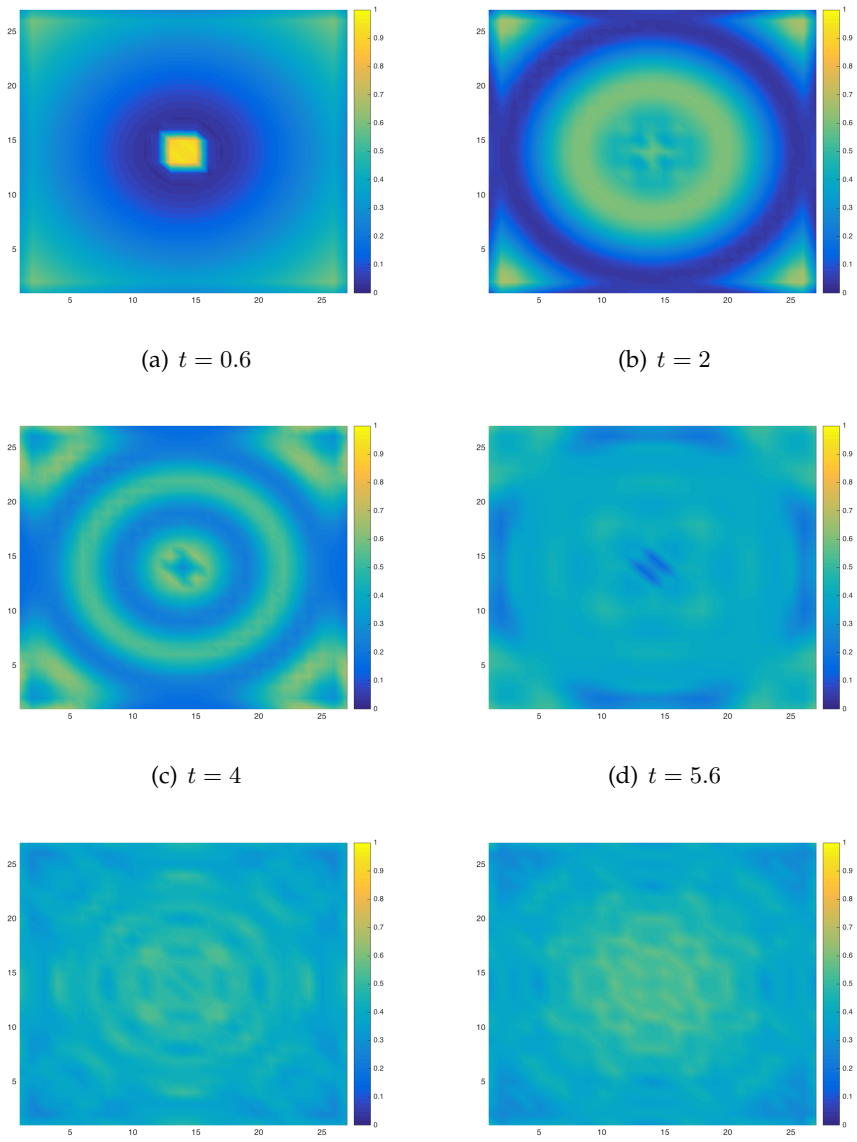

(a) $t = 0.6$ (b) $t = 2$

(c) $t = 4$ (d) $t = 5.6$

(e) $t = 9.2$ (f) $t = 12$

FIGURE 3.9: Nonhomogeneous linear model with diffusion on the lattice and interactions between nutrients and bacteria even between adjacent cells. The frames show the densities of the bacteria over the region at times 0.6, 2, 4, 5.6, 9.2, 12, respectively.

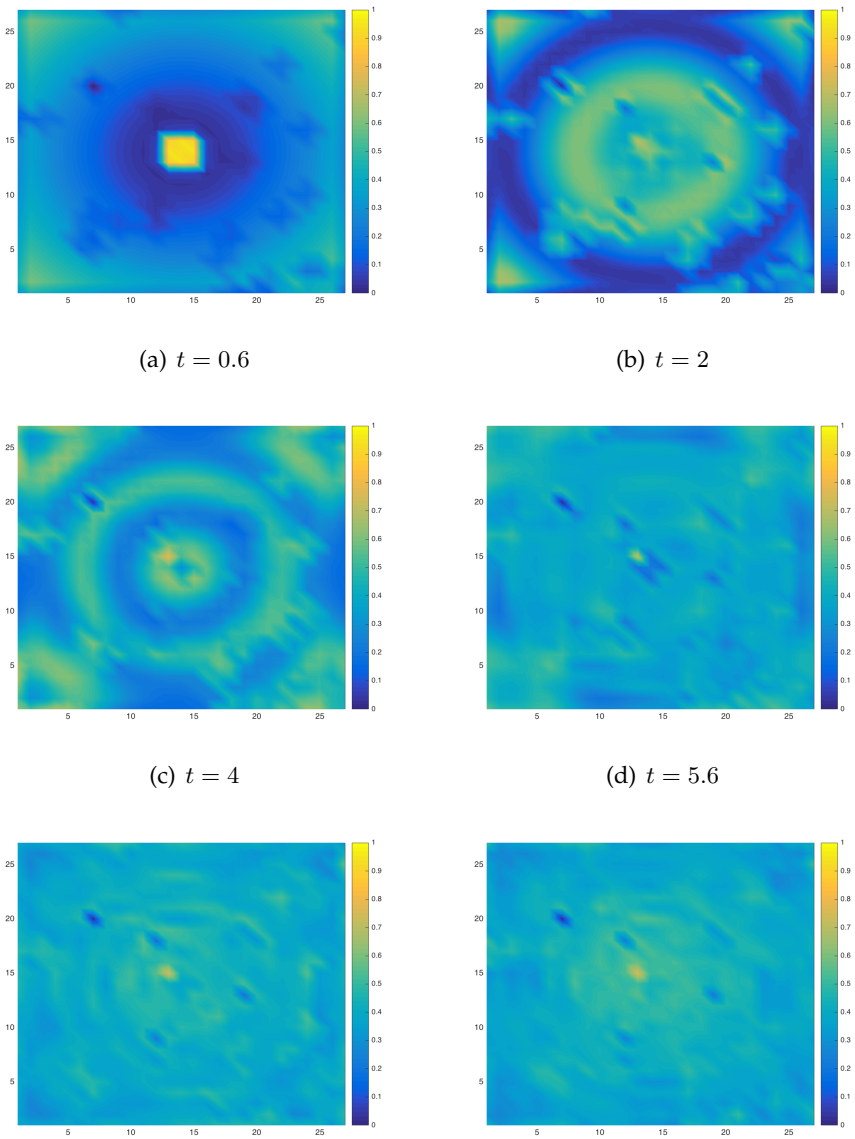

(a) $t = 0.6$ (b) $t = 2$

(c) $t = 4$ (d) $t = 5.6$

(e) $t = 9.2$ (f) $t = 12$

FIGURE 3.10: Nonhomogeneous linear model with diffusion on a lattice where some cells have parameters lowering the rates of change of all compartments. The frames show the densities of the bacteria over the region at times 0.6, 2, 4, 5.6, 9.2, 12, respectively.

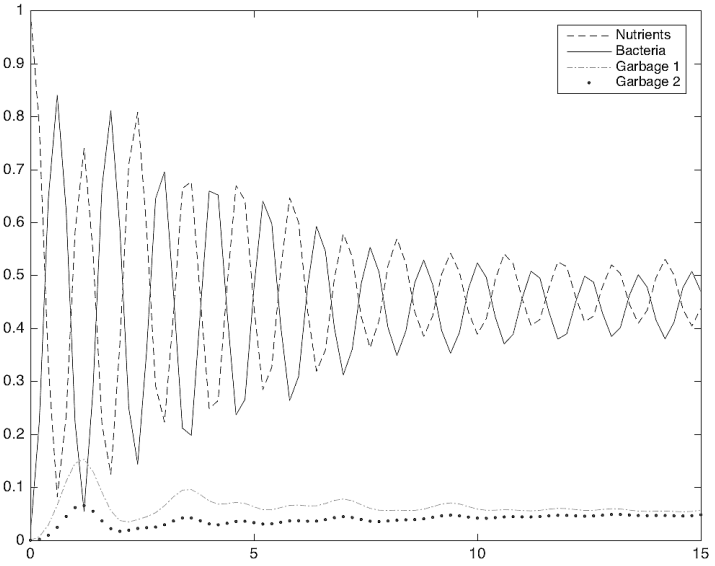

(a) Homogeneous model

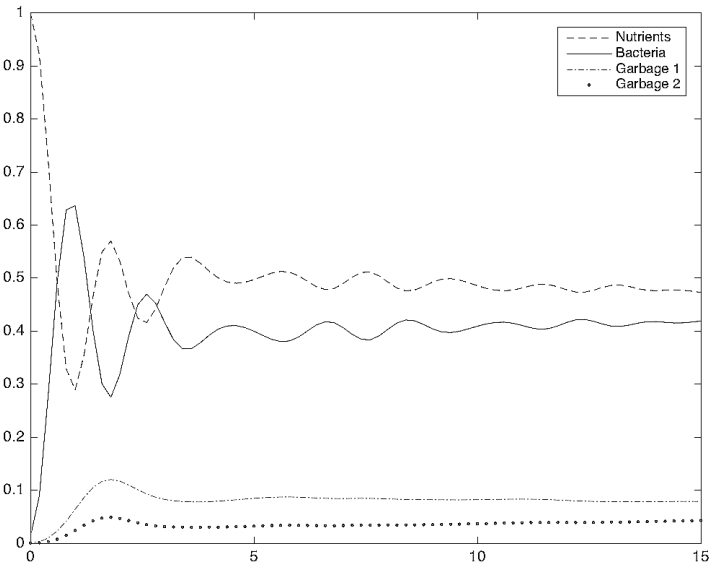

(b) Nonhomogeneous model

FIGURE 3.11: Time evolution of the mean of the densities of all the compartments over the entire region for the proposed models, respectively.

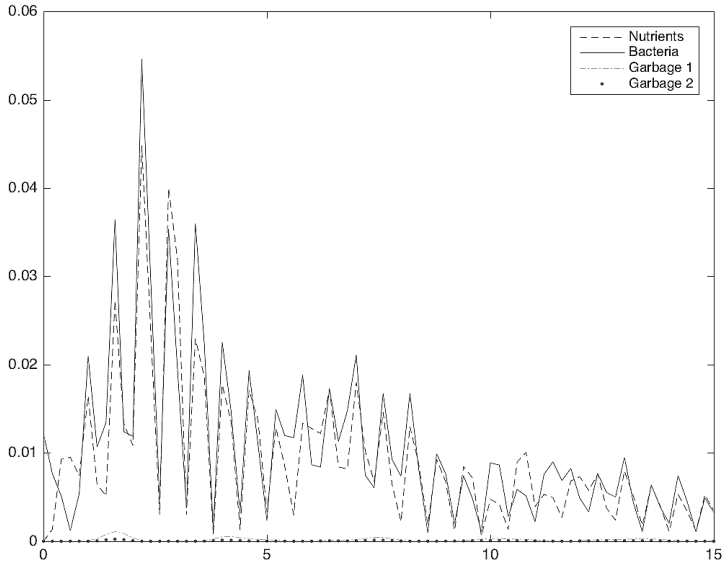

(a) Homogeneous model

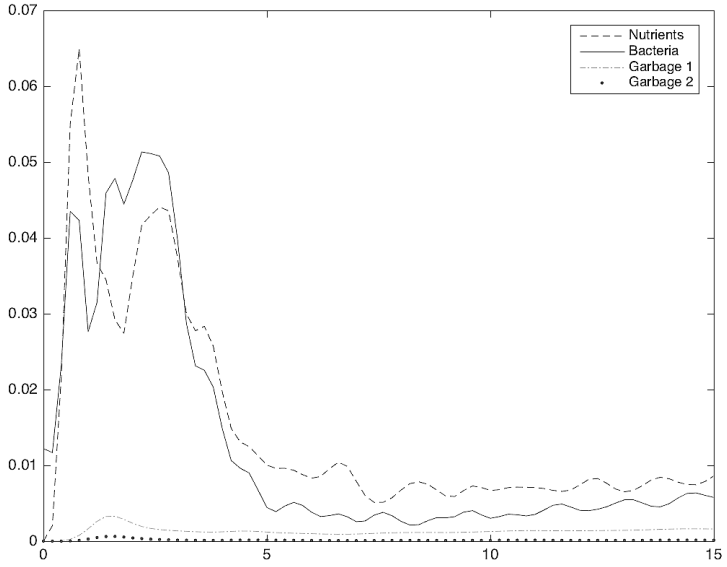

(b) Nonhomogeneous model

FIGURE 3.12: Time evolution of the variances of the densities of all the compartments over the entire region for the proposed models, respectively.

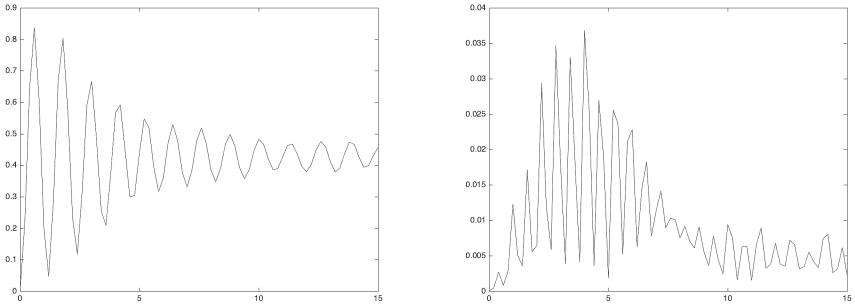

(a) Mean (b) Variance

FIGURE 3.13: Homogeneous model: time evolution of the mean value, (a), and the variance, (b), of the density of the bacteria on the holes.

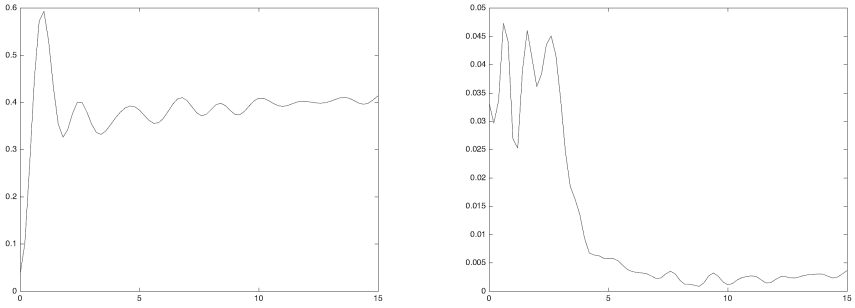

(a) Mean (b) Variance

FIGURE 3.14: Nonhomogeneous model: time evolution of the mean value, (a), and the variance, (b), of the density of the bacteria on the holes.

4 Political dynamics affected by turncoats

This Chapter deals with an operatorial theoretical model based on raising and lowering fermionic operators for the description of the dynamics of political parties affected by turncoat–like behaviors (Di Salvo and Oliveri, 2016a).

By observing the political landscape in place in Italy over the last years, appropriate macro–groups have been identified on the basis of the behavior of politicians in terms of disloyal attitude as well as openness towards accepting chameleons from other parties. The various subgroups of the political parties are described by fermionic operators and their evolution is ruled by a quadratic Hamiltonian operator in the Heisenberg representation.

4.1 Historical overview and motivation

Figuratively speaking, a *turncoat* is a person who changes allegiance from one loyalty or ideal to another one in an unscrupulous way to get maximum benefits and personal gain. The reason of the shift is frequently self–interest, and the faithless attitude in politics may come upon in a manifest way through an open and declared change of side, or in a veiled and subtle way in terms of incoherence in the voting secrecy (just think of those politicians from fragmented sub–factions who declare a certain ideology, but secretly give electoral support to a different cause).

For this political behavior, after the election speech of Agostino De Pretis on October 8th, 1882 (Sabbatucci, 1998) (*"If anyone wants to come into our ranks, if he wants to accept my modest program, if he wants to transform himself and become progressive, how can I reject him?"*), the term "transformism" has been coined: it refers to the method of making a flexible centrist coalition of government which isolated the extremes of the left and the right in Italian politics. On that occasion, Agostino De Pretis, the Italian Prime Minister in 1883, who was a member of the Constitutional Left party, moved to the right and reshuffled his government to include Marco Minghetti's Conservatives. The aim was to ensure a stable government that would avoid weakening the institutions by extreme shifts to the left or right. Depretis felt that a secure government could ensure calm in Italy. However, transformism fed into the debates that the Italian parliamentary system was weak and actually failing; it ultimately became associated with corruption and created a huge gap between 'Legal' (parliamentary and political) Italy, and 'Real' Italy where the politicians became increasingly isolated. With respect to the contemporary political landscape in place in Italy, a look at the behavior of politicians from various parties during the first thirty months of the XVII Italian Legislature reveals a high level of disloyal attitude and

openness towards accepting chameleons from other political groups in both the two houses of the Italian Parliament. Such kind of ugly phenomenon, which manifests in more than 300 changes of side during the period of 30 months under observation, emerges from the official data available in the Institutional web pages of the Chamber of Deputies[1] and the Senate of the Republic[2].

The general political elections of 2013 in Italy produced a result where three parties took more or less the same number of votes: the *Democratic Party* (PD), the *People of Freedom* (PdL) and the *Five Star Movement* (M5S). PD was really the first party in that election, but due to the different electoral rules for the two houses of Parliament, it got the majority of parliament seats only in the Chamber of Deputies. Then, the formation of a stable government required the formation of alliances between different parties. This determined a fragmentation of some political parties, the birth of new parliamentary groups, and a paroxysmal occurrence of changes of side of groups of parliament members.

Recently, operatorial techniques have been efficiently used to build dynamical models for the description of alliances in politics (Bagarello, 2015; Bagarello and Haven, 2016; Bagarello, 2016; Bagarello and Gargano, 2016b).

In the following, we define a simplified model, based on fermionic operators, whose dynamics is ruled by a time–independent self–adjoint Hamiltonian operator, that, despite its simplicity, is suitable to describe the dynamics of political party groups affected by turncoat–like behaviors of part of their members.

4.2 The linear conservative model

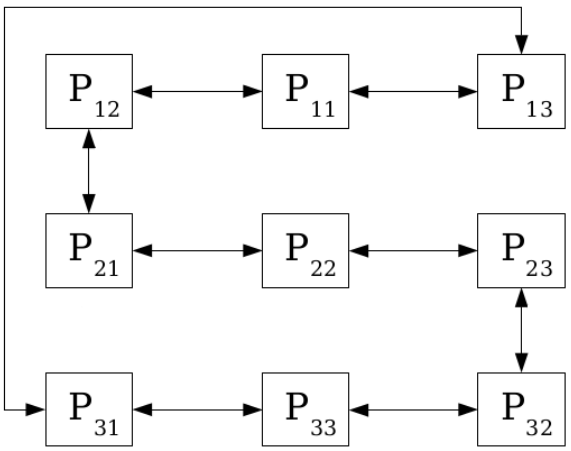

FIGURE 4.1: A schematic view to the simplified model of three parties.

[1] http://www.camera.it.
[2] http://www.camera.it.

The model presented in this Section (schematized in fig. 4.1) consists of nine groups of politicians P_{ij} $(i,j = 1,2,3)$, represented by fermionic operators, identified on the basis of three possible attitudes in relation to three main factions f_i $(i = 1,2,3)$ expressing three possible simplified political strategies. More precisely, at the initial time, f_1 represents a moderate faction, characterized by scarce openness to exchanges with other parties (external flows) and small propensity to transformations in ideological direction (internal flows), f_2 represents a fickle faction, highly permissive towards transitions between political groups and other ideologies sympathizers in the party itself, while f_3 stands for an extremist faction, intransigent against contaminations and influences from others. The operators used to describe the evolution of the system are to be intended in accordance with the key under which the compartments whose subscript indices are equal refer to those politicians who are loyal to the corresponding faction, while those having different subscript indices are related to the politicians who belong to a faction (the one associated with the first index) but are drawn towards another faction (the one associated with the second index).

As expected, the formulation adopted in the following is based on the assumptions stated in Section 1.2. In particular, the states of the system are vectors in the 2^9–dimensional Hilbert space $\mathcal{H}$ constructed as the linear span of the vectors

$$\varphi_{p_{11},p_{12},\ldots,p_{33}} := (P_{11}^\dagger)^{p_{11}}(P_{12}^\dagger)^{p_{12}}\cdots(P_{33}^\dagger)^{p_{33}}\varphi_{\mathbf{0}},$$

which give an orthonormal set of eigenstates of the number operators $\widehat{p}_{ij} = P_{ij}^\dagger P_{ij}$ $(i,j = 1,2,3)$, with $p_{ij} \in \{0,1\}$, $\varphi_{\mathbf{0}}$ being the vacuum state.

Once defined a vector state $\varphi_{p_{11},p_{12},\ldots,p_{33}}$ representing the initial configuration of the system, we compute the mean values

$$p_{ij}(t) = \langle \varphi_{p_{11},p_{12},\ldots,p_{33}},\, \widehat{p}_{ij}(t)\varphi_{p_{11},p_{12},\ldots,p_{33}}\rangle, \qquad i,j = 1,2,3, \tag{4.1}$$

and such averages are interpreted as the densities of the various compartments, *i.e.*, the consistencies of the various political groups of the model.

The dynamics of the political system is assumed to be governed by the self–adjoint time independent Hamiltonian operator

$$\begin{cases} H = H_0 + H_I, \qquad \text{with} \\ H_0 = \displaystyle\sum_{i,j=1}^{3} \omega_{ij}\, P_{ij}^\dagger\, P_{ij}, \\ H_I = \displaystyle\sum_{\substack{i,j=1 \\ j\neq i}}^{3} \lambda_i^{(j)} \left(P_{ii}P_{ij}^\dagger + P_{ij}P_{ii}^\dagger\right) + \sum_{\substack{i,j=1 \\ j\neq i}}^{3} \mu_{ij}\left(P_{ij}P_{ji}^\dagger + P_{ji}P_{ij}^\dagger\right), \end{cases} \tag{4.2}$$

embedding the main effects deriving from the interactions among the nine actors of the system. As usual, the real parameters ω_{ij} appearing in the first standard part H_0 express a measure of the inertia of the various compartments (see Section 2.2). Moreover, the real parameters $\lambda_i^{(j)}$ in H_I are used to describe the internal flows that occur within each faction, namely the minor ideological positions representing in some sense early warning of disloyalty, whereas the parameters μ_{ij} are related to the external flows

stemming from the real changes of side. Of course, requiring $\lambda_i^{(j)} = \mu_{ij} = 0$ $(i, j = 1, 2, 3)$, meaning that the components of the system do not interact, implies that the densities of the compartments of the system stay constant in time.

In the Heisenberg picture, the compartments of the model evolve in time according to the differential equations

$$\begin{cases} \dot{P}_{11} = i\left(-\omega_{11}P_{11} + \lambda_1^{(2)}P_{12} + \lambda_1^{(3)}P_{13}\right), \\ \dot{P}_{12} = i\left(-\omega_{12}P_{12} + \lambda_1^{(2)}P_{11} + \mu_{12}P_{21}\right), \\ \dot{P}_{13} = i\left(-\omega_{13}P_{13} + \lambda_1^{(3)}P_{11} + \mu_{13}P_{31}\right), \\ \dot{P}_{21} = i\left(-\omega_{21}P_{21} + \lambda_2^{(1)}P_{22} + \mu_{12}P_{12}\right), \\ \dot{P}_{22} = i\left(-\omega_{22}P_{22} + \lambda_2^{(1)}P_{21} + \lambda_2^{(3)}P_{23}\right), \\ \dot{P}_{23} = i\left(-\omega_{23}P_{23} + \lambda_2^{(3)}P_{22} + \mu_{23}P_{32}\right), \\ \dot{P}_{31} = i\left(-\omega_{31}P_{31} + \lambda_3^{(1)}P_{33} + \mu_{13}P_{13}\right), \\ \dot{P}_{32} = i\left(-\omega_{32}P_{32} + \lambda_3^{(2)}P_{33} + \mu_{23}P_{23}\right), \\ \dot{P}_{33} = i\left(-\omega_{33}P_{33} + \lambda_3^{(1)}P_{31} + \lambda_3^{(2)}P_{32}\right). \end{cases} \tag{4.3}$$

Once the system (4.3) has been solved, the evolution of the consistency of the faction f_i $(i = 1, 2, 3)$ is easily obtained, say $f_i(t) = \sum_{j=1}^{3} p_{ij}(t)$.

Since the total densities of political parties commute with H, that is the quantity $f_1+f_2+f_3$ is a constant of motion, the system is suitable to describe the density conservation of all the parliamentary seats.

To simplify the notation, let us set $Q_{3(i-1)+j} = P_{ij}$; introducing the column vector $Q = (Q_1, Q_2, Q_3, Q_4, Q_5, Q_6, Q_7, Q_8, Q_9)^T$ and the matrix

$$U = i \begin{pmatrix} -\omega_{11} & \lambda_1^{(2)} & \lambda_1^{(3)} & 0 & 0 & 0 & 0 & 0 & 0 \\ \lambda_1^{(2)} & -\omega_{12} & 0 & \mu_{12} & 0 & 0 & 0 & 0 & 0 \\ \lambda_1^{(3)} & 0 & -\omega_{13} & 0 & 0 & 0 & \mu_{13} & 0 & 0 \\ 0 & \mu_{12} & 0 & -\omega_{21} & \lambda_2^{(1)} & 0 & 0 & 0 & 0 \\ 0 & 0 & 0 & \lambda_2^{(1)} & -\omega_{22} & \lambda_2^{(3)} & 0 & 0 & 0 \\ 0 & 0 & 0 & 0 & \lambda_2^{(3)} & -\omega_{23} & 0 & \mu_{23} & 0 \\ 0 & 0 & \mu_{13} & 0 & 0 & 0 & -\omega_{31} & 0 & \lambda_3^{(1)} \\ 0 & 0 & 0 & 0 & 0 & \mu_{23} & 0 & -\omega_{32} & \lambda_3^{(2)} \\ 0 & 0 & 0 & 0 & 0 & 0 & \lambda_3^{(1)} & \lambda_3^{(2)} & -\omega_{33} \end{pmatrix},$$

the system of linear differential equations (4.3) can be expressed in matrix form as

$$\dot{Q} = UQ, \tag{4.4}$$

whereupon the solution may be clearly expressed as

$$Q(t) = V(t)Q(0), \tag{4.5}$$

with $V(t) = \exp(Ut)$. If we denote with $q_{3(i-1)+j} = p_{ij}$ the initial density of the generic compartment of the system, we have

$$q_{3(i-1)+j}(t) = p_{ij}(t) = \sum_{k=1}^{9} \left| V_{3(i-1)+j,k}(t) \right|^2 q_k,$$

i.e., the local densities at time t of the various compartments of the model, which are the physical observables that we consider relevant for a complete description of the political environment, are exactly obtained in a simple manner at the cost of computing the exponential of the 9×9 matrix Ut.

Of course, the interactions that we can model with a quadratic Hamiltonian imply that the dynamics we can deduce is at most quasi–periodic. In particular, if we choose, as a start, the following values of the parameters (consistent with the ideological and attitudinal interpretation of the parties given above),

$$\begin{array}{lll} \omega_{11} = 0.7, & \omega_{12} = 0.5, & \omega_{13} = 0.4, \\ \omega_{22} = 0.3, & \omega_{21} = 0.2, & \omega_{23} = 0.1, \\ \omega_{33} = 1, & \omega_{31} = 0.8, & \omega_{32} = 0.7, \\ \lambda_1^{(2)} = 0.5, & \lambda_1^{(3)} = 0.4, & \\ \lambda_2^{(1)} = 0.6, & \lambda_2^{(3)} = 0.7, & \\ \lambda_3^{(1)} = 0.4, & \lambda_3^{(2)} = 0.3, & \\ \mu_{12} = 0.1, & \mu_{13} = 0.2, & \mu_{23} = 0.3, \end{array} \tag{4.6}$$

and we suppose that the initial consistencies of the three factions under consideration are essentially the same, we get the evolution of the densities f_1, f_2 and f_3 shown in fig. 4.2. In this case, we can observe (at least in the considered time interval) how the model reproduces a dynamics according to which the moderate party's approach proves successful, the fickle party results scarcely promoted, whereas the strategy of the extremist party reveals to be losing.

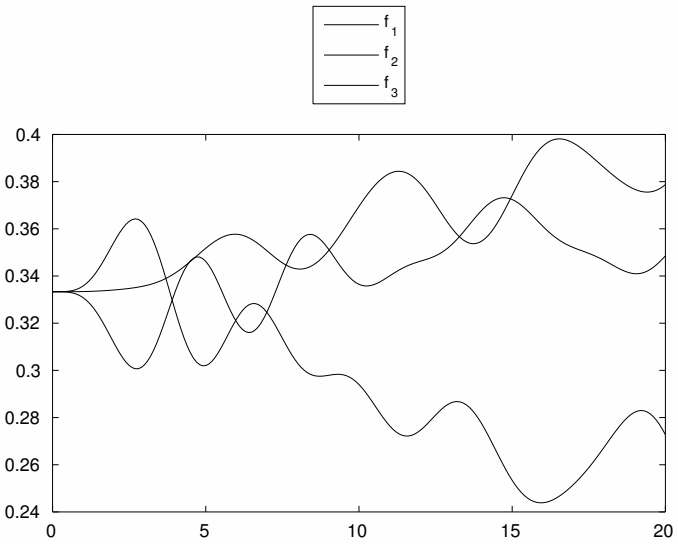

FIGURE 4.2: Linear model: evolution of the densities of politicians in each faction up to $t = 20$, with the parameters fixed as in (4.6).

4.3 Different behaviors depending on the cross interactions

In this Section, we perform a study of the parameters entering the model. Different assignments of values to the set of parameters involved in the model, apart from the initial datum, of course play a significant role in the evolution of the system giving rise to different dynamical behaviors.

The fact that each compartment of the considered model is associated to a specific political fringe (identified on the basis of the declared ideology and openness towards the other political groups) implicitly forces the assignment of the values to the inertia parameters ω_{ij} related to the tendency of each group to keep the same amount of members during the evolution as well as to the internal interaction parameters $\lambda_i^{(j)}$, which need to be inversely proportional to the loyalty to the corresponding faction. Moreover, it is clear from (4.2) that, in order to make the Hamiltonian operator self–adjoint, the parameters μ_{ij} definitely influences both the operator P_{ij} and the operator P_{ji}. We may therefore think to minimize the exchanges between only two of the main factions.

For the above reasons, in the numerical simulations shown in fig. 4.3, we fix the parameters ω_{ij} and $\lambda_i^{(j)}$ entering the model as follows:

$$\begin{array}{lll} \omega_{11} = 0.7, & \omega_{12} = 0.6, & \omega_{13} = 0.5, \\ \omega_{22} = 0.4, & \omega_{21} = 0.3, & \omega_{23} = 0.2, \\ \omega_{33} = 1, & \omega_{31} = 0.8, & \omega_{32} = 0.9, \\ \lambda_1^{(2)} = 0.25, & \lambda_1^{(3)} = 0.3, & \\ \lambda_2^{(1)} = 0.7, & \lambda_2^{(3)} = 0.75, & \\ \lambda_3^{(1)} = 0.15, & \lambda_3^{(2)} = 0.1. & \end{array} \tag{4.7}$$

This means that the third party is intended as the most severe and unwilling to betray or become contaminated with the other parties, the first one is slightly more prone towards the other ideologies, while the second one is characterized by a markedly open and fickle attitude. Of course, the parameters ω_{ii}, $i = 1, 2, 3$, are slightly larger than the parameters ω_{ij} ($i \neq j$) referring to the disloyal fringes of the i–th party. In fig. 4.3, different behaviors related to the choice of the values for the cross interaction parameters $\mu_{i,j}$ (determining the transitions among factions), as indicated in the figure, are shown: the first two subframes illustrate the alternative time evolutions of the system corresponding to the cases in which either f_1 or f_3 is characterized by a marked attitude towards switching side compared to the other groups (having very few interactions instead), while the last subframe refers to a situation of uniform disloyal tendency.

The influence of the parameters entering the model on the dynamics of the political system is the ingredient of the approach aimed at enriching the standard Heisenberg description of the dynamics of this model of the political environment that is presented in Section 8.1. In that context, the values initially assigned to the parameters entering the model are no longer constant all over the evolution of the system, but rather are subject to change at specific times so as to take into account the subsequent states reached by the system.

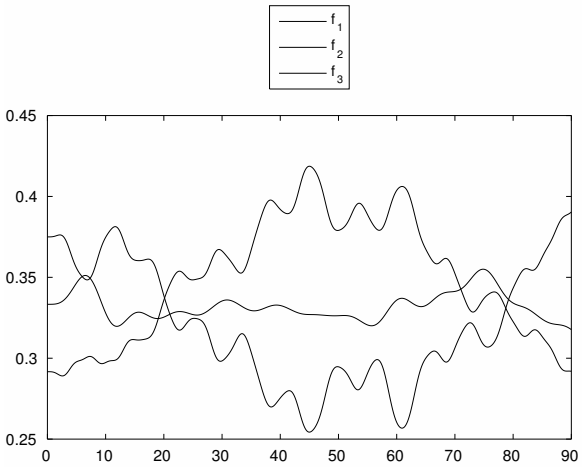

(a) $\mu_{12} = 0.1,\ \mu_{13} = 0.09,\ \mu_{23} = 0.01$

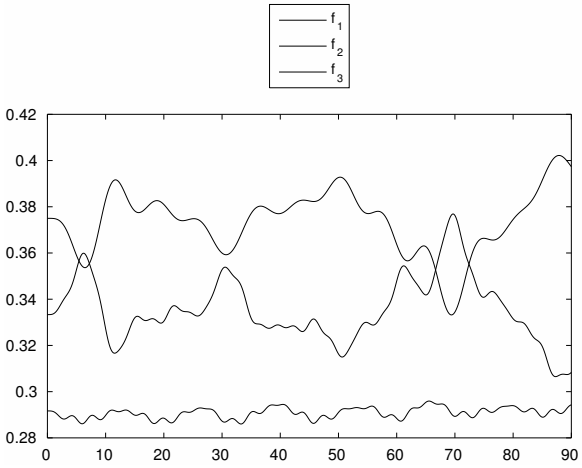

(b) $\mu_{12} = 0.01,\ \mu_{13} = 0.1,\ \mu_{23} = 0.09$

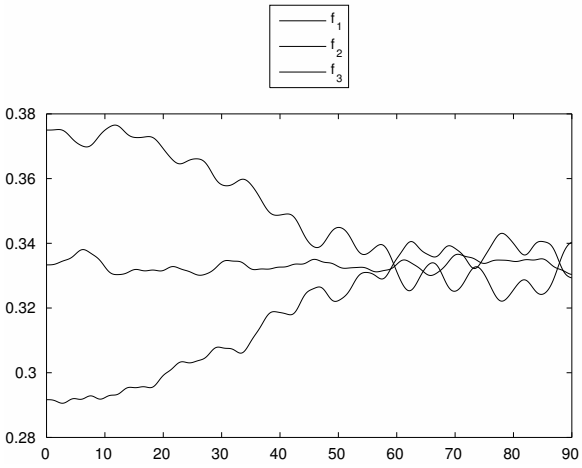

(c) $\mu_{12} = 0.04,\ \mu_{13} = 0.04,\ \mu_{23} = 0.04$

FIGURE 4.3: Linear model: time evolution of the densities of the three party groups up to $t = 90$ corresponding to the inertia parameters in (4.7) and different choices of the cross interaction parameters.

5 The rule–induced dynamics

In this Chapter, we discuss the possibility to expand the description of the time evolution of a macroscopic system by using some tools arising from quantum mechanics together with some specific rules. This completely innovative approach is useful when, for instance, the time evolution of a given system is governed not only by a Hamiltonian operator, as it happens for conservative closed microscopic systems or even for non-conservative microscopic open systems, but also by some external/internal action, periodically acting on the system, that is not easy to include in any Hamiltonian.

The extension whose aspects are discussed here is called (H, ρ)-*induced dynamics*, or, equivalently, *rule–induced dynamics*. According to this approach, the evolution of the system depends on its Hamiltonian, its initial conditions, and a *rule* ρ, *i.e.*, a suitable set of conditions acting repeatedly on the system itself (in such a case the rule can be seen as a sort of generalized projection operator), as well as on the values of the parameters entering the Hamiltonian operator (in some sense, this kind of rule adjusts the model on the basis of the current state reached by the system). The action of the rule (intended as a tool physically justified by the phenomena under analysis) on the system produces reliable changes on its original behavior; furthermore, we show that replacing the Heisenberg with the (H, ρ)-induced dynamics produces a simple, and somehow natural, way to prove that some relevant dynamical variables of the system converge, for large t, to some asymptotic values (Bagarello et al., 2016).

5.1 Modified descriptions of the dynamics

The key aspect when using raising and lowering operators in the analysis of the time evolution of some macroscopic system is that the time evolution of an observable X of the system $\mathcal{S}$ under consideration is given by $X(t) = \exp(iHt)X\exp(-iHt)$, where H is the Hamiltonian of $\mathcal{S}$. Despite of the fact that the method has been applied to very different situations, it is not expected to be a completely general strategy. For instance, if you require $\mathcal{S}$ to have a finite number of degrees of freedom, and if H is self–adjoint, time independent and quadratic, then the only possible outcomes are periodic or quasiperiodic. However, if we know that $\mathcal{S}$ decays to some *final state*, it is clear that such a description does not work. This is a case in which the framework needs to be enriched. A possibility, used, *e.g.*, in quantum optics, or for two or three level atoms (to describe some transition from one level to another) consists in using some effective Hamiltonian operator which is represented by a finite–dimensional not Hermitian matrix (Cherbal et al., 2007). Another well known way is considering the atoms interacting with some reservoir with an infinite number of degrees of freedom (Barnett and Radmore, 1997) at the price of dealing with a full system ($\mathcal{S}$ plus the reservoir) which is no longer finite dimensional.

This possibility has been used in several applications also because it admits interesting interpretations (Bagarello, 2015; Bagarello, 2016; Bagarello and Gargano, 2016a). However, from a technical point of view, this is probably not the easiest choice and, in fact, quite often one makes use of some finite dimensional effective Hamiltonian H_{eff}, with $H_{eff} \neq H_{eff}^\dagger$. To keep the situation simple, sometimes one describes a simplified version of the full system (many details of which get lost) by means of some master equation where, again, the dynamics is described by some finite matrix whose entries are properly chosen. This theory extends quantum mechanics beyond Hamiltonian dynamics, and finds powerful applications in quantum optics and quantum information (see Huang et al., 2008, and references therein). Often, when starting from the microscopic model for the full system, a series of approximations has to be made in order to be able to describe the open system dynamics in terms of the GKSL–master equation (Breuer and Petruccione, 2007). Naturally, these approximations are not generally valid, and the dynamical semigroup is not an exact description for all possible physical situations of interest. We propose a novel approach — the (H, ρ)–induced dynamics — with the aim of overcoming such difficulties in a way that is both straightforward and not expensive from a computational viewpoint.

Thus, in the sequel we deal with an extended version of the Heisenberg dynamics which allows us to take into account other effects which may occur during the time evolution of a given system $\mathcal{S}$. The strategy proposed here merges the general framework of the quantum dynamics, described by a Hamiltonian H, with some periodic (or not) effect which can not be included in H.

In particular, we first consider the case in which the dynamics is driven by a Hermitian Hamiltonian H, time independent, but, during the time evolution, some check on $\mathcal{S}$ occurs periodically, and this check can, in principle, change the state of the system itself. The check is what is called a *rule*, ρ, and the combined effect of H and ρ produces what is called the (H, ρ)-induced dynamics. This was applied in Bagarello et al., 2017 to an operatorial model of the Game of Life (described in Chapter 6), and in Bagarello and Gargano, 2016a to politics.

Moreover, in Di Salvo and Oliveri, 2016c; Di Salvo and Oliveri, 2016a a different viewpoint has been proposed: the rule periodically checks the state of the system and changes some of the values of the parameters entering the Hamiltonian, without modifying its functional form. In some sense, the strength of the interactions between the different parts of the system $\mathcal{S}$ are *adjusted* according to the current state (or its variation) of $\mathcal{S}$. This approach reveals quite efficient, as an example, in building an operatorial model of political parties affected by turncoat–like behavior (Di Salvo and Oliveri, 2016a), as described in detail in Chapter 8.

We briefly review the main definitions and results for the (H, ρ)-induced dynamics. Let $\mathcal{S}$ be the physical system we are interested in, and Q_j ($j = 1, \ldots, M$) a set of M commuting self-adjoint operators with eigenvectors $\varphi_{n_j}^{(j)}$ and eigenvalues $\alpha_{n_j}^{(j)}$:

$$[Q_j, Q_k] = Q_jQ_k - Q_kQ_j = 0, \qquad Q_j = Q_j^\dagger, \qquad Q_j\varphi_{n_j}^{(j)} = \alpha_{n_j}^{(j)}\varphi_{n_j}^{(j)}, \quad (5.1)$$

$j, k = 1, \ldots, M$, $n_j = 1, 2, 3, \ldots, N_j$, which can be finite or infinite. Setting $\mathbf{n} = (n_1, n_2, \ldots, n_M)$, the vector

$$\varphi_{\mathbf{n}} = \varphi_{n_1}^{(1)} \otimes \varphi_{n_2}^{(2)} \otimes \cdots \varphi_{n_M}^{(M)}$$

represents an eigenstate of all the operators Q_j, say

$$Q_j \, \varphi_{\mathbf{n}} = \alpha_{n_j}^{(j)} \, \varphi_{\mathbf{n}}. \tag{5.2}$$

The existence of a common eigenstate for all the operators Q_j is guaranteed by the fact that they mutually commute. It is convenient, and always true in our applications, to assume that these vectors are mutually orthogonal and normalized:

$$\langle \varphi_{\mathbf{n}}, \varphi_{\mathbf{m}} \rangle = \delta_{\mathbf{n},\mathbf{m}} = \prod_{j=1}^{M} \delta_{n_j, m_j}. \tag{5.3}$$

The Hilbert space $\mathcal{H}$ where $\mathcal{S}$ is defined is mathematically constructed, as usual, as the closure of the linear span of all the vectors $\varphi_{\mathbf{n}}$. Observe that there exists a one-to-one correspondence between $\mathbf{n}$ and the vector $\varphi_{\mathbf{n}}$: once we know $\mathbf{n}$, $\varphi_{\mathbf{n}}$ is clearly identified, and vice versa. Now, let $H = H^\dagger$ be a quadratic time independent self–adjoint Hamiltonian, ruling the evolution of $\mathcal{S}$, which, in general, does not commute with the Q_j's. This means that, in absence of any other information, to look at the time evolution of $\mathcal{S}$ it is possible to assume that the wave function $\Psi(t)$ describing $\mathcal{S}$ at time t evolves according to the Schrödinger equation, or, equivalently, that the operators acting on $\mathcal{H}$ at time t do, according to the Heisenberg equation (see Section 2.1).

The mean value of each operator Q_j in the state $\Psi(t)$ is given by computing $q_j(t) = \langle \Psi(t), Q_j \Psi(t) \rangle$; the obtained values allow us to define the related M-dimensional time-dependent vector $\mathbf{q}(t) = (q_1(t), q_2(t), \ldots, q_M(t))$.

We now introduce, rather generally, two different ways of extending the dynamics through the introduction of some *rules*.

In the first approach, described in Subsection 5.1.1, the rule ρ is a — not necessarily linear — map from $\mathcal{H}$ to $\mathcal{H}$. Its explicit action depends on the expression of $\mathbf{q}(t)$ at particular instants $k\tau$ ($k = 1, 2, \ldots$). In other words, according to how $\mathbf{q}(k\tau)$ looks like, ρ maps an input vector Φ_{in} into a different output vector Φ_{out}, that is $\rho(\Phi_{in}) = \Phi_{out}$. This is not very different from what happens in scattering theory, where an incoming state, after the occurrence of the scattering, is transformed into an outgoing state (Roman, 1965).

The second approach, described in Subsection 5.3.1, works on the space of the (in general) real parameters of the Hamiltonian H. Given a quadratic time independent self–adjoint Hamiltonian involving p real parameters, the rule ρ is a map from $\mathbb{R}^p$ to $\mathbb{R}^p$ that, at particular instants $k\tau$ ($k = 1, 2, \ldots$), on the basis of the actual state (or its variation) of the system, changes the values of the parameters. In such a way, the model *adjusts itself* and is able to describe more complex (and somehow realistic) behaviors.

5.1.1 The rule ρ as a map from $\mathcal{H}$ to $\mathcal{H}$

We discuss here a special definition of the rule ρ as a map from $\mathcal{H}$ to $\mathcal{H}$.

In general terms, suppose that at time $t = 0$ the system $\mathcal{S}$ is in a state $\mathbf{n}^0$ or, which is the same, $\mathcal{S}$ is described by the vector $\varphi_{\mathbf{n}^0}$. Then, once fixed a positive value of τ, this vector evolves in the time interval $[0, \tau[$ according to the Schrödinger recipe: $\exp(-iHt)\varphi_{\mathbf{n}^0}$. Let us set

$$\Psi(\tau^-) = \lim_{t\to\tau^-} \exp(-iHt)\varphi_{\mathbf{n}^0},$$

where t converges to τ from below. The notation τ^-, $2\tau^-$, ... as argument of Ψ is used here to emphasize that before τ, for instance, the time evolution is only due to H, while ρ really acts at $t = \tau$. Of course, the rule ρ may be defined in different ways. The key point common to all possible choices is that ρ behaves as a check over the system $\mathcal{S}$, and modifies some of its ingredients according to the result of this check. In particular, at time $t = \tau$, ρ is applied to $\Psi(\tau^-)$, and the output of this action is a new vector which we assume to be again an eigenstate of each operator Q_j, but with different eigenvalues, $\varphi_{\mathbf{n}^1}$. In other words, ρ *looks* at the explicit expression of the vector $\Psi(\tau^-)$ and, according to its form, returns a new vector $\mathbf{n}^1 = (n_1^1, \ldots, n_M^1)$; as a consequence, a new vector $\varphi_{\mathbf{n}^1}$ of $\mathcal{H}$ is obtained. Now, the procedure is iterated, taking $\varphi_{\mathbf{n}^1}$ as the initial vector, and letting it evolve with H for another time interval of length τ; we compute

$$\Psi(2\tau^-) = \lim_{t\to\tau^-} \exp(-iHt)\varphi_{\mathbf{n}^1},$$

and the new vector $\varphi_{\mathbf{n}^2}$ is deduced by the action of rule ρ on $\Psi(2\tau^-)$: $\varphi_{\mathbf{n}^2} = \rho(\Psi(2\tau^-))$. Then, in general, we have

$$\Psi(k\tau^-) = \lim_{t\to\tau^-} \exp(-iHt)\varphi_{\mathbf{n}^{k-1}}, \tag{5.4}$$

and

$$\varphi_{\mathbf{n}^k} = \rho\left(\Psi(k\tau^-)\right), \tag{5.5}$$

for all $k \geq 1$.

Let now X be a generic operator on $\mathcal{H}$, bounded or unbounded. In this last case, we will require that the various $\varphi_{\mathbf{n}^k}$ belong to the domain of $X(t) = \exp(iHt)X\exp(-iHt)$ for all $t \in [0, \tau]$.

Definition 5.2 *The sequence of functions*

$$x_{k+1}(t) := \langle \varphi_{\mathbf{n}^k}, X(t)\varphi_{\mathbf{n}^k} \rangle, \tag{5.6}$$

for $t \in [0, \tau]$ and $k \in \mathbb{N}_0$, is called the (H, ρ)–induced dynamics of X.

Some consequences of Definition 5.2, and some properties of the sequence $\underline{X}(\tau) = (x_1(\tau), x_2(\tau), x_3(\tau), \ldots)$ have been discussed in Bagarello et al., 2017. For instance, next theorem can be stated.

Theorem 5.3 *The following results concerning periodicity hold true.*

1. *If the rule ρ does not depend on the input, then*

$$\underline{X}(\tau) = (x_1(\tau), x_2(\tau), x_2(\tau), x_2(\tau), x_2(\tau), \ldots).$$

2. *Assume that a* $K > 0$ *exists such that* $\rho(\varphi_{\mathbf{n}^K}) = \varphi_{\mathbf{n}^K}$, *then*

$$\underline{X}(\tau) = (x_1(\tau), x_2(\tau), \ldots, x_{K+1}(\tau), x_{K+1}(\tau), x_{K+1}(\tau), \ldots)\,.$$

3. *Assume that* $K > 0$, $N \geq 0$ *exist such that* $\rho(\varphi_{\mathbf{n}^{(N+K)}}) = \varphi_{\mathbf{n}^N}$, *then*

$$\underline{X}(\tau) = (x_1(\tau), \ldots, x_N(\tau), x_{N+1}(\tau), \ldots, x_{N+K+1}(\tau), x_{N+1}(\tau), \ldots)\,.$$

Notice that from $\underline{X}(t) = (x_1(t), x_2(t), x_3(t), \ldots)$ it is possible to define a function of time in the following way:

$$\tilde{X}(t) = \begin{cases} x_1(t), & t \in [0, \tau[\\ x_2(t-\tau), & t \in [\tau, 2\tau[\\ x_3(t-2\tau), & t \in [2\tau, 3\tau[\\ \ldots & \ldots \end{cases} \tag{5.7}$$

It is clear that $\tilde{X}(t)$ may have discontinuities at times $k\tau$, for positive integers k. Of course, Theorem 5.3 gives conditions for $\tilde{X}(t)$ to admit some asymptotic value or to be periodic. We will return on this aspect later in Section 5.10.

5.3.1 The rule ρ as a map in the space of the parameters of H

In Subsection 5.1.1, we have introduced a rule ρ as a map acting on some *input vector* of $\mathcal{H}$ and returning an *output vector*, again belonging to $\mathcal{H}$. In other words, the effect of ρ is to change the state of the system. This is not the only possibility. In fact, we now discuss how a rule can be considered on $\mathcal{S}$ changing some aspects of the dynamics of $\mathcal{S}$. Let $\mathcal{S}$ be a system involving M fermionic modes whose evolution is ruled by the quadratic time independent self–adjoint Hamiltonian

$$H = \sum_{j=1}^{M} \omega_j a_j^\dagger a_j + \sum_{j=1}^{M-1} \sum_{k=j+1}^{M} \lambda_{j,k}(a_j a_k^\dagger + a_k a_j^\dagger), \tag{5.8}$$

containing the $p = M(M+1)/2$ real parameters (not necessarily all non vanishing) ω_j and $\lambda_{j,k}$.

Adopting the Heisenberg representation, the time evolution is given by

$$a_j(t) = \exp(iHt) a_j(0) \exp(-iHt),$$

or, equivalently, by the solution of the following linear system of ordinary differential equations:

$$\dot{a}_j(t) = i\Big(-\omega_j a_j(t) + \sum_{k=1}^{j-1} \lambda_{j,k} a_k(t) + \sum_{k=j+1}^{M} \lambda_{j,k} a_k(t)\Big), \quad j = 1, \ldots, M. \tag{5.9}$$

In principle, we have a system of $M 2^{2M}$ linear differential equations to be solved with suitable initial conditions for the matrices representing the fermionic operators a_j. However, since the system is linear, we may write it in compact form, say

$$\dot{A}(t) = UA(t), \tag{5.10}$$

where

$$A(t) = \begin{pmatrix} a_1(t) \\ a_2(t) \\ \vdots \\ a_M(t) \end{pmatrix},$$

while U is an $M \times M$ constant symmetric matrix such that $U_{j,j} = -i\omega_j$, $U_{j,k} = U_{k,j} = i\lambda_{j,k}$ ($j < k$), and each component of A is a $2^M \times 2^M$ matrix. The formal solution is immediately deduced:

$$A(t) = \exp(Ut)A(0) = V(t)A(0). \tag{5.11}$$

Thus, if $V_{\ell,m}(t)$ is the generic entry of the matrix $V(t)$, we have

$$a_\ell(t) = \sum_{k=1}^{M} V_{\ell,k}(t)a_k, \qquad \ell = 1, \ldots, M.$$

Now, we need to compute the mean value of the number operator

$$\hat{n}_\ell(t) = a_\ell^\dagger(t)a_\ell(t)$$

on an eigenvector $\varphi_{n_1,\ldots,n_M}$ of all the $\hat{n}_\ell(0)$,

$$\hat{n}_\ell\varphi_{n_1,\ldots,n_M} = n_\ell\varphi_{n_1,\ldots,n_M}, \qquad \ell = 1, \ldots, M.$$

It is easy to check that

$$n_\ell(t) = \langle\varphi_{n_1,\ldots,n_M}, \hat{n}_\ell(t)\varphi_{n_1,\ldots,n_M}\rangle = \sum_{k=1}^{M} |V_{\ell,k}(t)|^2 \, n_k \tag{5.12}$$

for all $\ell = 1, \ldots, M$, provides what we are looking for (representing the physical quantities which are relevant in the description of the system under analysis).

Starting from a quadratic Hamiltonian such as the one defined in (5.8), the alternative approach in order to enrich the dynamics proposed in this Subsection consists in a suitable adjustment of the model operated by specific conditions accounting for a sort of dependence on the current state of the system and repeatedly acting at specific times on the parameters entering the Hamiltonian operator. We stress that in such an approach only the strengths of the mutual interactions change, whereas the model preserves its functional structure. Combining the action of such kind of rule with the standard Heisenberg description of the dynamics, other than having a concrete meaning, really produces a simple, and somehow natural, way to prove that some relevant dynamical variables of the system converge, for large t, to some realistic asymptotic values.

Here is a brief sketch of this approach, leading to a (H, ρ)–induced dynamics slightly different from that above considered. Let us split the whole period during which the system evolves into time subintervals of duration τ. Then, the description of the dynamics of the system is determined by its Hamiltonian as well as its initial conditions, and extended by a set of conditions — *i.e.*, the rule — stepwise acting on it. The rule takes into account some effects occurring during the time evolution of the system. By means

of this approach, quite different behaviors arise depending on the explicit form of H, the initial conditions, the rule, and the length τ of each time subinterval.

Here, we use the variations of the mean values of the various compartments in some time intervals in order to modify the values of some of the parameters of the model; then, we consider a new Hamiltonian operator, having the same functional form as the previous one, but (in general) with a different set of the values of the involved parameters, and follow the evolution of the system under the action of this new Hamiltonian for the next time interval of length τ, and so on. Therefore, the global evolution will be ruled by a sequence of similar Hamiltonian operators, and the parameters entering the model are stepwise (in time) constant.

More in detail, we start considering a self–adjoint quadratic Hamiltonian operator $H^{(1)}$, the corresponding evolution of an observable X

$$X(t) = \exp(iH^{(1)}t)X\exp(-iH^{(1)}t), \tag{5.13}$$

and we compute its mean value

$$x(t) = \langle \varphi_{n_1,\dots,n_M},\, X(t)\varphi_{n_1,\dots,n_M}\rangle \tag{5.14}$$

in a time interval of length $\tau > 0$. The change of some of the parameters involved in $H^{(1)}$, on the basis of the values of the various $x(\tau)$, thus provides a new Hamiltonian operator $H^{(2)}$, having the same functional form as $H^{(1)}$. We now restart the evolution of the system as ruled by $H^{(2)}$ in another time interval of length $\tau > 0$, and so on. Therefore, the rule now has to be thought of as a map from $\mathbb{R}^p$ into $\mathbb{R}^p$ acting on the space of the p parameters involved in the Hamiltonian.

In general terms, consider a time interval $[0, T]$, and split it in $n = T/\tau$ subintervals of length τ (we assume here that n is integer). In the k–th subinterval $[(k-1)\tau, k\tau[$ consider a Hamiltonian $H^{(k)}$ ruling the dynamics. The global dynamics arises from the sequence of Hamiltonians

$$H^{(1)} \xrightarrow{\tau} H^{(2)} \xrightarrow{\tau} H^{(3)} \xrightarrow{\tau} \dots \xrightarrow{\tau} H^{(n)}, \tag{5.15}$$

the global evolution being obtained by gluing the local evolutions.

In every subinterval, we therefore have a system like

$$\dot{A}(t) = U^{(k)}A(t), \qquad t \in [(k-1)\tau, k\tau], \tag{5.16}$$

whose solution (representing A as an $N \times N$ matrix such that $A(0) = \mathbb{1}$, as done in Section 2.6) is just given by

$$A(t) = \exp(U^{(k)}t), \qquad t \in [(k-1)\tau, k\tau]; \tag{5.17}$$

joining the solutions in all the subintervals, we have globally

$$A(t) = \begin{cases} \exp(U^{(1)}t) & t \in [0, \tau], \\ \exp(U^{(2)}(t-\tau))\exp(U^{(1)}\tau) & t \in [\tau, 2\tau], \\ \exp(U^{(3)}(t-2\tau))\exp(U^{(2)}\tau)\exp(U^{(1)}\tau) & t \in [2\tau, 3\tau], \\ \dots & \dots \end{cases} \tag{5.18}$$

The fact that the parameters are changed according to the actual state (or

its variation) of the system means, in some sense, that the strength of the interactions among the compartments is repeatedly adjusted; as a result, asymptotic values of the mean values can be obtained. This aspect is developed in more detail in Section 5.10. Moreover, this kind of rule–induced step–wise dynamics clearly may generate discontinuities in the first order derivatives of the operators, but prevents the occurrence of jumps in their evolutions and, consequently, in the mean values of the number operators.

Stated differently, by adopting this rule, we are implicitly considering the possibility of having a time-dependent Hamiltonian. But the time-dependence is, in such a case, somehow hidden and of a very special form: in each interval $[(k-1)\tau, k\tau[$ the Hamiltonian does not depend on time, but in $k\tau$ some changes may occur, according to how the system is evolving.

5.4 On equilibria

In this Section, we show that the concept of (H, ρ)-induced dynamics can be efficiently used to describe systems which are expected to reach some stationary point or periodic orbit, during their time evolution, even when H is kept to be Hermitian.

Suppose that ρ is a map from $\mathcal{H}$ to $\mathcal{H}$. The following definitions are directly connected with Theorem 5.3.

Definition 5.5

1. *$x^\infty \in \mathbb{C}$ is an equilibrium for the (H, ρ)–induced dynamics of the operator X if, $\forall\, \epsilon > 0$, $\exists N_\epsilon > 0$ such that $|x_\ell(\tau) - x^\infty| < \epsilon$, for all $\ell > N_\epsilon$.*

2. *Given $\epsilon > 0$, $x^\infty \in \mathbb{C}$ is an ϵ-equilibrium for the (H, ρ)-induced dynamics of the operator X if $\exists N_\epsilon > 0$ such that $|x_\ell(\tau) - x^\infty| < \epsilon$, for all $\ell > N_\epsilon$.*

3. *The L-dimensional vector $(x_1^\infty, x_2^\infty, \ldots, x_L^\infty)$, $x_j^\infty \in \mathbb{C}$, is an L-equilibrium cycle for the (H, ρ)-induced dynamics of the operator X if, $\forall\, \epsilon > 0$, $\exists N_\epsilon > 0$ such that*

$$\sup_{\ell=1,\ldots,L} |x_{N_\epsilon + kL + \ell}(\tau) - x_\ell^\infty| < \epsilon,$$

for all $k = 0, 1, \ldots$.
In this case, we call L the period of the solution and $N_L = inf_{\epsilon>0} N_\epsilon$ the transient to reach the L-equilibrium cycle.

Remark 5.6 *If x^∞ is an equilibrium for the (H, ρ)-induced dynamics of the operator X, then it is also an ϵ-equilibrium, for all $\epsilon > 0$.*

Remark 5.7 *According to the definition given in Theorem 5.3, a 1-equilibrium cycle solution for the (H, ρ)-induced dynamics of the operator X is simply an equilibrium.*

The following results easily follow from Definition 5.5 and Theorem 5.3.

Theorem 5.8 *If the rule ρ does not depend on the input, or, more in general, if there exists $K > 0$ such that $\rho(\varphi_{\mathbf{n}^K}) = \varphi_{\mathbf{n}^K}$, then, for each operator X of the system, an equilibrium for the (H, ρ)-induced dynamics of the operator X does exist.*

Suppose rather that a $K > 0$ exists such that $\rho(\varphi_{\mathbf{n}^K}) = \varphi_{\mathbf{n}^0}$, and define

$$\bar{\epsilon} = \max_{j=1,\dots,K} \left| x^\infty - x^j(\tau) \right|,$$

with $x^\infty = \frac{1}{K}\sum_{j=1}^K x^j(\tau)$, then x^∞ is an $\bar{\epsilon}$-equilibrium for the (H,ρ)-induced dynamics of the operator X.

Once again, we do not give here the proof of the previous Theorem, which is very easy. It is clear that the interesting situation is when $\bar{\epsilon}$ is sufficiently small. When this is not so, we can not say much about the closeness of x^∞ to the various $x^j(\tau)$. In this case, it is more interesting the following result.

Theorem 5.9 *Suppose that $K > 0$ exists such that $\rho(\varphi_{\mathbf{n}^K}) = \varphi_{\mathbf{n}^0}$, then a $(K+1)$-cycle for the (H,ρ)-induced dynamics of the operator X exists, with $x_j^\infty = x^j(\tau)$.*

It is clear that, even if an equilibrium exists for the (H,ρ)-induced dynamics of a certain operator X, then it is not necessarily an equilibrium also for the (H,ρ)-induced dynamics of a different operator Y. In other words, using the function $\tilde{X}(t)$ introduced before, even if this function can admit some asymptotic value (or be periodic from some multiple of τ), the analogous function $\tilde{Y}(t)$ defined in analogy to (5.7) does not necessarily admit some asymptotic value.

5.10 Large time behaviors

In this Section, we describe, by using different techniques, a very simple two-mode system, and discuss its time evolution. In particular, we consider the limit $t \to \infty$.

5.10.1 An example: a two–mode system

In this Subsection, we describe the possibility of getting, in some simple and natural way, some asymptotic behavior for certain physical systems by means of the (H,ρ)-induced dynamics, but not only, by discussing in some details a very simple example, originally introduced in Bagarello and Oliveri, 2013.

Consider the Hamiltonian of the system $\mathcal{S}$ under analysis, having two (fermionic) degrees of freedom,

$$H = H_0 + \lambda H_I, \qquad H_0 = \omega_1 a_1^\dagger a_1 + \omega_2 a_2^\dagger a_2, \quad H_I = a_1^\dagger a_2 + a_2^\dagger a_1. \tag{5.19}$$

Of course, when $\lambda = 0$ there is no interacting contribution in H.

The eigenstates of the number operators $\hat{n}_j := a_j^\dagger a_j$ are easily constructed: if $\varphi_{0,0}$ is the *ground vector* of $\mathcal{S}$, $a_1\varphi_{0,0} = a_2\varphi_{0,0} = 0$, the only non–trivial, linearly independent, vectors of our Hilbert space $\mathcal{H}$ are

$$\varphi_{0,0}, \qquad \varphi_{1,0} := a_1^\dagger \varphi_{0,0}, \qquad \varphi_{0,1} := a_2^\dagger \varphi_{0,0}, \qquad \varphi_{1,1} := a_1^\dagger a_2^\dagger \varphi_{0,0}.$$

This means that $dim(\mathcal{H}) = 4$, and we have

$$\hat{n}_1\varphi_{n_1,n_2} = n_1\varphi_{n_1,n_2}, \qquad \hat{n}_2\varphi_{n_1,n_2} = n_2\varphi_{n_1,n_2}. \tag{5.20}$$

The equations of motion for the annihilation operators $a_j(t)$ are

$$\begin{aligned} \dot{a}_1(t) &= -i\omega_1 a_1(t) - i\lambda a_2(t), \\ \dot{a}_2(t) &= -i\omega_2 a_2(t) - i\lambda a_1(t), \end{aligned} \tag{5.21}$$

which can be solved with the initial conditions $a_1(0) = a_1$ and $a_2(0) = a_2$. The solution looks like

$$\begin{aligned} a_1(t) &= \frac{1}{2\delta}\left(a_1\left((\omega_1-\omega_2)\Phi_-(t) + \delta\Phi_+(t)\right) + 2\lambda a_2\Phi_-(t)\right), \\ a_2(t) &= \frac{1}{2\delta}\left(a_2\left(-(\omega_1-\omega_2)\Phi_-(t) + \delta\Phi_+(t)\right) + 2\lambda a_1\Phi_-(t)\right), \end{aligned} \tag{5.22}$$

where

$$\begin{aligned} \delta &= \sqrt{(\omega_1-\omega_2)^2 + 4\lambda^2}, \\ \Phi_+(t) &= 2\exp\left(-\frac{it(\omega_1+\omega_2)}{2}\right)\cos\left(\frac{\delta t}{2}\right), \\ \Phi_-(t) &= -2i\exp\left(-\frac{it(\omega_1+\omega_2)}{2}\right)\sin\left(\frac{\delta t}{2}\right). \end{aligned}$$

Then the functions $n_j(t) := \langle\varphi_{n_1,n_2}, \hat{n}_j(t)\varphi_{n_1,n_2}\rangle$ are the following:

$$\begin{aligned} n_1(t) &= \frac{n_1(\omega_1-\omega_2)^2}{\delta^2} + \frac{4\lambda^2}{\delta^2}\left(n_1\cos^2\left(\frac{\delta t}{2}\right) + n_2\sin^2\left(\frac{\delta t}{2}\right)\right), \\ n_2(t) &= \frac{n_2(\omega_1-\omega_2)^2}{\delta^2} + \frac{4\lambda^2}{\delta^2}\left(n_2\cos^2\left(\frac{\delta t}{2}\right) + n_1\sin^2\left(\frac{\delta t}{2}\right)\right). \end{aligned} \tag{5.23}$$

These functions are interpreted, in agreement with what already stated, as the densities of two species, $\mathcal{S}_1$ and $\mathcal{S}_2$, interacting in a given (small) region. The interaction Hamiltonian H_I in (5.19) describes a sort of predator–prey mechanism, and this is reflected by the solutions in (5.23), which show how the two densities, because of the interaction between $\mathcal{S}_1$ and $\mathcal{S}_2$, oscillate between zero and one. In fact, if $\lambda = 0$, $n_j(t) = n_j$, and the densities stay constant. Notice that these formulas automatically imply that $n_1(t) + n_2(t) = n_1 + n_2$, independently of t and λ: the oscillations are such that they sum up to zero.

Hereafter, we develop a different aspect of this model consisting in the possibility of getting some limiting values for $n_1(t)$ and $n_2(t)$ for large values of t, when $\lambda \neq 0$.

The first trivial remark is that the functions $n_1(t)$ and $n_2(t)$ in (5.23) do not admit any asymptotic limit, except when $n_1 = n_2$ (or if $\lambda = 0$, which is excluded here). In this case, clearly, $n_1(t) = n_2(t) = n_1 = n_2$. If, on the other hand, $n_1 \neq n_2$, then both $n_1(t)$ and $n_2(t)$ always oscillate in time. This is not surprising. In fact it is easy to prove the following statement:
if $\mathcal{S}$ is a system living in a finite dimensional Hilbert space, and if its dynamics is driven by a time-independent, self-adjoint, Hamiltonian H, then its dynamics is necessarily periodic or quasi-periodic.

This claim implies, first of all, that an asymptotic limit exists only in the trivial case in which no dynamics at all exists or, better to say, when each

observable of the system keeps its initial value. To prove the claim, it is sufficient to observe that, if $H = H^\dagger$ is an $M \times M$ matrix, then an unitary matrix U exists such that $UHU^{-1} = H_d$, which is a diagonal matrix with M (not necessarily different) real eigenvalues $E_1, E_2, \ldots, E_M$. Then, if $\hat{n}$ is an observable of $\mathcal{S}$, its time evolution can be written as

$$\hat{n}(t) = \exp(iHt)\hat{n}\exp(-iHt) = U^{-1}\exp(iH_d t)\left(U\hat{n}U^{-1}\right)\exp(-iH_d t)U,$$

which is periodic when all couples of eigenvalues are commensurable, while is quasi–periodic otherwise. If H_d commutes with $U\hat{n}U^{-1}$, then $\hat{n}(t) = \hat{n}$, and its large time behavior is clearly trivial. Otherwise, $\hat{n}(t)$ keeps on oscillating, and no asymptotic value is reached. This is essentially what is described by formulas (5.23), where the focus is not really on the operators $\hat{n}_1$ and $\hat{n}_2$, but on their mean values.

If $\mathcal{S}$ lives in a finite dimensional Hilbert space, the previous simple argument shows that no time-independent, self-adjoint, Hamiltonian H makes the job. Hence, we have to add some extra ingredients, or change something in the Hamiltonian. Here, we show how the use of a rule, other than having a concrete meaning, can describe a somehow realistic asymptotic value for the observables of $\mathcal{S}$.

In order to show this, we first rewrite (5.23) as follows:

$$N(t) = T_t N(0), \tag{5.24}$$

where

$$N(t) = \begin{pmatrix} n_1(t) \\ n_2(t) \end{pmatrix}, \; T_t = \frac{1}{\delta^2}\begin{pmatrix} \delta^2 - 4\lambda^2\sin^2\left(\frac{\delta t}{2}\right) & 4\lambda^2\sin^2\left(\frac{\delta t}{2}\right) \\ 4\lambda^2\sin^2\left(\frac{\delta t}{2}\right) & \delta^2 - 4\lambda^2\sin^2\left(\frac{\delta t}{2}\right) \end{pmatrix}. \tag{5.25}$$

Of course, the components of $N(t)$ return the expressions of $n_1(t)$ and $n_2(t)$ for all time. But, as we have already discussed, this can only produce a periodic (or quasi–periodic) time evolution. Let us now see what happens if we insert a rule ρ in the time evolution of the system.

The rule ρ can be thought of as a measure of $n_1(t)$ and $n_2(t)$ repeated at time $\tau, 2\tau, 3\tau, \ldots$ It is known that performing a measure on a quantum system is a delicate operation, which modifies the system itself. For this reason, there is no reason a priori to say that the result of a measure at time $k\tau$ (after having measured the system at time $\tau, 2\tau, \ldots, (k-1)\tau$) would be exactly the same as the one deduced directly from (5.25), *i.e.*, $n_1(k\tau)$ and $n_2(k\tau)$, as we are going to show now.

The first measure gives $N_1(\tau) := N(\tau) = T_\tau N(0)$. Then, according to what discussed in Section 5.1.1, we let the system evolve out of this new initial condition $N_1(\tau)$ for another time step: $N_2(\tau) := T_\tau N_1(\tau) = T_\tau^2 N(0)$, and so on. In this way, we produce a sequence

$$N_\ell(\tau) = T_\tau^\ell N(0), \tag{5.26}$$

for all $\ell \geq 1$.

In order to compute $N_l(\tau)$, and its limit for ℓ diverging, we first observe that T_t is a self–adjoint matrix, so it can be easily diagonalized. In particular,

we get

$$U^{-1}T_tU = \begin{pmatrix} \lambda_1(t) & 0 \\ 0 & \lambda_2(t) \end{pmatrix} =: \Lambda_t,$$

where

$$U = \frac{1}{\sqrt{2}}\begin{pmatrix} 1 & -1 \\ 1 & 1 \end{pmatrix}, \qquad \lambda_1(t) = 1, \quad \lambda_2(t) = \frac{1}{\delta^2}\left(\delta^2 - 8\lambda^2 \sin^2\left(\frac{\delta t}{2}\right)\right).$$

Then

$$T_\tau^\ell = U\Lambda_\tau^\ell U^{-1} = U\begin{pmatrix} 1 & 0 \\ 0 & \lambda_2^\ell(\tau) \end{pmatrix} U^{-1},$$

so that $N_\ell(\tau) = T_\tau^\ell N(0)$ can converge if $\lambda_2^\ell(\tau)$ does converge when ℓ diverges. This is what happens whenever the parameters δ, τ and λ satisfy the following inequalities:

$$0 < 8\lambda^2 \sin^2\left(\frac{\delta t}{2}\right) < \delta^2. \tag{5.27}$$

In fact, when this is true, $\lambda_2(\tau) \in]0,1[$, and therefore $\lim_{\ell\to\infty} \lambda_2^\ell(\tau) = 0$. Hence,

$$\lim_{\ell\to\infty} N_l(\tau) = \begin{pmatrix} n_1(0) \\ 0 \end{pmatrix}, \tag{5.28}$$

which clearly shows that a non trivial equilibrium can be reached in this case. However, if the parameters do not satisfy (5.27), the asymptotic behavior of $N_\ell(\tau)$ can be completely different. In fact, taking, for instance, $\tau = \frac{\pi}{\delta}$ and $\lambda = \sqrt{\frac{3}{8}}\,\delta$, and then fixing $\delta = 1$ for simplicity, we deduce that $\lambda_2(\tau) = -2$, so that $\lim_{\ell\to\infty} |\lambda_2(\tau)|^\ell = \infty$: it is evident, therefore, that the role of the values assigned to the parameters of H is in fact essential.

The conclusion of the analysis of this simple example is therefore the following: even in presence of a self-adjoint Hamiltonian, a simple two-mode fermionic system admits a non trivial asymptotic limit for a large variety of the parameters of the model, at least if a *stop and go* rule[1] (according to the approach described in Subsection 5.1.1) is assumed. However, the same rule can also produce a non converging dynamics for special choices of the parameters.

As discussed in Subsection 5.3.1, using a rule which modifies the state of the system is not the unique choice, but rather one can also think to modify the parameters of the Hamiltonian. Then, consider again the same model with two fermionic modes ruled by the Hamiltonian (5.19), and suppose now that the rule acts on the space of parameters. More precisely, assume that the rule modifies at fixed times $k\tau$ ($k = 1, 2, \ldots$) only the parameters ω_1 and ω_2 in (5.19) according to the variations of n_1 and n_2 in the intervals $[0, k\tau]$ (rule $\tilde{\rho}_A$) or $[(k-1)\tau, k\tau]$ (rule $\tilde{\rho}_B$).

Let us fix the initial values of the parameters, say $\omega_1 = 1/\sqrt{3}$, $\omega_2 = 1$, $\lambda = 1/\sqrt{5}$, and the initial conditions $n_1 = 0.8$, $n_2 = 0.6$. Without applying any rule, we have (see fig. 5.1), as one expects, a never ending oscillating behavior of both $n_1(t)$ and $n_2(t)$.

[1] The reason why we call the one used here a *stop and go* rule is because we just *stop* to measure n_1 and n_2, and then we *go* again, till the next measure.

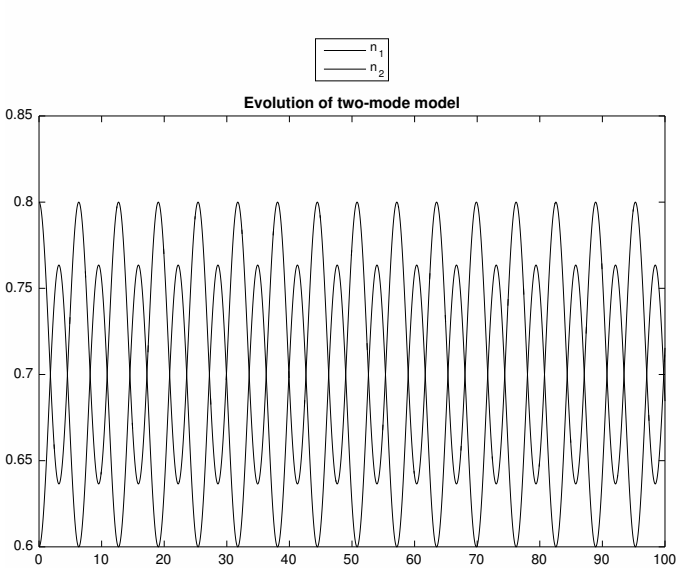

FIGURE 5.1: Time evolution of the mean values: oscillating behavior.

By taking the rule

$$\begin{aligned} \tilde{\rho}_A(\omega_1) &= \omega_1(1+\delta_1), \qquad & \delta_1 &= n_1(k\tau) - n_1(0), \\ \tilde{\rho}_A(\omega_2) &= \omega_2(1+\delta_2), \qquad & \delta_2 &= n_2(k\tau) - n_2(0), \end{aligned} \tag{5.29}$$

fig. 5.2 shows how the system reaches some asymptotic states; the rate of decay of oscillating behaviors is smaller as the value of τ is increased. Notice that, since $n_1(t) + n_2(t)$ is a constant, $\delta_1 + \delta_2 = 0$, so that the variations of the inertia parameters ω_1 and ω_2 are opposite.

By taking the rule

$$\begin{aligned} \tilde{\rho}_B(\omega_1) &= \omega_1(1+\delta_1), \qquad & \delta_1 &= n_1(k\tau) - n_1((k-1)\tau), \\ \tilde{\rho}_B(\omega_2) &= \omega_2(1+\delta_2), \qquad & \delta_2 &= n_2(k\tau) - n_2((k-1)\tau), \end{aligned} \tag{5.30}$$

fig. 5.3 shows how the system tends to reach again some asymptotic states.

The conclusion of the analysis of this simple model is that the rules, both the one defined on $\mathcal{H}$ and those working on the space of the parameters, strongly affect the behavior of the system where they are defined, producing serious differences. For this reason, they seem to be a valid alternative to the standard open system procedure, usually adopted in quantum optics or, more recently, in the analysis of some macroscopic systems.

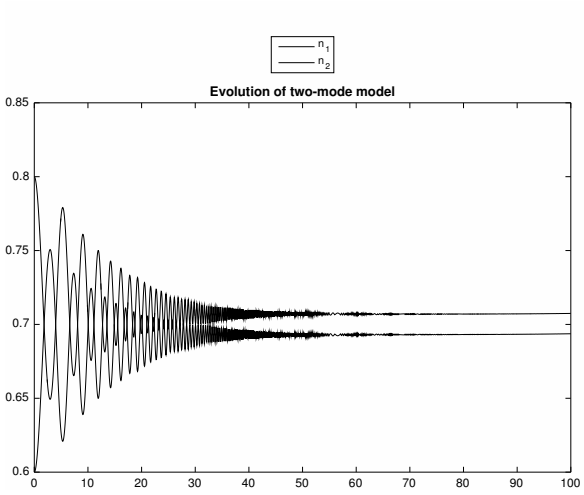

(a) $\tau = 1$

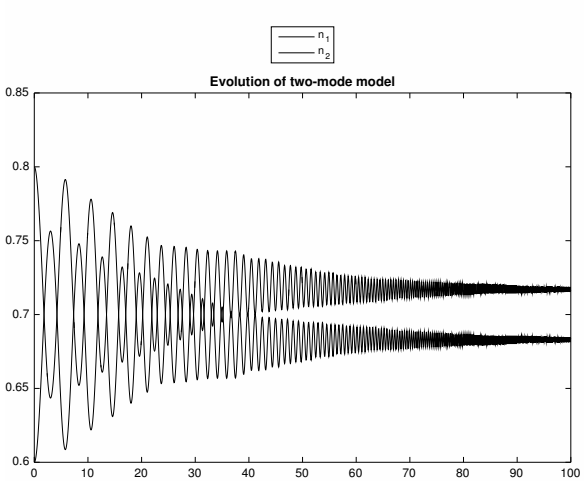

(b) $\tau = 2$

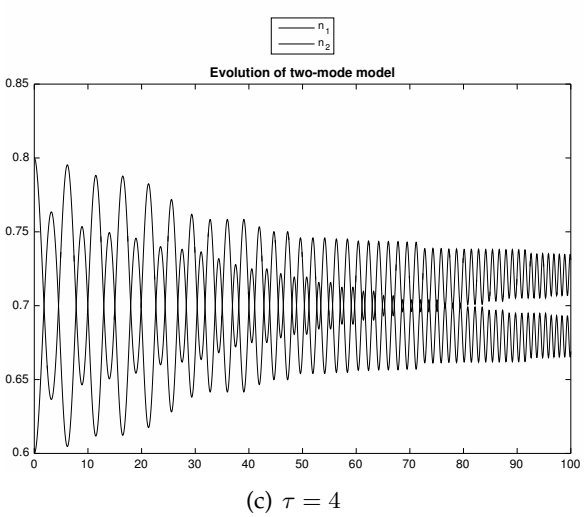

(c) $\tau = 4$

FIGURE 5.2: Time evolution with rule $\tilde{\rho}_A$.

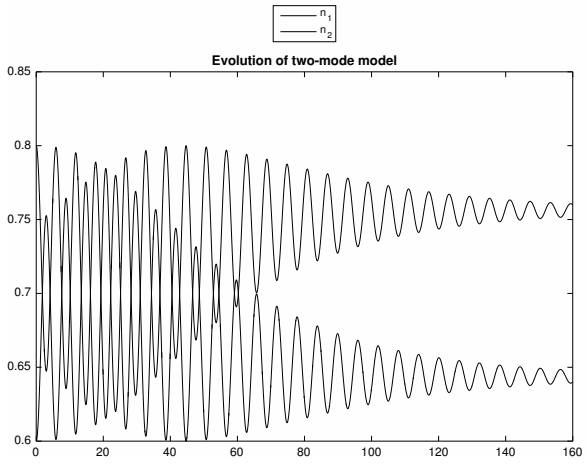

(a) $\tau = 1$

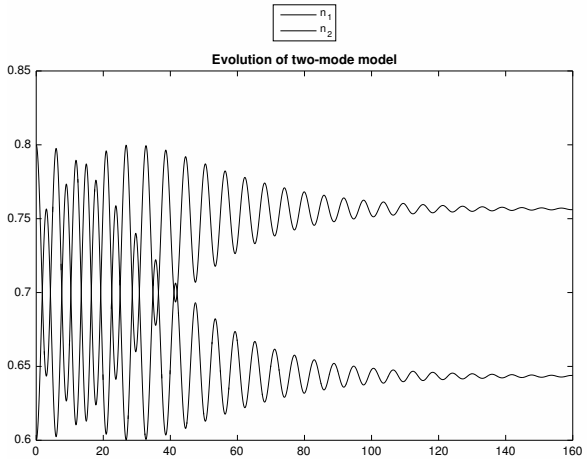

(b) $\tau = 2$

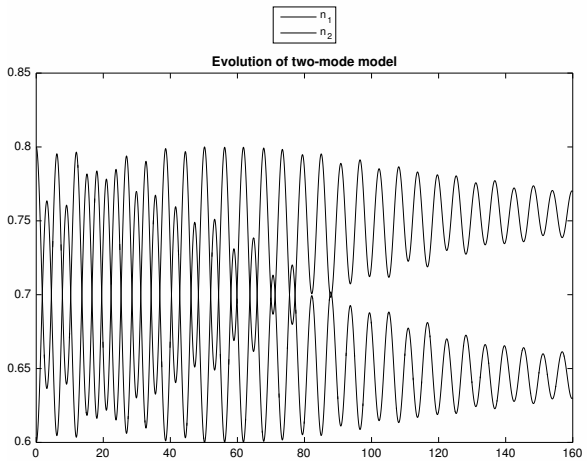

(c) $\tau = 4$

FIGURE 5.3: Time evolution with rule $\tilde{\rho}_B$.

6 Dynamics with rule acting on the system: Quantum GoL

In this Chapter, we apply the general ideas concerning the (H, ρ)-induced dynamics presented in Chapter 5 to extend the classical Game of Life, and we analyze several aspects of this extension. The described dynamics, which is obtained by considering the combined action of the Hamiltonian H of the system and a suitable set ρ of conditions acting repeatedly on the system itself, is not necessarily periodic or quasi-periodic, as one could imagine for conservative systems with a finite number of degrees of freedom. In fact, it may have quite different behaviors depending on the explicit forms of H, ρ, as well as on the initial conditions. The results here reported belong to the joint paper Bagarello et al., 2017.

6.1 Classical setting and new perspectives

The Game of Life (hereafter, *GoL*) can be thought of as a sort of a dynamical system $\mathcal{S}$ in which one is interested in the changes of the local densities of a given population $\mathcal{P}$ living in a lattice $\mathcal{R}$. In the generic cell C_j of $\mathcal{R}$, the density of the population changes according to what happens in the other cells surrounding C_j itself (typically, the eight surrounding cells characterizing the so-called Moore neighborhood); in particular, this change is driven by the sum of the densities of the populations in these surrounding cells. In other words, the *GoL* is a two-dimensional cellular automaton in which each cell at any time assumes only two possible values: 0 if the cell is in a dead state, 1 if the cell is alive. At each *generation*, a given cell undergoes a transition according to specific rules based on its own state and on the states of the surrounding cells. More formally, the *GoL* can be written as the cellular automaton

$$A_{GoL} = \{Z^2_{GoL}, \mathcal{N}, \{0,1\}, f\},$$

where Z_{GoL} is the set of all integers such that Z^2_{GoL} represents the two-dimensional array of the cellular space, $\mathcal{N}$ is the Moore neighborhood index, $\{0,1\}$ is the set of the possible states of a cell, and $f : \{0,1\}^{|\mathcal{N}|+1} \rightarrow$

$\{0,1\}$ is the transition function defined as

$$f(1,\{\alpha\}) = 1 \text{ if } \left(\left(\sum_{\alpha\in\mathcal{N}}\alpha = 2\right) \vee \left(\sum_{\alpha\in\mathcal{N}}\alpha = 3\right)\right), \tag{6.1}$$

$$f(1,\{\alpha\}) = 0 \text{ if } \left(\left(\sum_{\alpha\in\mathcal{N}}\alpha < 2\right) \vee \left(\sum_{\alpha\in\mathcal{N}}\alpha > 3\right)\right), \tag{6.2}$$

$$f(0,\{\alpha\}) = 1 \text{ if } \left(\sum_{\alpha\in\mathcal{N}}\alpha = 3\right), \tag{6.3}$$

$$f(0,\{\alpha\}) = 0 \text{ if } \left(\sum_{\alpha\in\mathcal{N}}\alpha \neq 3\right). \tag{6.4}$$

Here , $\{\alpha\}$ is the set of all state values in $\mathcal{N}$, and $|\mathcal{N}|$ is the cardinality of $\mathcal{N}$. These rules mimic the basic processes of life and death: rule (6.1) represents condition for sustainable life, rule (6.2) represents death due to under or over population, rule (6.3) represents a birth condition, and rule (6.4) corresponds to the permanence of a death state condition. Cells are generally updated synchronously, *i.e.*, they undergo state transitions at the same time, although in some papers there are variations implementing also asynchronous evolutions (see, for instance, Lee et al., 2004).

The use of quantum ideas for cellular automata (QCA) dates back to the 1980's (Feynman and Shor, 1982; Deutsch, 1985; Grössing and Zeilinger, 1988), and has attracted the interest of several scientists during the last decades. The motivation behind these approaches mainly relies on the possibility of reproducing, by using generalized structures, quantum phenomena such as interference, or entanglement effects. In this context, various *quantum* versions of the Game of Life have been developed. In Flitney and Abbott, 2010, by using standard arguments in the QCA, the state $|\psi\rangle$ of a cell is defined as a superposition of the states $|1\rangle$ (life) and $|0\rangle$ (death), forming a qubit $|\psi\rangle = c_1|1\rangle + c_0|0\rangle$, and the process of birth-death-sustain of a cell is reproduced through the combination of suitable birth and death operators. A different quantum version of the Game of Life, based on the number operator, and involving a Hamiltonian operator which includes mechanisms resembling the standard rules of the Game of Life, is developed in Bleh, Calarco, and Montangero, 2012.

The quantum version of the *GoL* introduced in this Chapter, hereafter *QGoL*, is not intended as an attempt to study any quantum property of the QCA, but just as a proposal of a deterministic method describing the structure of peculiar cellular automata by means of an enriched concept of rule, and under the assumption that, during consecutive transients, the system is driven by an energy-like operator, *i.e.* the Hamiltonian operator H, describing the most relevant mechanisms occurring in the system itself. Therefore, differently from the *GoL*, we shall consider a quantic dynamics of the population before applying the rule ρ, which somehow extends the rule introduced in (6.1)-(6.4). The new state deduced after the rule is implemented is then considered as the starting point for the next iteration of the time evolution, which is again driven by H. At the end of this new iteration, ρ is applied once again, and a new state is deduced. And so on. Of course, the dynamics one deduces in this way is driven by several ingredients, and

various scenarios can arise.

6.2 The framework for the Quantum Game of Life

In this Section, we introduce the operatorial framework for the variant of the classical *GoL* called Quantum Game of Life (*QGoL*). The model is constructed as follows: to each cell of the lattice a fermionic variable, taking value 0 or 1 only[1], is attached , and each possible configuration is given as a vector on the Hilbert space $\mathcal{H}$ described below. The quantum approach we want to describe is based on the assumption that the observables of the system $\mathcal{S}$ we are interested to, among which there is the state of each cell, are described by operators acting on $\mathcal{H}$.

We suppose that the system $\mathcal{S}$ is made up of a single population $\mathcal{P}$ living on a square lattice $\mathcal{R}$ made by L^2 cells. At time zero, each cell may be dead or alive (states that are represented by the values 0 or 1, respectively). This setting is well described by using a two state vector φ_{n_α} for any single cell, where $\alpha \in \{1, \dots, L^2\}$ labels the cell itself, and $n_\alpha = 0, 1$, and by building these vectors up in a family of fermionic operators, say $\{a_\alpha\}_{\alpha\in\{1,\dots,L^2\}}$, according to the formalism described in Section 1.2. In this way, we have that the eigenvalues $n_\alpha = 0, 1$ of the number operator $N_\alpha = a_\alpha^\dagger a_\alpha$ for the cell C_α describe exactly the status of that cell (dead or alive), whereas the state vector of the system

$$\varphi_{\mathbf{n}} = \otimes_{\alpha=1}^{L^2} \varphi_{n_\alpha}, \quad \mathbf{n} = (n_1, n_2, ..., n_{L^2}), \tag{6.5}$$

describes the status of each cell in $\mathcal{R}$. The Hilbert space $\mathcal{H}$ is constructed by taking the closure of the linear span of all these vectors. The scalar product is the natural one. In particular, in each cell the scalar product reduces to the one in $\mathbb{C}^2$. The CAR in $\mathcal{R}$ extend those above:

$$\{a_\alpha, a_\beta^\dagger\} = \delta_{\alpha,\beta} \mathbb{1}, \qquad \forall \alpha, \beta, \tag{6.6}$$

where a_α is now a $2^{L^2} \times 2^{L^2}$ matrix operator satisfying

$$\begin{aligned} a_\alpha \varphi_{\mathbf{n}} &= 0 \quad \text{if } n_\alpha = 0, \\ a_\alpha^\dagger \varphi_{\mathbf{n}} &= 0 \quad \text{if } n_\alpha = 1, \\ N_\alpha \varphi_{\mathbf{n}} &= a_\alpha^\dagger a_\alpha \varphi_{\mathbf{n}} = n_\alpha \varphi_{\mathbf{n}}. \end{aligned}$$

The self-adjoint Hamiltonian describing the diffusion of a population in a closed region through fermionic operators (see Bagarello, Gargano, and Oliveri, 2015; Gargano, 2014) is assumed here to be

$$H = \sum_{\alpha=1}^{L^2} a_\alpha^\dagger a_\alpha + \sum_{\alpha,\beta=1}^{L^2} p_{\alpha,\beta} \left(a_\alpha a_\beta^\dagger + a_\beta a_\alpha^\dagger \right), \tag{6.7}$$

where $p_{\alpha,\beta}$ are non-negative real parameters such that $p_{\alpha,\beta} = 1$ if $\alpha \neq \beta$ and the cell α is comprised in the Moore neighborhood of the cell β, and $p_{\alpha,\beta} = 0$ otherwise. Notice that letting the parameters $p_{\alpha,\beta}$ range over all positive real value, and not only zero and one, as it is in Bagarello, Gargano,

[1] Equivalently, one could use spin variables and work with Pauli matrices.

and Oliveri, 2015, means that the speed of diffusion from one cell to another may be changed. However, for the sake of simplicity, this possibility is avoided here.

Consider now the essential variation with respect to the classical *GoL*, that is, before the generation of a new state, we fix a *transient time* τ such that in the time interval $[0, \tau[$ the states of the neighboring cells interact governed by the Hamiltonian H given in (6.7) according to the laws of quantum mechanics. Hence, as time t increases, $t < \tau$, $\mathcal{S}$ is no more in its initial state, $\phi_{\mathbf{n}^0}$, but instead in the evolved state $\exp(-iHt)\phi_{\mathbf{n}^0}$, which, in general, is a superposition of the vectors $\varphi_{\mathbf{n}}$ defined in (6.5). Following the scheme described in Bagarello, 2012, we relate the mean values of the number operators N_α to the new states of each cell. The evolution of the number operators is given by the law

$$N_\alpha(t) := \exp(iHt)N_\alpha(0)\exp(-iHt),$$

and their mean values on some suitable state $\phi_{\mathbf{n}^0}$ describing the system at $t = 0$ by means of

$$n_{\alpha,0}(t) = \langle \phi_{\mathbf{n}^0}, N_\alpha(t)\phi_{\mathbf{n}^0}\rangle = \|a_\alpha \exp(-iHt)(t)\varphi_{\mathbf{n}^0}\|^2. \tag{6.8}$$

Because of the CAR, the values $n_{\alpha,0}(t)$ belong to the range $[0, 1]$, for all $\alpha \in \{1, \dots, L^2\}$ and all $t \geq 0$. Hence, they can be endowed with a probabilistic meaning: if $n_{\alpha,0}(t) \ll 1$ then the cell α has high probability to be in a dead state.

Thus, let t vary in the interval $[0, \tau[$. After this interval has elapsed, that is at time τ, the rule is applied synchronously to all the cells, so that the upgraded states are all either 0 or 1, and the new state vector, obtained through (6.5), is $\varphi_{\mathbf{n}^1}$. This process is iterated for several generations. The whole procedure can be schematized as follows.

loop {From generation k to generation $k + 1$}

- For each cell α set $n_{\alpha,k}(0) = n_{\alpha,k}$, with $n_{\alpha,k} = 0$ or 1, and construct $\varphi_{\mathbf{n}^k}$ through (6.5).
- Compute $\exp(-iH\tau)\varphi_{\mathbf{n}^k}$ and the related $n_{\alpha,k}(\tau)$, in analogy with (6.8), out of it.
- Apply the rule synchronously to $\exp(-iH\tau)\varphi_{\mathbf{n}^k}$ to compute $\mathbf{n}^{k+1}$. In each cell you will have $n_{\alpha,k+1} = 0$ or 1.
- Set $k \to k + 1$.

end loop

In such a way, we obtain in each cell a sequence of states $n_{\alpha,k}$, where the index k labels the generic k-th generation. The conditions determining the fact that, at each generation, $n_{\alpha,k}$ is set to 0 or 1 are expressed by the applied rule. Specifically, the rule ρ imposed here for the generation of the

new state is defined as follows:

$$\rho_\sigma(n_{\alpha,k}=1)=1 \text{ if } \left(2-\sigma\leq\sum_{\beta\in\mathcal{N}} n_{\beta,k}\leq 3+\sigma\right), \tag{6.9}$$

$$\rho_\sigma(n_{\alpha,k}=1)=0 \text{ if } \left(\sum_{\beta\in\mathcal{N}} n_{\beta,k}<2-\sigma\right)\vee\left(\sum_{\beta\in\mathcal{N}} n_{\beta,k}>3+\sigma\right), \tag{6.10}$$

$$\rho_\sigma(n_{\alpha,k}=0)=1 \text{ if } \left(3-\sigma\leq\sum_{\beta\in\mathcal{N}} n_{\beta,k}\leq 3+\sigma\right), \tag{6.11}$$

$$\rho_\sigma(n_{\alpha,k}=0)=0 \text{ if } \left(\sum_{\beta\in\mathcal{N}} n_{\beta,k}<3-\sigma\right)\vee\left(\sum_{\beta\in\mathcal{N}} n_{\beta,k}>3+\sigma\right), \tag{6.12}$$

where σ is a positive parameter, which can be seen as a measure of the deviation from the original classical rule. In particular, if $\sigma = 0$, we recover essentially the rule expressed by (6.1)-(6.4). Through this procedure we obtain a sequence of functions $n_{\alpha,k}(t)$ (with $t \in [0,\tau[$), which define the (H,ρ)-induced dynamics for the number operators N_α ($\alpha = 1,\ldots,L^2$).

We remark here that, if we look at the standard *GoL*, the time plays no role: what is really relevant is the rule ρ. This can be easily recovered, in the described scheme, just taking $\tau = 0$, or assuming that $H = 0$, which are, therefore, two limiting cases of this strategy. On the other hand, if we assume that ρ is the identity map (it means essentially that we have no rule at all), we trivially go back to the standard quantum dynamics.

A second important consideration concerns the formation of periodic orbits. As a matter of fact, we stress that, because of the finite dimensionality of the quantum system and of the finite number of the possible states of each cell, each initial condition necessarily generates a periodic solution (the worst possible case is that an initial state $\phi_{\mathbf{n}^0}$ returns in itself after $2^{L^2}-1$ generations).

6.3 The dynamics of the QGoL: results and comparative analysis

This Section is devoted to a detailed analysis, by means of different tools, of the results that can be deduced from the operatorial model of Game of Life described above. At first, we study the influence of the parameters τ and σ on the (H,ρ)-induced dynamics of the *QGoL*; in fact, the value of τ defines the time range during which only the Hamiltonian–driven evolution is active before the application of the rule (6.9)–(6.12), whereas the value of σ is intended as a measure of the deviation of the new rule with respect to the one originally given in (6.1)–(6.4). Successively, we analyze the output of the model by means of both the spectral and blob analysis, with the aim of describing differences and similarities between the *QGoL* and the *GoL*.

All the simulations shown below are performed on a two–dimensional square lattice of size L^2, with $L = 33$, by choosing initial configurations in which the state of each cell is initialized in a random way, with equal probabilities to have value 0 or 1. The results obtained from the *QGoL* evolution are compared to the ones deduced from the simulations of the *GoL* so as to highlight the main effects due to the $(H,\rho)-$induced dynamics.

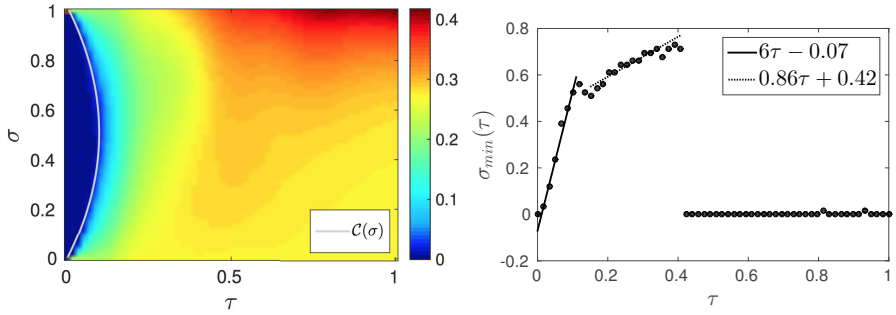

(a) Distribution of $\Delta^{GoL}_{QGoL}(\tau, \sigma)$ (b) $\sigma_{min}(\tau)$ for $0 \leq \tau \leq 1$

FIGURE 6.1: **(a)** The distribution $\Delta^{GoL}_{QGoL}(\tau, \sigma)$ of the L_1-error norms between the states of the cells obtained by the *QGoL* and the *GoL* at the second generation. For a fixed σ, Δ^{GoL}_{QGoL} essentially increases with the time τ in which the Hamiltonian–driven evolution takes place. The dependence of $\Delta^{GoL}_{QGoL}(\tau, \sigma)$ on τ may be expressed as follows: for $\tau < 0.4$, $\Delta^{GoL}_{QGoL}(\tau, \sigma)$ increases as σ approaches 0 or 1, while for $\tau > 0.4$ the error increases with σ. The white curve is the quadratic curve $\mathcal{C}(\sigma) = -0.337\sigma^2 + 0.384\sigma$ approximating the contour level $\Delta^{GoL}_{QGoL}(\tau = 0.1, \sigma = 0.5) = 0.02$. **(b)** The minimum $\sigma_{min}(\tau)$ of $\Delta^{GoL}_{QGoL}(\tau, \cdot)$ for a fixed τ. Different linear growth rates are visible for three τ ranges; for $\tau > 0.4$ $\sigma_{min}(\tau) \approx 0$, which is explicative of the presence of a phase transition for $\tau \simeq 0.4$.

6.3.1 The parameters τ and σ

The parameter τ defines the time range of the (H, ρ)–induced dynamics of the system before the rule is applied, whereas the parameter σ gives a measure of how much the rule for the generation of a new state in the quantum setting differs from the set of conditions used in the classical case. Obviously, for $\tau = 0$ there is no Hamiltonian–driven dynamics at all, and, therefore, if $\sigma = 0$, we recover the classical behavior of the *GoL*. To study how the parameters τ and σ modify the classical evolution, we evaluate first of all the following L_1-error norm between the states of the cells obtained by the quantum and the classical games of life at the second generation ($K = 2$):

$$\Delta^{GoL}_{QGoL}(\tau, \sigma) = \frac{1}{L^2} \sum_{\alpha=1}^{L^2} |n_{\alpha,2} - \mathring{n}_{\alpha,2}|, \tag{6.13}$$

where $n_{\alpha,2}$ and $\mathring{n}_{\alpha,2}$ are the states in the cell α reached by the *QGoL* and the *GoL*, respectively. Hence, $\Delta^{GoL}_{QGoL}(\tau, \sigma) = 0$ when $n_{\alpha,2} = \mathring{n}_{\alpha,2}$ for all α, *i.e.*, when the *QGoL* and the *GoL* actually coincide (at the second generation, and so at all generations). In order to consider more robust results, we compute the distribution $\Delta^{GoL}_{QGoL}(\tau, \sigma)$ by averaging the differences obtained from 100 different random initial conditions for fixed τ and σ.

The distribution $\Delta^{GoL}_{QGoL}(\tau, \sigma)$ is shown in fig. 6.1(a) for $0 \leq \tau, \sigma \leq 1$. The way in which τ affects Δ^{GoL}_{QGoL} is clear: Δ^{GoL}_{QGoL} increases with τ. This is in agreement with the fact that $\tau > 0$ corresponds to an effect which is absent in the classical situation, since, in the latter case, no time evolution exists at all. In the *GoL*, in fact, the rule only, applied again and again, determines the different generations. The dependence of $\Delta^{GoL}_{QGoL}(\tau, \sigma)$ on

σ is much richer, since it is also related to the value of τ. For $\tau < 0.4$, $\Delta^{GoL}_{QGoL}(\tau, \sigma)$ increases as σ approaches 0 or 1, while it decreases for intermediate values of σ. On the other hand, for $\tau > 0.4$ the L_1-error norm increases with τ and with σ, taking its minimum value for $\sigma = 0$. This is essentially what one could expect, since larger values of τ and σ represent major differences from the classical situation. Nevertheless, it is interesting to notice that, for $\tau < 0.4$, $\sigma = 0$, we have a maximum value for $\Delta^{GoL}_{QGoL}(\tau, \sigma)$. This suggests that, even if $\sigma = 0$ (so that the new rules and the classical ones do coincide), the time evolution of the system driven by H is already enough to significantly modify the behavior of the system. In fig. 6.1(a), the quadratic curve $\mathcal{C}(\sigma) = -0.337\sigma^2 + 0.384\sigma$, approximating the contour level $\Delta^{GoL}_{QGoL}(\tau = 0.1, \sigma = 0.5) = 0.02$, is also shown. This contour level surrounds the region $\tau < \mathcal{C}(\sigma)$ in which Δ^{GoL}_{QGoL} has its lowest values, and, as it will be detailed in Section 6.4, it allows to characterize the region of τ and σ where the periodicity of a periodic orbit of the *QGoL* case differs from the *GoL* case.

The performed numerical simulations also suggest that, in general, for a fixed τ, there is always a value $\sigma_{min}(\tau)$ for which $\Delta^{GoL}_{QGoL}(\tau, \sigma_{min}(\tau))$ reaches a minimum. In particular, for very small values of τ, there exist ranges of parameter σ for which $\Delta^{GoL}_{QGoL}(\tau, \sigma)$ vanishes, so that the *QGoL* and *GoL* dynamics coincide: for instance, for $\tau = 0.01$, we obtain $\Delta^{GoL}_{QGoL}(\tau, \sigma) = 0$ for $0.009 < \sigma < 0.99$. This fact suggests, once again, that the role of the action of H is more relevant than the change in the rule ρ (*i.e.*, the passage from the classical rule to the new one). For later convenience, if for a fixed τ we have a range of minima $[\sigma_1, \sigma_2]$ of $\Delta^{GoL}_{QGoL}(\tau, \sigma)$, then we fix $\sigma_{min}(\tau) = \sigma_1$. The trend of $\sigma_{min}(\tau)$ is plotted in fig. 6.1(b), where a piecewise linear behavior with three different slopes is visible. $\sigma_{min}(\tau)$ appears increasing for $\tau \leq 0.4$; in particular, for $\tau \leq 0.1$, $\sigma_{min}(\tau)$ has a linear growth rate of 6, while for $0.1 < \tau \leq 0.4$ the linear growth rate is much lower (close to 0.87). For $\tau > 0.4$ $\sigma_{min}(\tau) \approx 0$. It looks like a phase transition for $\tau \simeq 0.4$, even if, so far, the reason for such a transition is not clear.

6.3.2 Spectral analysis

Here, we perform a statistical study of the *QGoL* by using the classical tools of the spectral analysis. In particular, for a fixed cell α, the Fourier transform of its state $n_{\alpha,k}$ at the various generations $k = 0, \ldots, T-1$ is given by

$$\tilde{n}_{\alpha,k}(f) = \frac{1}{T} \sum_{t=0}^{T-1} n_{\alpha,k} \exp\left(-i \frac{2\pi t f}{T}\right), \tag{6.14}$$

and the Fourier power spectrum is defined as

$$S(f) = \sum_{\alpha=1}^{L^2} |\tilde{n}_{\alpha,k}(f)|^2. \tag{6.15}$$

Moreover, we consider the density of alive cells at the k–th generation, say

$$D^k = \frac{1}{L^2} \sum_{\alpha=1}^{L^2} n_{\alpha,k}. \tag{6.16}$$

Roughly speaking, the power spectrum $S(f)$ gives information on the frequencies excited due to the possible presence of an equilibrium cycle solution of period T/f. The density of alive cells D^k is the ratio of alive cells for each generation k, and a stationary or periodic behavior of D^k gives information about the possible periodicity of the solution (in the sense defined in Section 5.4).

It is well known that the *GoL* has $1/f$ noise (Ninagawa, Yoneda, and Hirose, 1998), *i.e.*, its power spectrum behaves like $1/f$ at low frequencies, and in general cellular automata can have a power spectrum of the kind f^α (Ninagawa, 2008). A system showing a $1/f$ power spectrum is such that its current state is influenced by the history of the system itself; $1/f$ noise can be observed in a wide variety of phenomena such as the voltage of vacuum tubes, the rate of traffic flow, and the loudness of music. The presence of the $1/f$ behavior of the power spectrum has also been found in Lee et al., 2004 in the case of an asynchronous version of the *GoL*. Evidence of the $1/f$ noise is given in fig. 6.2(a), where the power spectrum for the *GoL* is shown for a random initial condition and $T = 4096$ generations (similar results arise, of course, also from the several numerical simulations performed using different random initial conditions). In this case, if $\tau = 0$ and $\sigma = 0$, we obtain a 2-equilibrium cycle after a transient of 277 generations (see the density of alive cells depicted in fig. 6.2(b)). Hence, in the power spectrum, there is a final peak at the frequency 2048, due to the fact that a 2-equilibrium cycle solution is a periodic orbit with period $\Omega = 2$ giving strength to the frequency $T/\Omega = 2048$. By fitting the spectrum $S(f)$ with a function Cf^α with a least square method, we obtain in the range $f = 1, \ldots, 2000$ the values $C = 0.4$ and $\alpha = -1.033$, which are consistent with the predicted $1/f$ of the power spectrum. Let us now move on to consider the *QGoL* case. The fig. 6.2(a) also shows the power spectra obtained in correspondence to $\tau = 0.1$ and various values of σ. As far as the values $\sigma = 0.1, 0.25$ are concerned, the spectrum is characterized by low power density at almost all frequencies with a peak at the first frequency $f = 0$: this is due to the fact that, after an initial transient, the whole system stabilizes to a 1-equilibrium cycle solution after very few generations. In fact, starting from the same random initial condition used for the *GoL*, the *QGoL* stabilizes to a 4–equilibrium and 6–equilibrium cycle solution for $\sigma = 0.1$ and $\sigma = 0.25$, respectively. For higher values of σ ($\sigma = 0.5$), the spectrum has almost all frequencies excited, with a clear low power behavior for small frequencies. The fitting with the function Cf^α for $f = 0, \ldots, 200$ returns $C = 0.45$ and $\alpha = -0.15$ for $\sigma = 0.5$. The circumstance that almost all the frequencies are excited, with decreasing amplitude, means that the solution does not show (at least for the number of generations here considered) any periodicity or equilibrium. However, this is just an appearance caused by the need to truncate the process because of complexity limitations, since, as already pointed out, each initial condition necessarily generates a periodic solution. This suggests that, in order to detect the periodic structure in the solution, a larger number of generations is needed.

For increasing values of τ ($\tau = 0.25, 0.5$), the situation does not change for $\sigma \leq 0.5$, since all the power spectra are similar to those observed in case of $\tau = 0.1$ and $\sigma = 0.1, 0.25$; thus, there is a 1–equilibrium cycle solution after few iterations, as the density of alive cells in figs. 6.3(b) and 6.4(b) shows. For $\tau = 0.25, 0.5$ and $\sigma = 1$ a peak at $f = 0$ is observed, and the remaining

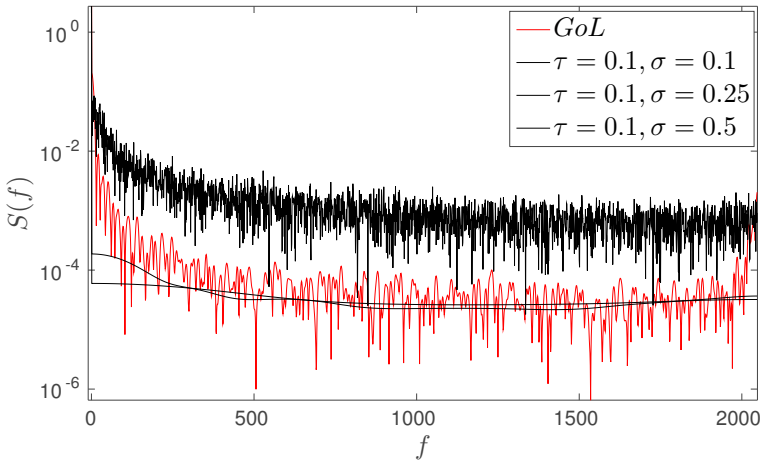

(a) Power spectrum for the *GoL*, and the *QGoL* for $\tau = 0.1$

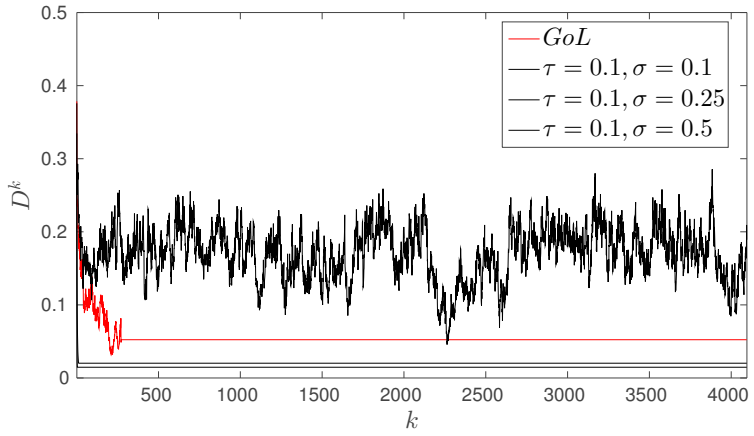

(b) Density of alive cell for the *GoL*, and the *QGoL* for $\tau = 0.1$

FIGURE 6.2: **(a)** Power spectrum of the *GoL* and the *QGoL* for $\tau = 0.1$ and various values of σ after $T = 4096$ generations starting from a random initial condition. The *GoL* exhibits a $1/f$ power spectrum, and has a 2–equilibrium cycle solution after a transient of 277 generations (see the density of the alive cell in **(b)**) leading to the peak in the frequency $f = 2048$ of the spectrum. The *QGoL* spectrum exhibits for $\sigma = 0.1, 0.25$ a low power density as a consequence of a 1–equilibrium cycle solution obtained after very few generations, while for $\sigma = 0.5$ has a $1/f^{0.15}$ behavior with all frequencies excited due to the fact that no periodic orbit has emerged yet (see **b)**).

frequencies appear excited with an amplitude similar to a "noise" signal, meaning that the evolution is virtually orderless, with a high number of alive cells in each generation (see figs. 6.3(b) and 6.4(b)): still in this case, during the computed generations no equilibrium periodic solution arises.

Comparing the obtained results with the ones relative to the *GoL*, it may be observed that, for small values of τ and σ, corresponding to small expected variations from the classical situation, we recover equilibrium solutions with periods which are smaller than those found for $\tau = \sigma = 0$. On

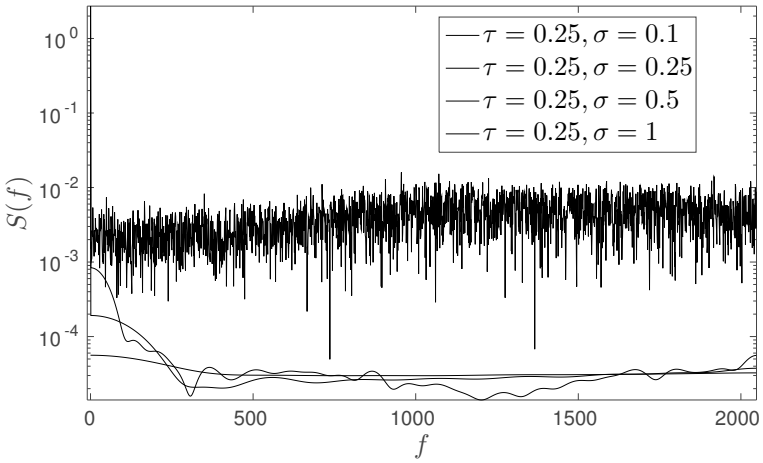

(a) Power spectrum for $\tau = 0.25$

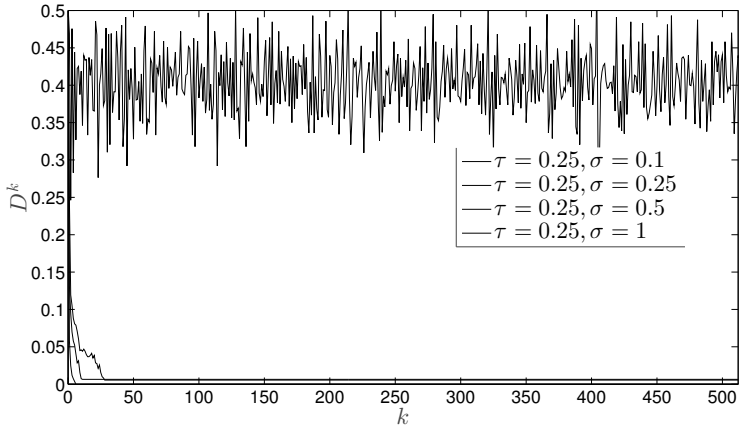

(b) Density of alive cell for $\tau = 0.25$

FIGURE 6.3: **a)** Same as fig. 6.2(a) for $\tau = 0.25$. Also in this case, for $\sigma \leq 0.5$ the power spectrum has low power density with a peak at the frequency $f = 0$ due to a 1–equilibrium solution, whereas for $\sigma > 0.5$ the spectrum has a noisy behavior with a high number of alive density cell (see figure **b)**).

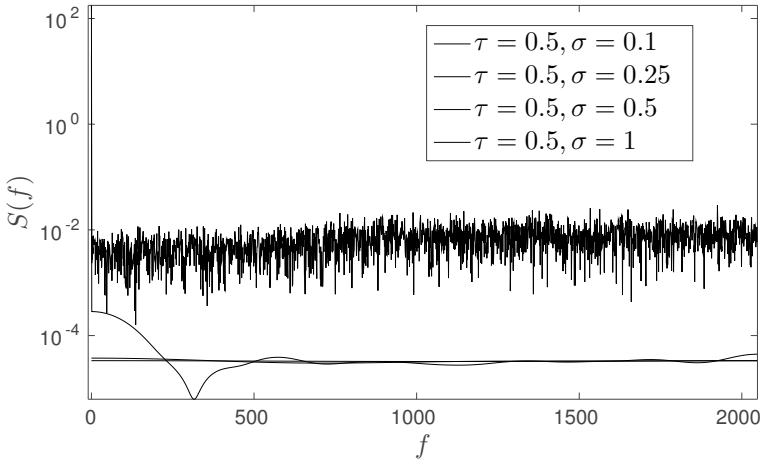

(a) Power spectrum for $\tau = 0.5$

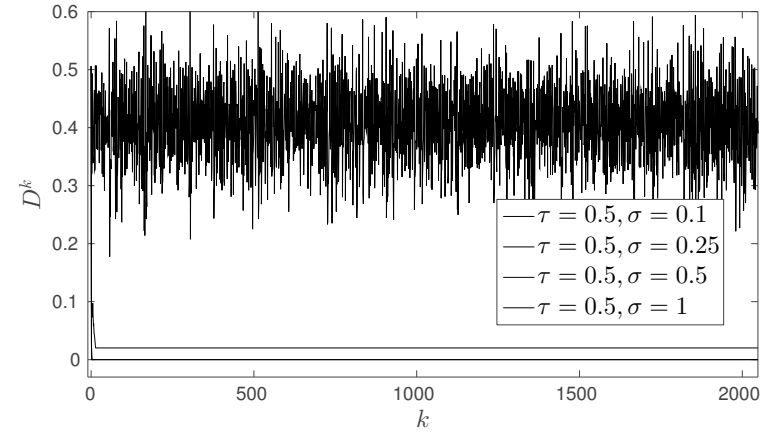

(b) Density of alive cell for $\tau = 0.5$

FIGURE 6.4: **a)** Same as fig. 6.2(a) for $\tau = 0.5$. The results in this case are similar to those obtained for $\tau = 0.25$ (see fig. 6.3(a)).

the other hand, however, for τ and σ close to 1, and for the generations computed during the performed numerical simulations, no equilibrium seems to arise, so that the situation is really different from the one corresponding to the classical *GoL*. However, as previously stated, a periodic solution necessarily exists also when adopting the proposed operatorial formulation, even if the transient period, for large values of τ and σ, may become so long that the equilibrium is not observed during the numerical tests. To give an insight on this aspect of the solutions, a case study with $L = 5$ is considered in Section 6.4, and all possible equilibria together with their transients are characterized.

6.3.3 Blob analysis

This Subsection deals with the so-called blob analysis (Lindeberg, 1994) of the generations of both the *GoL* and the *QGoL*. More precisely, each generation, that is essentially a distribution of 0 (for dead cells) and 1 (for alive cells) over a lattice, can be represented as a binary image. In particular, we perform the analysis of the 8–connected largest alive components (the *blobs*) in the binary images corresponding to the states of the system during the evolution of the *GoL* and the *QGoL*. By means of a forward scan of the lattice, each time an alive cell is encountered, we use it as a seed for the reconstruction of the binary large object of alive neighboring cells it belongs to.

For different choices of the parameters τ and σ, the analysis of the blobs detected during the evolution of the system has been carried out up to a stationary or periodic behavior of the patterns, with particular focus on the following properties:

- total number of blobs for configuration;
- area of each blob;
- perimeter of each blob;
- centroid of each blob;
- centroid of the whole configuration.

Area, perimeter and circularity are features used in shape analysis. The area of an alive connected region can be accurately estimated by counting the number of the cells of value 1 of the region. To obtain a good perimeter estimator, a contour following procedure using distances in taxicab geometry has been performed. To compute the circularities, the ratio between perimeters and areas of the various regions has been simply considered.

Comparing the evolution of the number of alive cells and the amount of connected regions, normalized with respect to the size of the lattice and the largest possible number of its connected components, respectively, the graphs plotted in figs. 6.5(a) and 6.5(b) and in figs. 6.6(a) and 6.6(b) reveal similar trends for the two curves, without strong fluctuations after few steps either in the quantum case or in the classical one. As already discussed in Subsection 6.3.2, for values of the parameter σ less than 0.5 the evolution of the *QGoL* is characterized by the achievement of stability within the first few steps (unlike the corresponding classical evolution),

whereas, for values of σ greater than or equal to 0.5, a significant delay in reaching a stable configuration compared to the classical case, which on average stabilize at most within about a thousand steps, is observed.

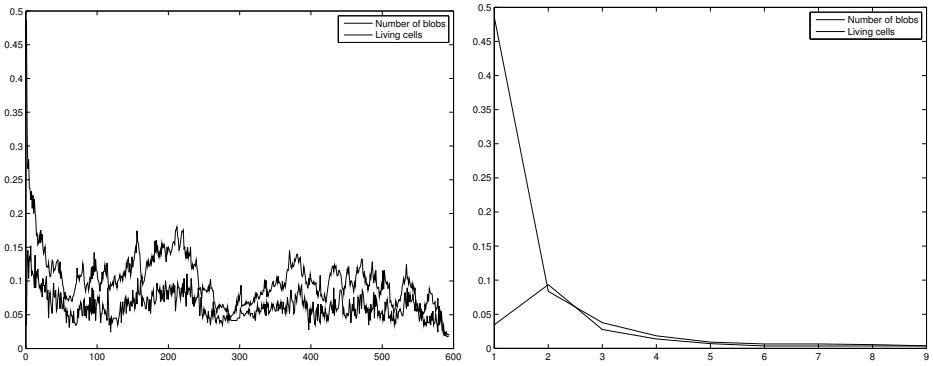

(a) *GoL* producing a 2–equilibrium cycle solution from step 594.

(b) *QGoL* for $\tau = 0.25$ and $\sigma = 0.1$ stable from step 9.

FIGURE 6.5: Number of living cells and blobs for the *GoL*, 6.5(a), and the *QGoL*, 6.5(b), for parameters $\tau = 0.25$ and $\sigma = 0.1$, normalized with respect to the dimension of the lattice and the maximum number of connected objects in it, respectively. The evolution trends of the amount of alive cells and of the connected regions are similar either in the classical or in the quantum case. For the same initial condition, the *QGoL* stabilizes to a 1–equilibrium cycle solution after very few generations, while the corresponding *GoL* generates a cyclic solution of period 2 from step 594.

The trends of the maximum, minimum and average value of the circularity parameters of the polygons corresponding to the blobs in different configurations provide a measure of how the shape of these connected regions deviates from the square shape (for which this value equals 4 divided by the number of neighboring cells). The maximum value of the circularity is reached in the case of single isolated alive cells or groups of living cells with at most one vertex in common. In the quantum case with $\tau = 0.1$, these types of connected components appear almost always, unlike the corresponding configurations in the classical case (see figs. 6.7(a) and 6.7(b)). In any case, as expected for a very short quantum interaction, the general trend of the curves for the shape parameters looks similar both for the *GoL* and the *QGoL*. As τ increases, however, as shown in figs. 6.8(a) and 6.8(b), the values corresponding to the shapes of the connected components tend to the average values.

Concerning the analysis of the centroids, the frequencies of the occurrence of the center of mass of the whole binary images in the various cells of the lattice at each step of the classical and the quantum evolution have been analyzed. The study performed for successive generations shows that, as depicted in figs. 6.9(a) and 6.9(b), while for the *GoL* the highest frequencies are arranged in a fairly broad, irregular and not always centered area, for quantum games evolving for long times before reaching the stability a shrinkage of this region to a distribution area with few centralized pixels is observed.

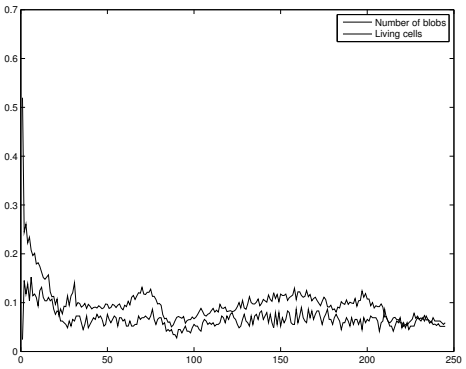

(a) *GoL* producing a 2–equilibrium cycle solution from step 245.

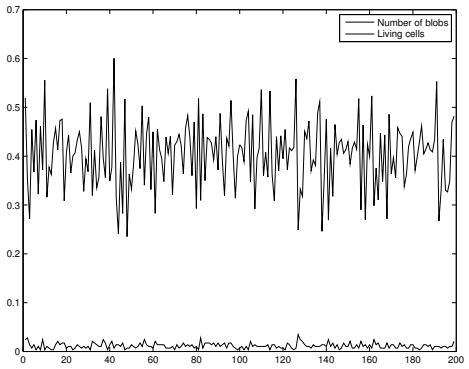

(b) *QGoL* for $\tau = 0.5$ and $\sigma = 1$ not yet stable at step 4096.

FIGURE 6.6: Number of living cells and blobs for the *GoL*, 6.6(a), and the *QGoL*, 6.6(b), for parameters $\tau = 0.5$ and $\sigma = 1$, normalized with respect to the dimension of the lattice and the maximum number of connected objects in it, respectively. The evolution trends of the amount of alive cells and of the connected regions are similar either in the classical or in the quantum game of life. For the same initial condition, the *GoL* generates a 2–equilibrium cycle solution after 245 generations, while the corresponding *QGoL* requires a significantly higher number of generations to reach the equilibrium.

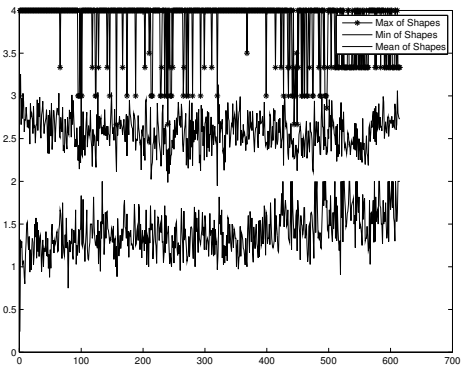

(a) Blobs' circularity parameters for the *GoL*.

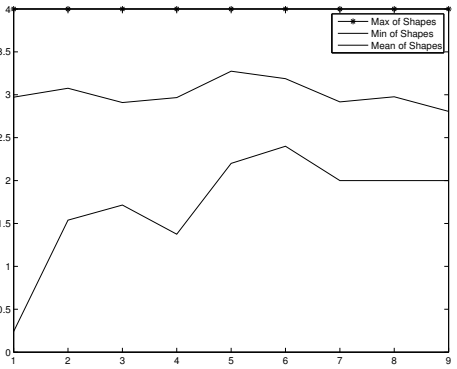

(b) Blobs' circularity parameters for the *QGoL*, for $\tau = 0.1$ and $\sigma = 0.25$.

FIGURE 6.7: Trends of the maximum, minimum and average value of the circularity parameters of the polygons corresponding to the blobs at each generation of the *GoL*, 6.7(a), and the *QGoL*, 6.7(b), for parameters $\tau = 0.1$ and $\sigma = 0.25$. The fact that the maximum of the circularities of the blobs equals 4 at each step of the *QGoL* attests the presence of single isolated alive cells or groups of living cells with at most one vertex in common during all the quantum evolution. Blobs with such a shape are not always detected in the classical case.

Moreover, the sample correlation coefficient of the cluster corresponding to the centroids of the connected regions at every generation has been taken into account.

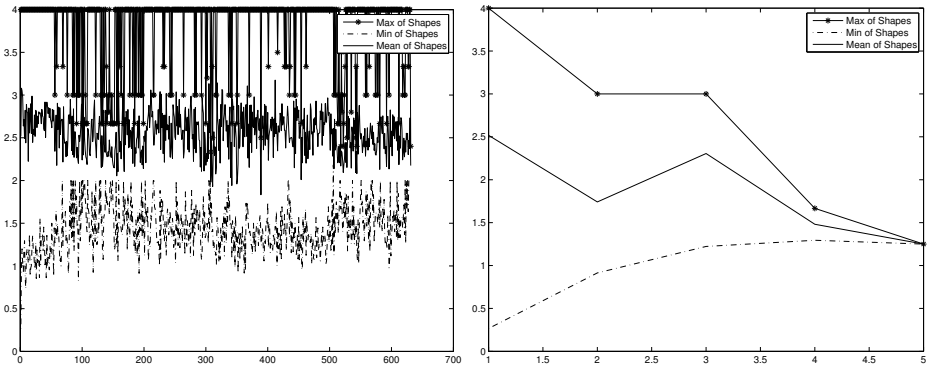

(a) Blobs circularity parameters for the *GoL*.

(b) Blobs circularity parameters for the *QGoL*, for $\tau = 0.5$ and $\sigma = 0.25$.

FIGURE 6.8: Trends of the maximum, minimum and average value of the circularity parameters of the polygons corresponding to the blobs at each generation of the *GoL*, 6.8(a), and the *QGoL*, 6.8(b), for parameters $\tau = 0.5$ and $\sigma = 0.25$. For values of τ greater than 0.1, the circularity parameters of the blobs flatten to the average value.

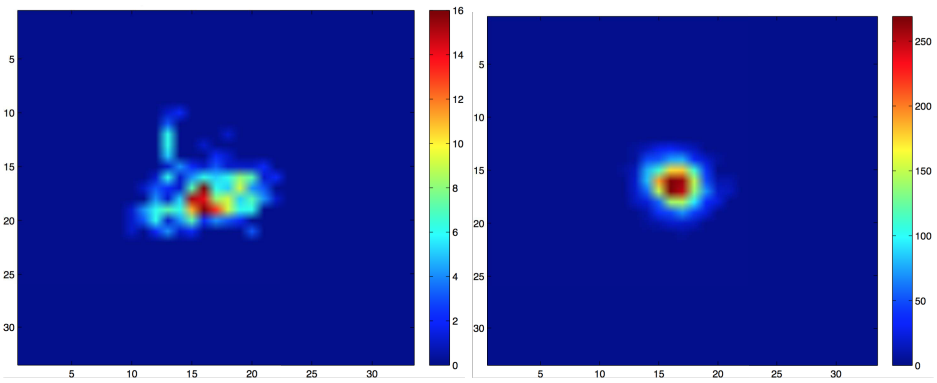

(a) Centroid occurrences for the *GoL*.

(b) Centroid's occurrences for the *QGoL*, for $\tau = 0.1$ and $\sigma = 0.5$.

FIGURE 6.9: Number of occurrences of the center of mass of the whole system after each generation of the *GoL*, 6.9(a), and the *QGoL* for parameters $\tau = 0.1$ and $\sigma = 0.5$, 6.9(b), in the various cells of the lattice. Classical evolutions are generally characterized by the arrangement of the highest frequencies in an irregular, not centrally localized area. For quantum systems stabilizing after many generations (such as the case considered in 6.9(b)), instead, centroid occurrences appear enclosed in a narrow area composed of few centralized pixels.

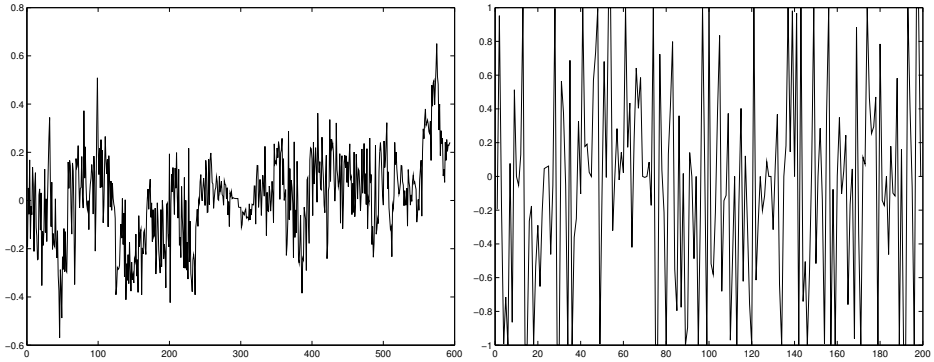

(a) Sample correlation of blobs' centroids for the *GoL*.

(b) Sample correlation of blobs' centroids for the *QGoL*, for $\tau = 0.25$ and $\sigma = 1$.

FIGURE 6.10: Sample correlation coefficients of the centroids of the various connected regions at each generation of the *GoL*, 6.10(a), and the *QGoL*, 6.10(b), for parameters $\tau = 0.25$ and $\sigma = 1$. In the case of quantum systems with τ greater than or equal to 0.25, the centroids of the blobs tend to assume configurations with direct or inverse correlation.

The trends recorded for values of τ greater than or equal to 0.25, associated with significant expected variations from the classical situation, highlight the fact that, as shown in figs. 6.10(a) and 6.10(b), to a lack of sample correlation between the centers of mass of the blobs in the case of the classical game of life corresponds, rather, in the quantum setting, a tendency of these centroids to be arranged in configurations with direct or inverse correlation.

6.4 A case study in a small domain

In this Section, in order to get an in-depth look at the dynamics of the model of the QGoL, a case study of the *GoL* and the *QGoL* dynamics in a small domain, namely choosing $L = 5$, is presented. Since in this case we have 2^{25} possible initial conditions, we may perform in a reasonable time a complete analysis of all scenarios that can arise in the classical *GoL* and how they differ from their quantum version. As remarked previously, for all the initial conditions, $\phi^l_{\mathbf{n}}, l = 0, \ldots, 2^{25} - 1$, a periodic behavior, in the sense that is explained in Section 5.4, will emerge. Each initial condition (a distribution of 0 and 1 in the 25 cells of the lattice) can be considered as the binary representation of an integer in the range $[0, 2^{25} - 1]$; therefore, one can think to label each initial condition with the corresponding integer.

For $\tau = \sigma = 0$, *i.e.*, in the classical *GoL*, following the evolution for all initial conditions, we get that the possible evolutions lead to periodic solutions, and that the observed periods are 1, 2, 3, 4, 5, 10, and 20. Since the data so obtained show that many initial conditions lead to the same periodic solutions, we can group the initial conditions in equivalence classes, see Table 6.1.

A first interesting analysis consists in considering the length of the transient for the different periodic solutions. Below, we report the observed data. For the initial conditions leading to the 1-equilibrium cyclic solutions,

Period Ω	1	2	3	4	5	10	20
# of initial conditions	3455	1225	200	200	20	60	20

TABLE 6.1: List all the possible values of the period Ω for the *GoL* in the case $L = 5$, and number of equivalence classes of initial conditions leading to an Ω-periodic solution.

the length of transients has a mean value of about 8; most initial configurations have very short transients (less than 7 generations), and, as the length of transients increases (its maximum is 51), the number of the initial conditions admitting them decays exponentially. For initial conditions leading to the 2–equilibrium cyclic solutions, the situation is quite the same: the length of transients has a mean value of about 5; most initial conditions have very short transient (less than 5 generations), and, as the length of transients increases (its maximum is 23), the number of the initial conditions admitting them decays exponentially. For initial configurations leading to the 3–equilibrium cyclic solutions, the length of transients is in the range 1 to 4, and most of the initial conditions have one or two transient generations.

For initial conditions leading to the 4–equilibrium cyclic solutions, the length of transients has a mean value of about 8; most of the initial conditions have a transient length between 1 and 13, and the maximum value is 32. For initial conditions leading to the 5–equilibrium cyclic solutions, the length of transients has a mean value of about 5, which is also the value with the highest frequency; most of the remaining initial conditions exhibit almost uniformly distributed transients of length equal to 1, 6, 7 and 8 (which is the maximum). For initial conditions leading to the 10–equilibrium cyclic solutions, the length of transients is in the range 1 to 10, and the distribution is almost uniform except for the extrema of the interval. Finally, for initial conditions leading to the 20–equilibrium cyclic solutions, the length of transients has a mean value of about 4, and most of the initial conditions have a transient length between 1 and 2, while the maximum number of transients is 15.

Consider now the behavior exhibited by the *QGoL*, and let $T^{\ell}(\tau, \sigma)$ be the number of transient generations needed to reach a $P^{\ell}(\tau, \sigma)$-periodic solution for a generic initial condition labeled with ℓ. In the case of the classical *GoL* evolution ($\tau = 0$, $\sigma = 0$), we have the values of $P^{\ell}(0, 0)$ (1, 2, 3, 4, 5, 10, 20, respectively). To investigate how $T^{\ell}(\tau, \sigma)$ and $P^{\ell}(\tau, \sigma)$ are affected in the (H, ρ)–dynamics by the parameters τ and σ, we compute the following mean distributions

$$\mathcal{T}_P(\tau, \sigma) = \frac{1}{N_P} \sum_{k_P=1}^{N_P} \left(T^{j_{k_P}}(\tau, \sigma) - T^{j_{k_P}}(0, 0) \right), \tag{6.17}$$

$$\Omega_P(\tau, \sigma) = \frac{1}{N_P} \sum_{k_P=1}^{N_P} \left(P^{j_{k_P}}(\tau, \sigma) - P^{j_{k_P}}(0, 0) \right), \tag{6.18}$$

where $j_1, \ldots, j_{N_P}$ label the initial conditions leading to a P-periodic solution. $\mathcal{T}_P(\tau, \sigma)$ and $\Omega_P(\tau, \sigma)$ allow us to determine where the transient and the periodic orbit length of the equilibrium cycle solution change according to the parameter τ and σ with respect to the *GoL*, as they are a measure of

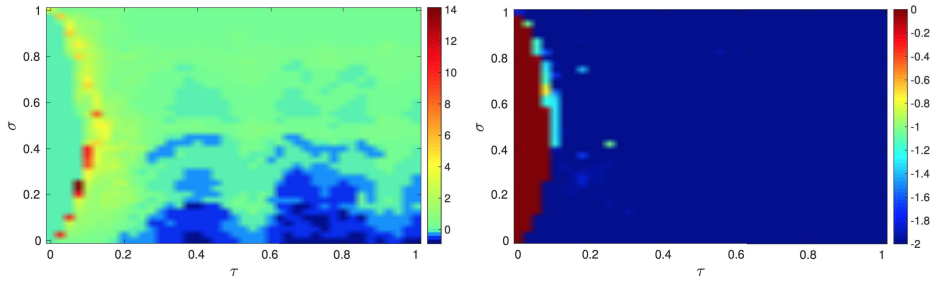

(a) $\mathcal{T}_3(\tau, \sigma)$ (b) $\Omega_3(\tau, \sigma)$

FIGURE 6.11: The distribution $\mathcal{T}_P(\tau, \sigma)$ in **(a)**, and $\Omega_P(\tau, \sigma)$ in **(b)** for the period $P = 3$. For $\tau < \mathcal{C}(\sigma)$, $\mathcal{T}_P(\tau, \sigma)$ and $\Omega_P(\tau, \sigma)$ vanish, hence there is no substantial difference between the *QGoL* and the *GoL* case. The most relevant differences arise for $\tau \approx \mathcal{C}(\sigma)$ where it is evident how in the *QGoL* case the solution is an equilibrium cyclic solution having a period lower than the one obtained in the*GoL* case and the length of transient before reaching the orbit is higher than the one in the *GoL* case. For $\tau > \mathcal{C}(\sigma)$ the situation is quite different: the periodicity of the *QGoL* solution is in general lower than the one in the *GoL* case, and the length of transient before reaching the orbit can decrease or increase with respect to the *GoL* case according to the various values of τ and σ.

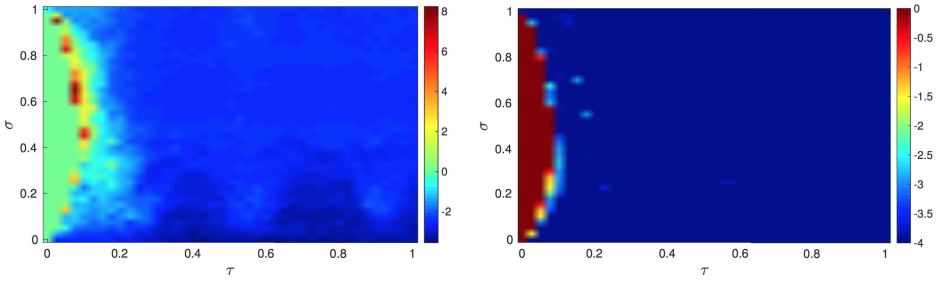

(a) $\mathcal{T}_5(\tau, \sigma)$ (b) $\Omega_5(\tau, \sigma)$

FIGURE 6.12: Same as fig. 6.11 for $P = 5$. Also in this case the main differences between the *GoL* and the *QGoL* evolution are visible for $\tau \approx \mathcal{C}(\sigma)$, and, compared to the case $P = 3$, the length of the transient of the equilibrium cycle solution in the *QGoL* case is always lower than the one in the *GoL* case.

the variations between the *GoL* and the *QGoL* case. The results are shown in figs. 6.11 and 6.14 for the periodic orbit lengths $P = 3, 5, 10, 20$. Notice that, in terms of the transient length, the most relevant differences arises for $\tau = 0.1, \sigma > 0.5$ along the curve $\tau = \mathcal{C}(\sigma) = -0.337\sigma^2 + 0.384\sigma$ for $P = 5, 10, 20$, while for $P = 3$ the peaks are reached for $\tau < 0.1, \sigma < 0.5$ again along the curve $\tau \approx \mathcal{C}(\sigma)$.

For $\tau < \mathcal{C}(\sigma)$, it is observed that $\mathcal{T}_P(\tau, \sigma)$ and $\Omega_P(\tau, \sigma)$ vanish, meaning that for $\tau < \sigma$ there is no substantial difference between the *QGoL* and the *GoL* case. On the other hand, for $\tau > \mathcal{C}(\sigma)$ the length of the periodic orbit $P^l(\tau, \sigma)$ is dramatically lower than the *GoL* case.

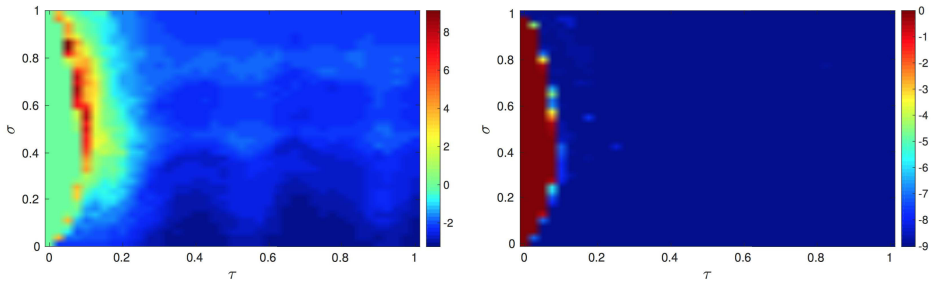

(a) $\mathcal{T}_{10}(\tau, \sigma)$ (b) $\Omega_{10}(\tau, \sigma)$

FIGURE 6.13: Same as fig. 6.11 for $P = 10$. The results are similar to those obtained in the case $P = 5$.

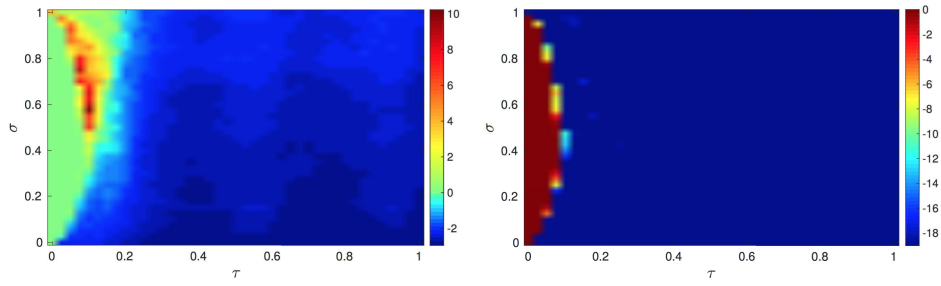

(a) $\mathcal{T}_{20}(\tau, \sigma)$ (b) $\Omega_{20}(\tau, \sigma)$

FIGURE 6.14: Same as fig. 6.11 for $P = 20$. The results are similar to those obtained in the case $P = 5, 10$.

7 Dynamics with rule acting on the model: bacterial populations

In this Chapter, we carry on the analysis of the models already introduced in Chapter 3 by examining the effects of combining the operatorial approach with the additional introduction of specific conditions acting periodically on the model itself, and combining their action with the usual quantum definition of the time evolution (see Chapter 5). Specifically, the evolution in a time interval is obtained by gluing the evolutions in a finite set of adjacent subintervals. In each subinterval the Hamiltonian is time independent, but the values of the parameters entering the Hamiltonian may be changed by the rules at the end of a subinterval on the basis of the actual state of the system, so as to express the change of the rates of interactions which reasonably take place in the considered closed bacterial ecosystem during its evolution (Di Salvo and Oliveri, 2016c; Bagarello et al., 2016).

7.1 The extended step–wise linear model in a single cell

The purpose of the following discussion is the description of the long–term survival of a bacterial population (considered in a single cell) by means of the application of specific rules modifying the original linear model presented in Section 3.2 accordingly to the state reached by the system after several time steps.

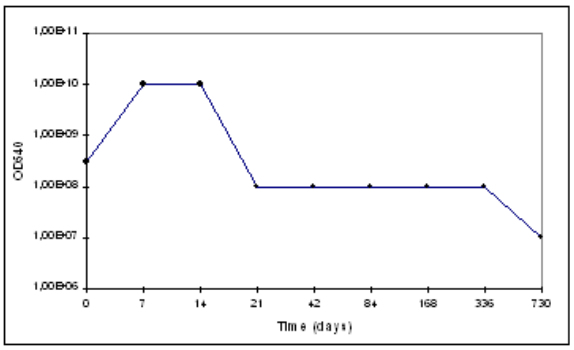

FIGURE 7.1: Viability data of a batch culture of *P. aeruginosa* monitored weekly for a period of 24 months in the case in which no nutrients were added after bacterial inoculum for all the observation period (Carnazza et al., 2008).

In practice, we consider the Heisenberg dynamics of the closed ecosystem for a time interval of length τ before applying the rule ρ; then, we assume the state reached by the system as the starting point for the next iteration of the time evolution, now governed by the new time–independent Hamiltonian operator deduced after the rule acting on the parameters has worked. At the end of this new iteration, ρ is applied again, a new set of values for the parameters deduced, and a new integration performed. The global evolution in the whole time interval we are interested in is thus obtained by gluing the evolutions in a finite set of adjacent subintervals. The stepwise dynamics we deduce in this way is driven by the particular functional form of the Hamiltonian H, the initial values for the parameters and the initial status of the system, and, of course, the rule ρ.

In particular, two different rules, ρ_1 and ρ_2, have been devised by taking into account the dynamical mechanisms implied by the variation of the scarcely recyclable garbage (7.1) and the nutrients (7.2), respectively; also, different values of τ have been tested. The specific aim is to reproduce the qualitative behavior of viability data (see fig. 7.1) of bacterial batch cultures where no nutrients at all were added after bacterial inoculum (Carnazza et al., 2008).

More explicitly, the rule ρ_1 for the generation of the new set of values for the parameters describing the interactions among the compartments on the basis of the variation of n_4 is defined as follows:

$$\begin{aligned}
&\text{if } \; n_4(k\tau) - n_4((k-1)\tau) > 0 \\
&\qquad \begin{cases} \rho_1(\lambda) = \lambda(1-0.4), \\ \rho_1(\nu_1^{(2)}) = \nu_1^{(2)}(1-0.4), \\ \rho_1(\nu_2^{(2)}) = \nu_2^{(2)}(1-0.4), \end{cases} \\
&\text{else} \\
&\qquad \begin{cases} \rho_1(\lambda) = \lambda(1+0.4), \\ \rho_1(\nu_1^{(2)}) = \nu_1^{(2)}(1+0.4), \\ \rho_1(\nu_2^{(2)}) = \nu_2^{(2)}(1+0.4), \end{cases}
\end{aligned} \tag{7.1}$$

where $k = 1, 2, \ldots$. In a very simple way, ρ_1 checks if the density of the scarcely recyclable garbage has increased compared to that of the previous step, and then modifies the values of the involved interaction parameters.

The numerical simulations shown in fig. 7.2 have been produced by choosing the inital values for the parameters $\omega_1 = 0.3$, $\omega_2 = 0.2$, $\omega_3 = 0.4$, $\omega_4 = 0.5$, $\lambda = 0.3$, $\nu_1^{(1)} = 0.25$, $\nu_1^{(2)} = 0.2$, $\nu_2^{(1)} = 0.15$, $\nu_2^{(2)} = 0.1$, the initial densities for the compartments $n_1 = 1$, $n_2 = 0.1$, $n_3 = 0$, $n_4 = 0.1$, and by imposing the rule ρ_1 after a time interval of length $\tau = 2$, $\tau = 5$ or $\tau = 10$, respectively. Due to the facts that the density of the scarcely recyclable waste material has reasonably damped oscillations and that, since it turns into nutrients rather hardly, this garbage has a low influence on the transformation of the system, it is visible how, for values of length τ of the interval of quantum evolution below 10, ρ_1 seems not to be a fitting rule for the description of the long–term survival of the bacteria, whereas for $\tau = 10$ the results are quite satisfactory.

We thus consider a second rule ρ_2 based on the control of the variation of the density of the nutrients at each step and acting both on the values of

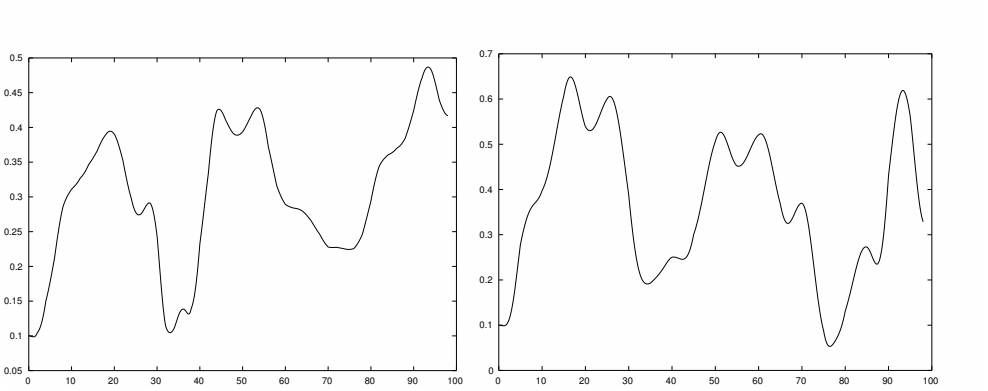

(a) $\tau = 2$ (b) $\tau = 5$

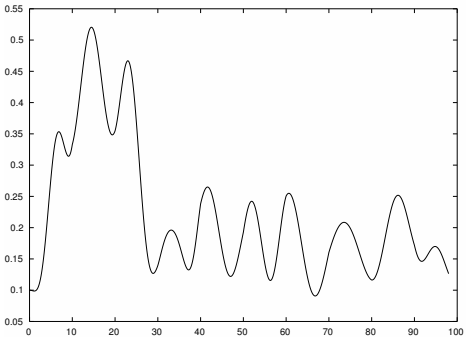

(c) $\tau = 10$

FIGURE 7.2: Time evolution of the density of the bacteria using the stepwise linear model: the rule ρ_1, based on the dynamical mechanisms implied by the variations of the scarcely recyclable garbage, is imposed after a time interval of length $\tau = 2$, (a), $\tau = 5$, (b), or $\tau = 10$, (c).

the inertia and of the involved interaction parameters according to the law

$$\begin{aligned}
&\text{if } n_1(k\tau) - n_1((k-1)\tau) > 0 \\
&\quad \begin{cases}
\rho_2(\omega_1) = \omega_1(1-0.4), \\
\rho_2(\omega_2) = \omega_2(1-0.4), \\
\rho_2(\omega_3) = \omega_3(1+0.2), \\
\rho_2(\omega_4) = \omega_4(1+0.2), \\
\rho_2(\lambda) = \lambda(1+0.4), \\
\rho_2(\nu_1^{(1)}) = \nu_1^{(1)}(1-0.4), \\
\rho_2(\nu_2^{(1)}) = \nu_2^{(1)}(1-0.4),
\end{cases} \\
&\text{else} \\
&\quad \begin{cases}
\rho_2(\omega_1) = \omega_1(1+0.4), \\
\rho_2(\omega_2) = \omega_2(1+0.4), \\
\rho_2(\omega_3) = \omega_3(1-0.2), \\
\rho_2(\omega_4) = \omega_4(1-0.2), \\
\rho_2(\lambda) = \lambda(1-0.4), \\
\rho_2(\nu_1^{(1)}) = \nu_1^{(1)}(1+0.4), \\
\rho_2(\nu_2^{(1)}) = \nu_2^{(1)}(1+0.4),
\end{cases}
\end{aligned} \tag{7.2}$$

with $k = 1, 2, \ldots$.

The graphs plotted in fig. 7.3 represent an evidence of how, even for small values of τ, the proposed approach, combining the action of the Hamiltonian H with a suitable rule able to adjust the model to the evolution of the system, provides a valuable description of what is observed in a bacterial population in a closed environment. The exact way in which the rules ρ_1 and ρ_2 change the values of the parameters entering the model in a specific case is reported in Tables 7.1 and 7.2. Even in the event that some stress factor is introduced for the scarcely recyclable garbage, the step–wise linear model employing the rule ρ_2 proves to be efficient in describing the expected behavior, characterized by a gradual decay of the densities of all the compartments of the system, as visible in fig. 7.4.

The numerical simulations obtained by considering the evolution of the system for consecutive time intervals in accordance with the Heisenberg representation and repeatedly imposing the rules ρ_1 or ρ_2, intended to account for the changes of the metabolic activity of bacteria (and, hence, in their interaction parameters) due to the increased density of the scarcely recyclable garbage or to a lack of nutrients, demonstrate the validity of the proposed stepwise method in describing the behavior of the bacteria, differently from what happens by adopting the standard linear model, even when we use the final values for the parameters deriving from several applications of the rule (as shown in fig. 7.5). Moreover, in such a simple way, the complexity limitations imposed by the fast growth of the size of the problem in the case of nonlinear models are avoided.

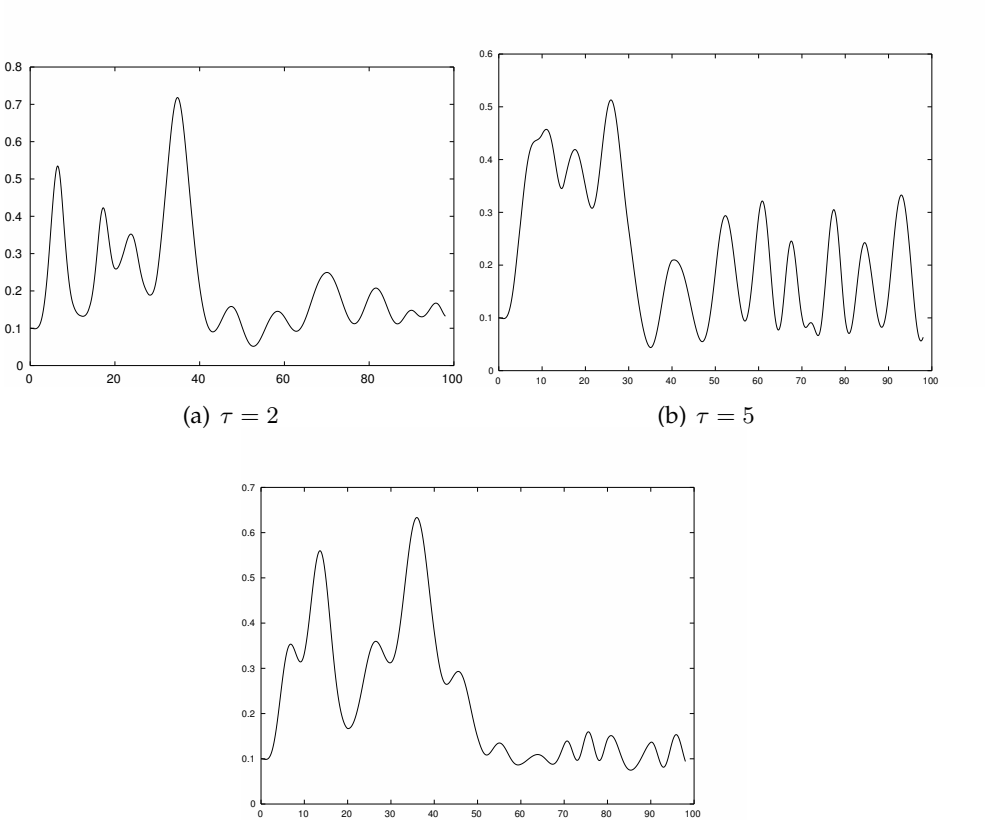

(a) $\tau = 2$ (b) $\tau = 5$

(c) $\tau = 10$

FIGURE 7.3: Time evolution of the density of the bacteria using the stepwise linear model: the rule ρ_2, based on the dynamical mechanisms implied by the variation of the nutrients, is imposed after a time interval of length $\tau = 2$, (a), $\tau = 5$, (b), or $\tau = 10$, (c).

	$]0, 10]$	$]10, 20]$	$]20, 30]$	$]30, 40]$	$]40, 50]$	$]50, 60]$	$]60, 70]$	$]70, 80]$	$]80, 90]$	$]90, 100]$
λ	0.300	0.300	0.180	0.252	0.353	0.212	0.296	0.178	0.107	0.149
$\nu_1^{(2)}$	0.200	0.200	0.120	0.168	0.235	0.141	0.198	0.119	0.071	0.100
$\nu_2^{(2)}$	0.100	0.100	0.060	0.084	0.118	0.071	0.099	0.059	0.036	0.050

TABLE 7.1: Stepwise linear model using the rule ρ_1 with $\tau = 10$: values of the parameters in the various time intervals.

	$]0, 10]$	$]10, 20]$	$]20, 30]$	$]30, 40]$	$]40, 50]$	$]50, 60]$	$]60, 70]$	$]70, 80]$	$]80, 90]$	$]90, 100]$
ω_1	0.300	0.300	0.420	0.252	0.353	0.212	0.127	0.076	0.046	0.064
ω_2	0.200	0.200	0.280	0.168	0.235	0.141	0.085	0.051	0.030	0.043
ω_3	0.400	0.400	0.320	0.384	0.307	0.369	0.442	0.531	0.637	0.510
ω_4	0.500	0.500	0.400	0.480	0.384	0.461	0.553	0.664	0.796	0.637
λ	0.300	0.300	0.180	0.252	0.151	0.212	0.296	0.415	0.581	0.349
$\nu_1^{(1)}$	0.250	0.250	0.350	0.210	0.294	0.176	0.106	0.064	0.038	0.053
$\nu_2^{(1)}$	0.150	0.150	0.210	0.126	0.176	0.106	0.064	0.038	0.023	0.032

TABLE 7.2: Stepwise linear model using the rule ρ_2 with $\tau = 10$: values of the parameters in the various time intervals.

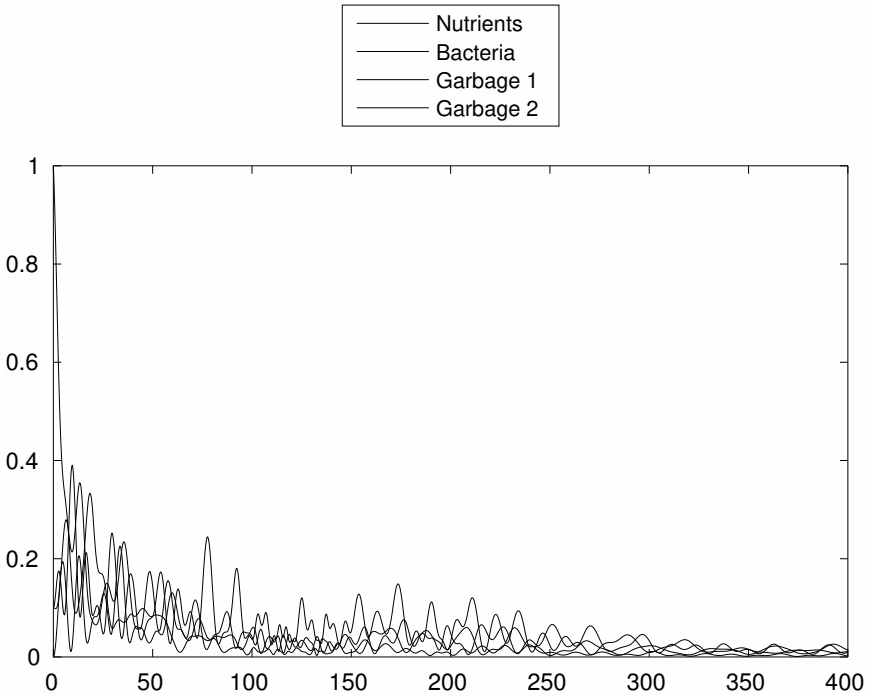

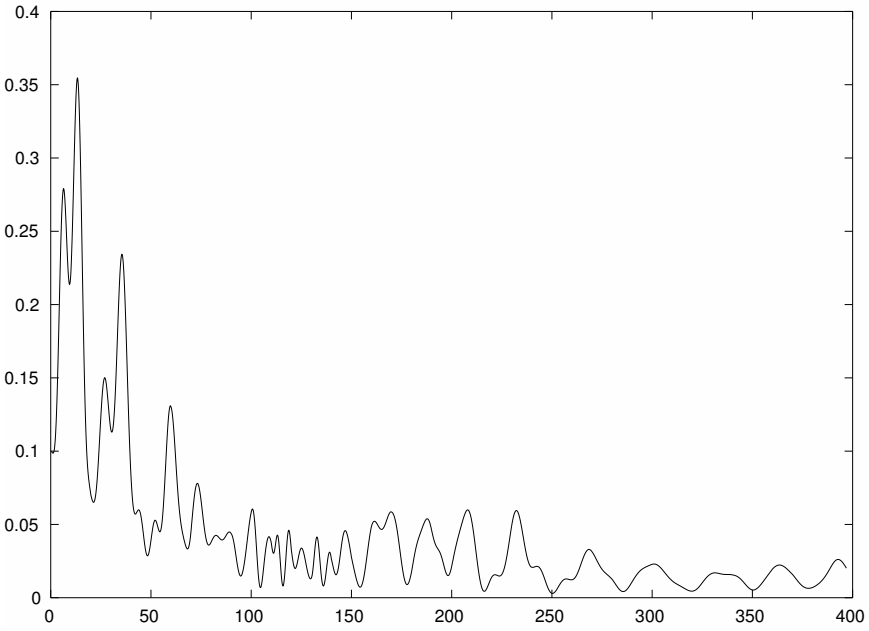

(b) Non–conservative case: bacteria

FIGURE 7.4: Time evolution of the densities of all the compartments of the ecosystem, (a), and of the bacteria, (b), using the stepwise linear model in the non–conservative case and imposing the rule ρ_2 after a time interval of length $\tau = 10$.

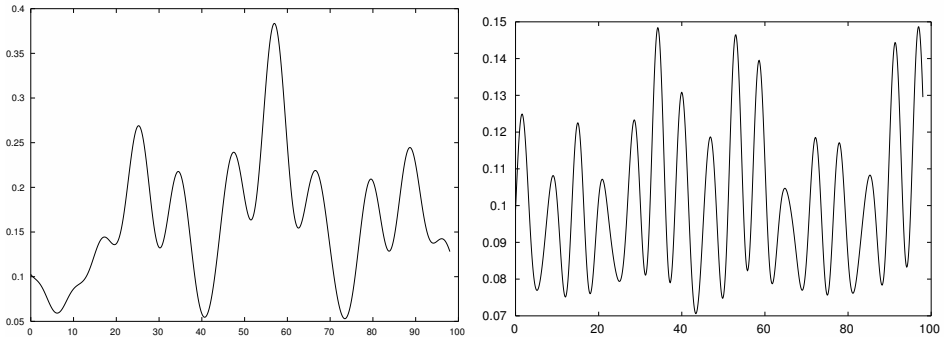

(a) ρ_1 (b) ρ_2

FIGURE 7.5: Time evolution of the density of the bacteria using the linear model with the final values of the parameters obtained applying either the rule ρ_1, (a), or the rule ρ_2, (b), after 10 time intervals of length $\tau = 10$.

7.2 Rule–induced dynamics for the long–term survival of bacteria in a square region

In this Section, we consider an example of operatorial model for the description in a finite 2D region of the long–term survival of bacterial populations belonging to certain genera, among which *Bacillus* and *Clostridium*, whose metabolism is such as to procure the survival for an indefinite time in terms of latent life when under negative stimuli (see Chapter 3). The results here reported belong to the joint manuscript (Bagarello et al., 2016).

The spatial model here analyzed is intended to generalize the ideas discussed in Di Salvo and Oliveri, 2016b; Di Salvo and Oliveri, 2016c, where the dynamics of the various trophic levels in a closed ecosystem has been investigated by applying operatorial techniques and further introducing specific rules acting periodically on the system. In particular, we consider here a fermionic model in a finite, closed, two-dimensional region, made by L^2 cells, involving four compartments in each cell, say the nutrients, the bacteria and two different garbages (playing different roles in the ecosystem, see Section 3.1), as schematized in fig. 3.2. To describe colony morphology in stressed/aged bacterial populations, we consider a region represented by a regular $L \times L$ square grid (see fig. 3.5). According to the usual interpretation, the number operators are used to describe the evolution of the local densities of the different compartments. Once we have fixed a suitable functional form for the Hamiltonian operator, say the one defined in Equation (3.9), we now move to describe the effect of combining the usual quantum definition of the dynamics with the action of a specific rule changing periodically the values of the involved parameters.

The way in which the rule acts is inspired by the observation of the biological dynamics of bacterial colonies where the living bacteria, as the nutrients disappear, besides reducing their metabolism, begin to use as nutrients the components of dead cells. In particular, the modifications of the parameters entering the Hamiltonian operator are intended to account for

the changes of the metabolic activity of bacteria (and, hence, their interaction parameters) due to the increased density of the non recyclable garbage or to a lack of nutrients.

Start considering nonhomogeneous regions characterized by cell–dependent parameters such that, when moving away from the center, the inertia parameters decrease and the interaction parameters moderately grow. Precisely, we initially look at the values assigned to the parameters in Di Salvo and Oliveri, 2016b, namely $\omega_{1,\alpha} = 0.3/(1+d_\alpha)$, $\omega_{2,\alpha} = 0.1/(1+d_\alpha)$, $\omega_{3,\alpha} = 0.3/(1+d_\alpha)$, $\omega_{4,\alpha} = 0.4/(1+d_\alpha)$,$\lambda_{2,\alpha} = 0.5d_\alpha$, $\lambda_{3,\alpha} = 0.4d_\alpha$, $\lambda_{4,\alpha} = 0.2d_\alpha$, $\nu_{2,\alpha} = 0.6d_\alpha$, $\nu_{3,\alpha} = 0.4d_\alpha$, provided that $d_\alpha \neq 0$, where d_α is the Euclidean distance (normalized to 1) between the cell α and the central one; moreover, $\mu_{2,\alpha} = 0.3$ ($\alpha = 1, \ldots, L^2$), whereas $p_{\alpha,\beta} = p_{\beta,\alpha}$ is vanishing for $\alpha = \beta$, equal to $1/d^2(\alpha,\beta)$, where $d(\alpha,\beta)$ is the Euclidean distance between the adjacent cells α and β, and zero elsewhere.

We take into account the dynamical mechanisms implied in each cell by the variation $D_{4,\alpha}$ of the scarcely recyclable garbage after any period of quantum evolution of the system of length τ,

$$D_{4,\alpha} = n_{4,\alpha}(k\tau) - n_{4,\alpha}((k-1)\tau), \qquad k > 1,\ \alpha = 1, \ldots, L^2,$$

to generate a new set of values for some of the parameters of the model according to the rule ρ acting as

$$\begin{cases} \rho(\omega_{2,\alpha}) = \omega_{2,\alpha}(1 + 10D_{4,\alpha}), \\ \rho(\lambda_{2,\alpha}) = \lambda_{2,\alpha}(1 - 10D_{4,\alpha}), \\ \rho(\lambda_{4,\alpha}) = \lambda_{4,\alpha}(1 - 10D_{4,\alpha}), \\ \rho(\nu_{3,\alpha}) = \nu_{3,\alpha}(1 - 10D_{4,\alpha}). \end{cases} \tag{7.3}$$

Numerical simulations of the stepwise model, describing the evolution of the system for consecutive time intervals in accordance with the Heisenberg representation and imposing repeatedly the rule ρ, have been compared to those obtained in Section 3.4 by considering the evolution according to the standard nonhomogeneous linear model (see figs. 3.9 to 3.12). The employed initial conditions are such that the nutrients are uniformly distributed with maximum local density on the entire region, the bacteria appear with maximum local density only in a restricted central area, whereas the two garbages are uniformly empty.

As visible in fig. 7.6, though the diffusion has the effect of distributing the bacteria all over the lattice (kept in mind that the radial inhomogeneity of the parameters determines the formation of symmetrical patterns), the validity of the proposed stepwise method, differently from what happens by adopting the standard linear model, is shown by the fact that the application of the rule ρ after several time steps improves the description of the behavior of bacterial populations in terms of long–term survival.

The mean values and the variances of the densities of all the compartments of the ecosystem exhibit in the case of the stepwise approach, as well as in the case of the standard approach (see figs. 3.11 and 3.12), an oscillating behavior with decreasing variations and the tendency to stabilize, in the case of the mean values, and to become smaller and smaller, in the case of the variances (see fig. 7.7 for the evolutions corresponding to the simulation

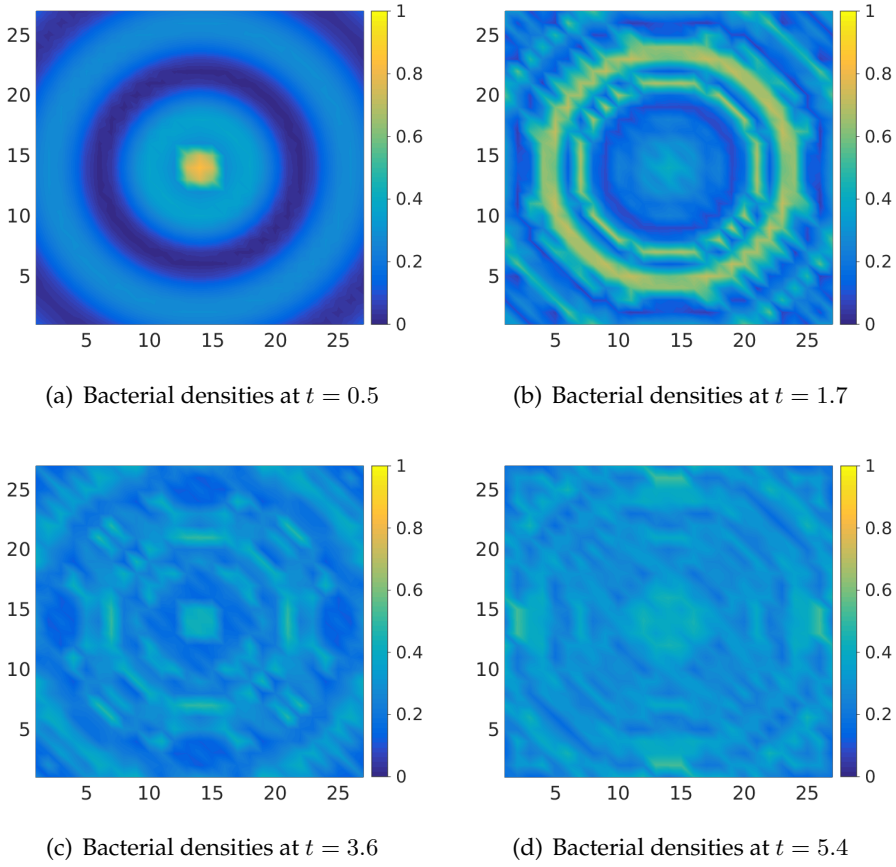

(a) Bacterial densities at $t = 0.5$

(b) Bacterial densities at $t = 1.7$

(c) Bacterial densities at $t = 3.6$

(d) Bacterial densities at $t = 5.4$

FIGURE 7.6: Stepwise nonhomogeneous spatial linear model with the rule ρ and $\tau = 1$. The frames show for each row the densities of the bacteria over the entire region at times 0.5, 1.7, 3.6, 5.4 respectively.

shown in fig. 7.6). The introduction of the rule results in an opposition to the destruction of the oscillations caused by the diffusion processes.

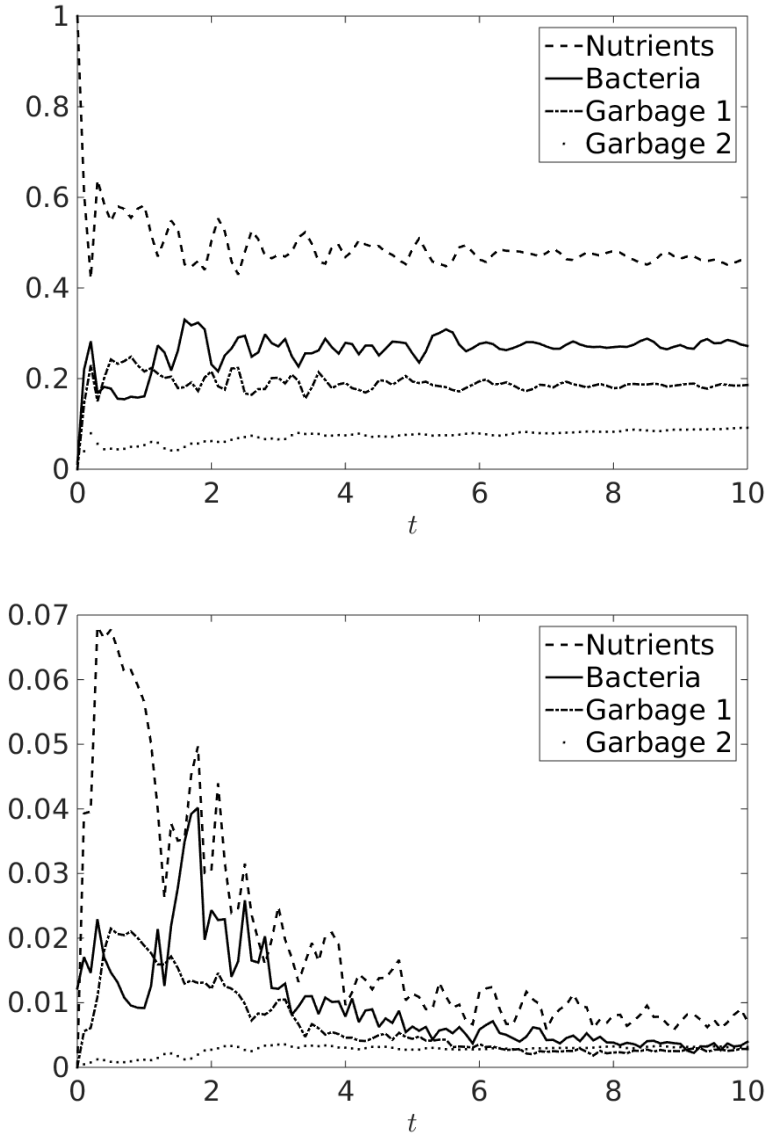

FIGURE 7.7: Time evolution of the mean, (a), and the variance, (b), of the densities of all the compartments of the ecosystem over a region described by means of the stepwise nonhomogeneous spatial linear model with the rule ρ and $\tau = 1$.

8 (H, ρ)–induced political dynamics and the role of turncoats

In this Chapter, we discuss an extension of the analysis of the party system dynamics described in Chapter 4, by combining the action of the Hamiltonian of the system with certain rules acting periodically on it in such a way that the parameters entering the linear conservative model, and describing the political style of the various parties, are repeatedly changed (so as to express a sort of dependence of them upon the variations of the mean values of the observables (Di Salvo and Oliveri, 2016a; Di Salvo, Gorgone, and Oliveri, 2016b)).

Moreover, in Section 8.3, we deal with two more sophisticated models, which consist in collections of similar models accounting for the effects of politicians' turncoat habits either inside the central government, or on the voters' opinion. The mutual influences are suitably graded.

8.1 Basic approach with rule acting on the model

The simulations shown during the dissertation in Chapter 4, as expected for the adopted linear model, provide an evolution of the densities that does not admit any asymptotic limit, that is the consistencies of the parties always oscillate in time. To describe some kind of "more interesting" dynamics, we need to add some extra ingredients, or change something in the form of H. The possibility consisting in assuming a different Hamiltonian containing terms of order greater than two would require the computation at each instant of time of the exponential of a $2^9 \times 2^9$ matrix, or, equivalently, the numerical solution of a system of $9 \cdot 2^{18}$ nonlinear differential equations to obtain the time evolution of the system in the Heisenberg representation. This approach becomes almost intractable from a computational point of view if we want to consider more realistic models with a larger number of political groups. In order to bypass the huge problem of the increase of the computational costs, we use here the approach of the (H, ρ)–induced dynamics explained in Chapter 5. In particular, starting from a quadratic Hamiltonian such as the one defined in (4.2), we enrich the description of the dynamics by accounting for the influence that the information about the subsequent states reached by the system has on the political style of the various parties (described by the specific values assigned to the parameters). We stress that in such an approach only the strengths of the mutual interactions change, whereas the structure of the original model is preserved.

If we consider the time interval $[0, T]$, split it in $n = T/\tau$ subintervals of length τ, and imagine the dynamics in the k–th subinterval $[(k-1)\tau, k\tau[$ ruled by an Hamiltonian operator $H^{(k)}$, the evolution of the mean values of

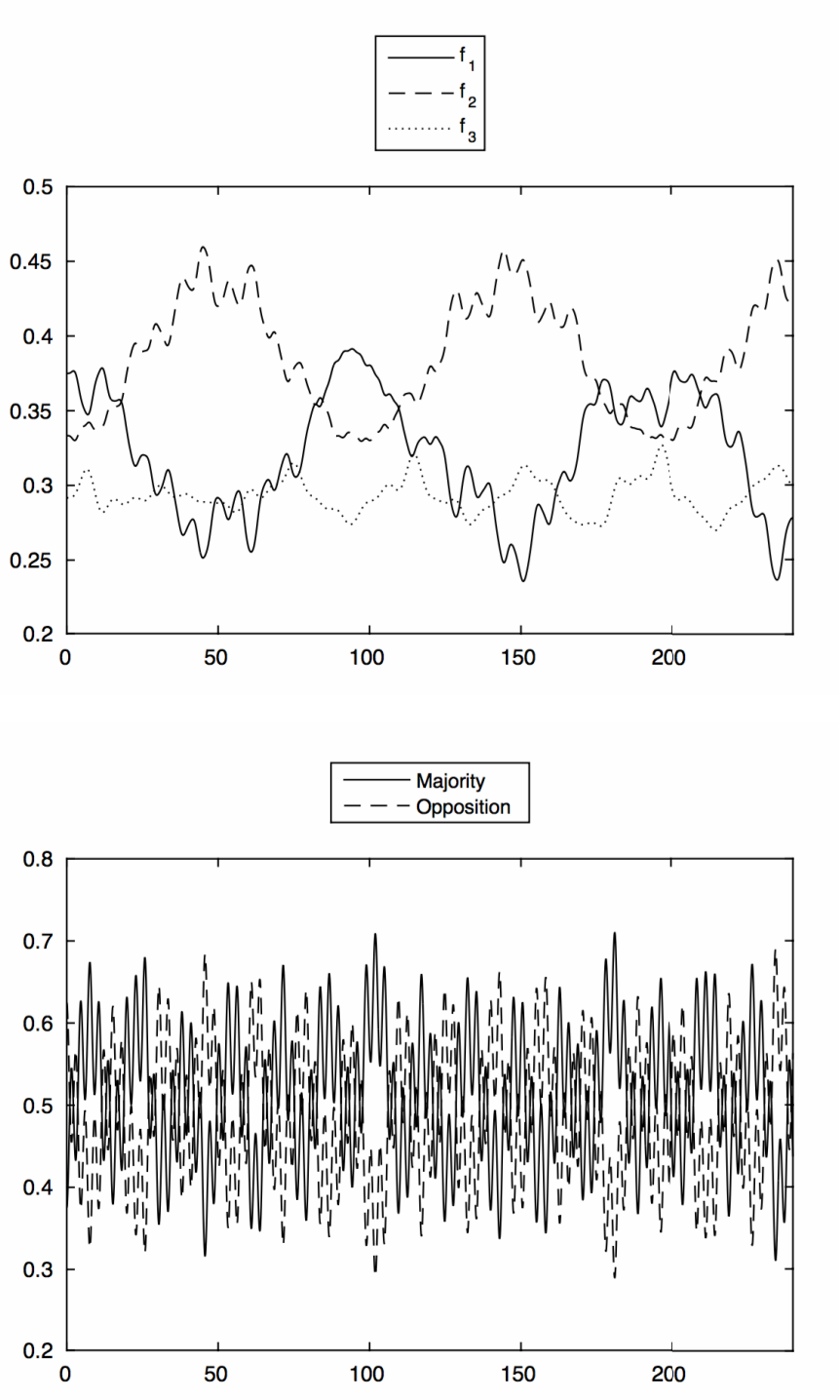

FIGURE 8.1: Linear model (no rule): time evolution of the densities of the three factions (top) and of the consistency of the parliamentary majority and opposition (bottom) up to $t = 250$. The time is scaled to the total number of weeks in the five–year term of office.

the observable of the system we are interested in is obtained according to the approach presented and discussed in Section 5.1.

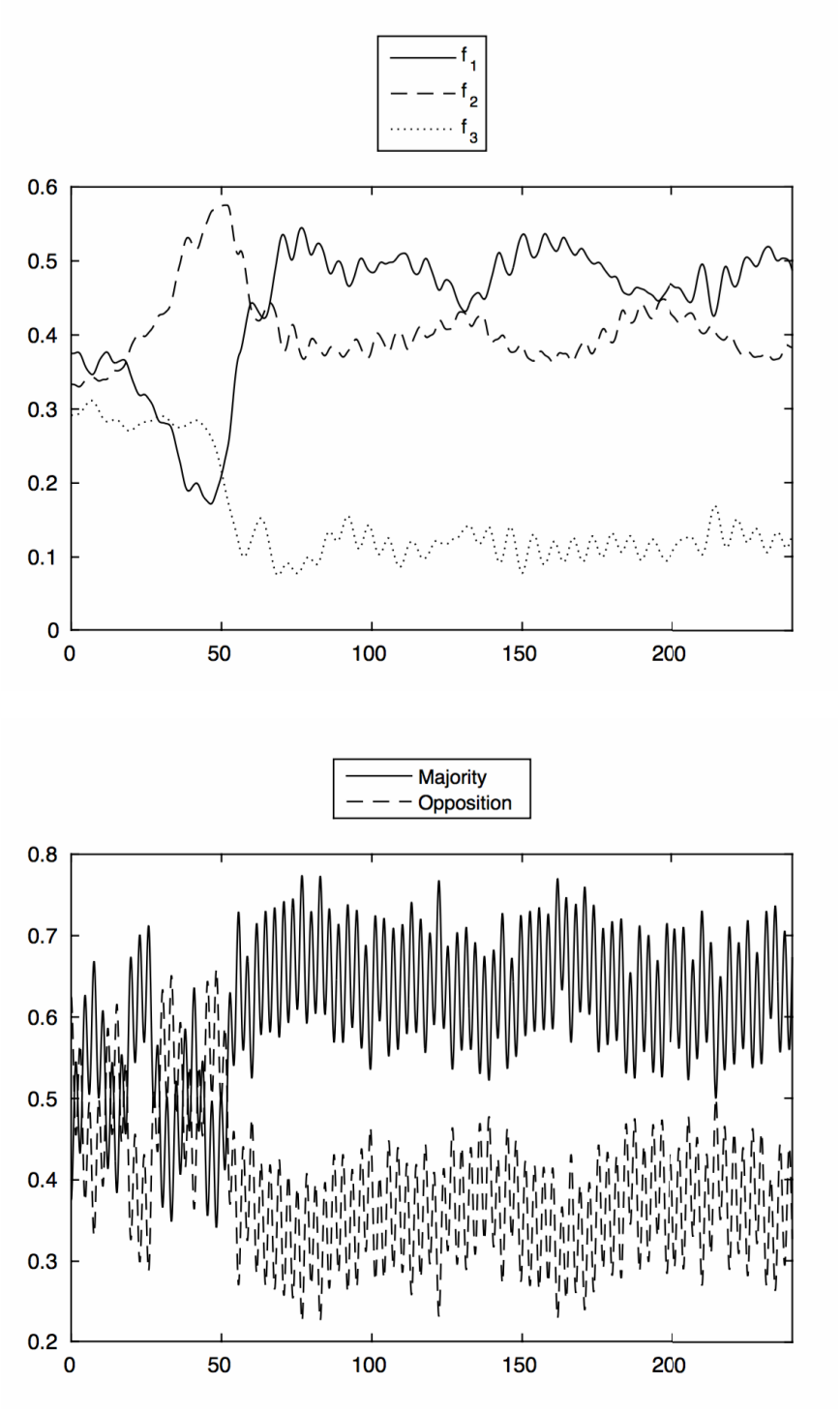

FIGURE 8.2: Stepwise linear model using the rule ρ_1 with $\tau = 5$: time evolution of the densities of the three factions (top) and of the consistency of the parliamentary majority and opposition (bottom) up to $t = 250$. The time is scaled to the total number of weeks in the five–year term of office.

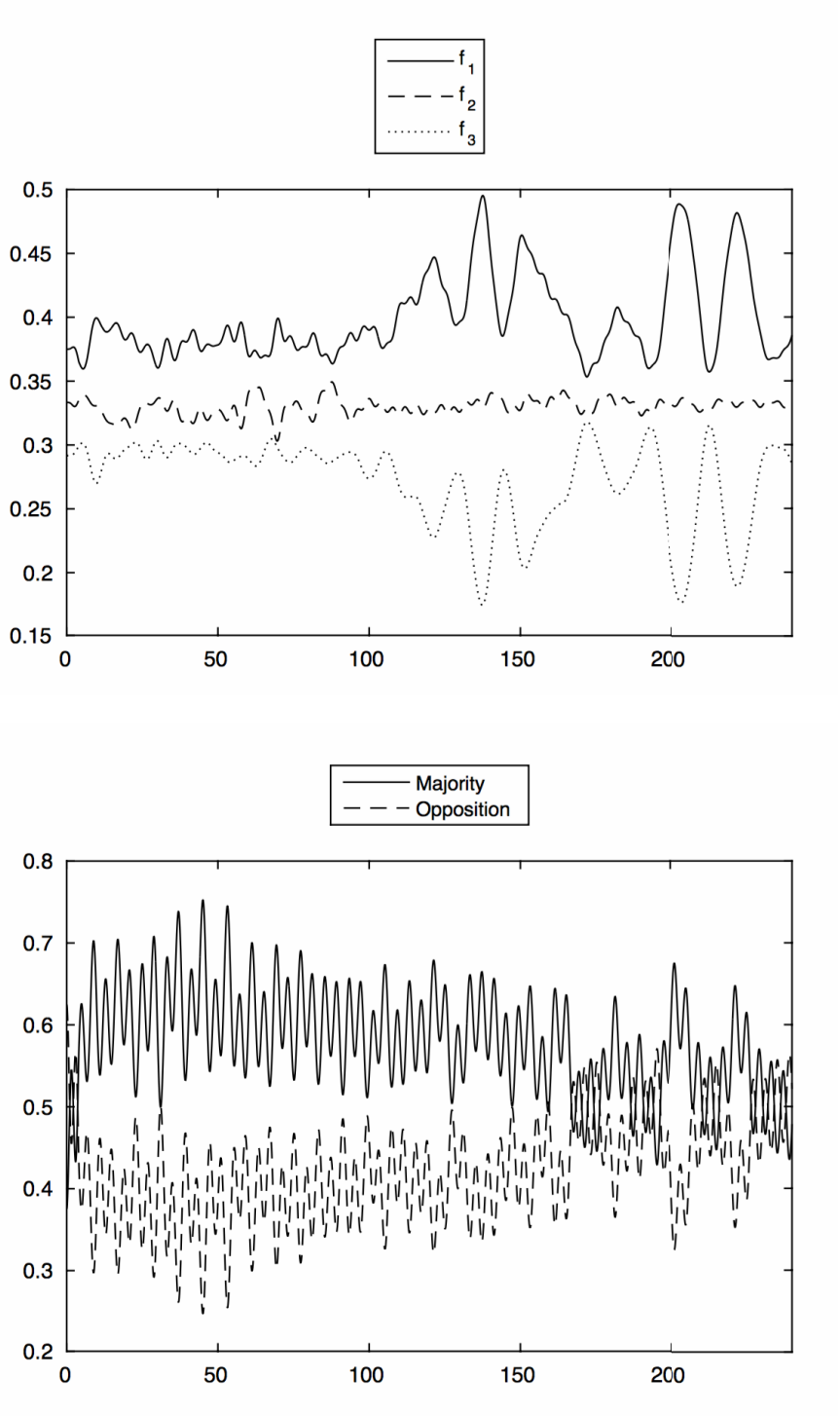

FIGURE 8.3: Stepwise linear model using the rule ρ_2 with $\tau = 5$: time evolution of the densities of the three factions (top) and of the consistency of the parliamentary majority and opposition (bottom) up to $t = 250$. The time is scaled to the total number of weeks in the five–year term of office.

Thus, let us consider a general political system in which three major factions are outlined, each one of them internally subdivided according to the political attitudes of its members into three fringes as schematically shown in fig. 4.1. We assume that the nature of the factions is characterized by the choice of values for the parameters of the model as in (4.7) along with $\mu_{12} = 0.1$, $\mu_{13} = 0.09$, $\mu_{23} = 0.01$; moreover, let us take the initial consistencies such that the first faction is predominant, but not significantly, compared to the sum of the remaining two. In other words, let us imagine that at the beginning of a parliamentary term there is a moderate party (f_1) which struggles to keep the majority of seats and has not the right numbers to govern alongside a fickle faction (f_2) and an extremist one (f_3). Taking into account the turncoat attitudes of the various actors of our model, reasonable estimates of the numerical consistence of the parliamentary majority and opposition to the faction f_j are obtained by considering the densities $M_j = f_j + \sum_{\substack{k=1 \\ k\neq j}}^{3} p_{kj}$ and $O_j = \sum_{\substack{k,\ell=1 \\ k,\ell\neq j}}^{3} p_{k\ell}$, respectively.

The description of the evolution of such a political system by means of the linear model (4.4) in the case where no rule is applied produces the results shown in fig. 8.1.

In order to account for the changes in political views and party affiliations due to the evolution and the mutual interactions between the compartments of the political system, we consider two different rules (ρ_1 and ρ_2) periodically acting on some of the parameters of the model in such a way to have remarkable effects on the evolution of the system. More explicitly, once the variations of the densities of the main factions

$$D_j = f_j(k\tau) - f_j((k-1)\tau), \qquad k \geq 1, \quad j = 1, 2, 3, \tag{8.1}$$

have been computed after a period of length τ of the Heisenberg–like evolution of the political system, the first rule ρ_1 consists in the conditions

$$\begin{cases} \rho_1(\omega_{jj}) = \omega_{jj}(1 + D_j), \\ \rho_1(\omega_{j\ell}) = \omega_{j\ell}(1 - D_j), \quad \ell \neq j, \end{cases} \qquad j, \ell = 1, 2, 3, \tag{8.2}$$

which are intended to modify, according to the evolution of each faction, the tendency of the loyal fringes to remain constant in time contrarily to those of the disloyal ones. The time evolutions of the system and of the consistency of the parliamentary majority and opposition obtained by means of the stepwise linear model applying the rule ρ_1 after every time step of length $\tau = 5$ are shown in fig. 8.2.

The resulting dynamics can be further adapted in favor of the leading party f_1 through the set of conditions ρ_2, taking into account the variations

$$d_{j\ell} = p_{j\ell}(k\tau) - p_{j\ell}((k-1)\tau), \qquad k \geq 1, \ j, \ell = 1, 2, 3, \tag{8.3}$$

of the densities of each compartment $p_{j\ell}$ of the model, and introducing further conditions on the internal interaction parameters:

$$\begin{cases} \rho_2(\omega_{j\ell}) = \omega_{j\ell}(1 + d_{j\ell}), \\ \rho_2(\lambda_{j\ell}) = \lambda_{j\ell}(1 - d_{j\ell}), \quad \ell \neq j, \end{cases} \qquad j, \ell = 1, 2, 3. \tag{8.4}$$

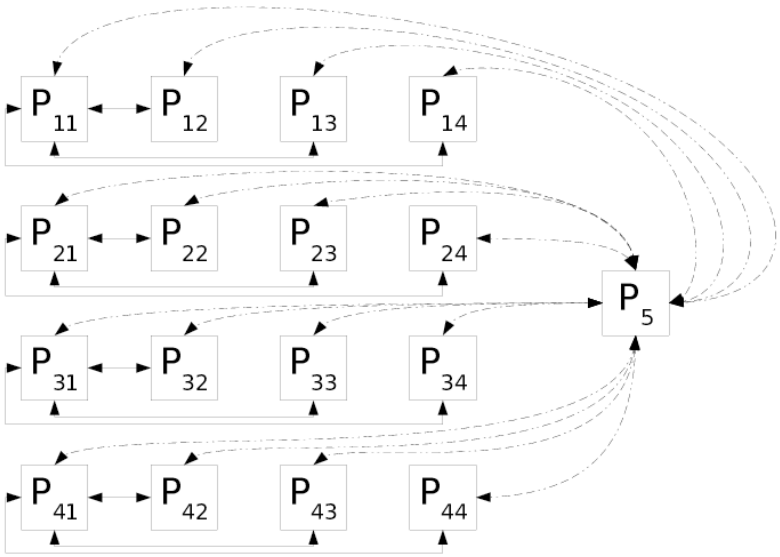

FIGURE 8.4: A schematic view to the model describing the main parties interacting in the Italian XVII Legislature.

Notice that, due to the fact that the system under consideration is conservative, at any given time the variations $d_{j\ell}$ (as well as D_j), $j, \ell = 1, 2, 3$, will never have the same sign. This results in a consolidation of the factions whose density is growing associated with an incentive to variability for the other factions whose density is decreasing, *i.e.*, ρ_2 acts increasing (lowering, respectively) the value of the inertia parameters and lowering (increasing, respectively) the values of the internal interaction parameters in order to suppress or promote the internal disloyalty flows. Therefore, the periodic application of the rule ρ_2 accounts for the tendency of the candidates to *jump on the bandwagon* and, as visible in fig. 8.3, the stepwise model well describes the situation in which the leading faction reaches a good numerical consistency compared to the other factions, and maintains a majority of overall seats in the parliament.

Despite of the simplicity of the proposed model, the obtained numerical simulations seem to capture some relevant features (*e.g.* the reinforcement of moderate factions) of the dynamics of political parties affected by turncoat–like behaviors.

8.2 A case study: the dynamics of turncoats in the Italian XVII Legislature

The political parties taking part to the Italian XVII Legislature have been grouped according to ideology and attitudes into five main factions: the center–left coalition (f_1), the center–right coalition (f_2), the center coalition (f_3), the Five Star Movement (f_4), and the set of all the minor parties,

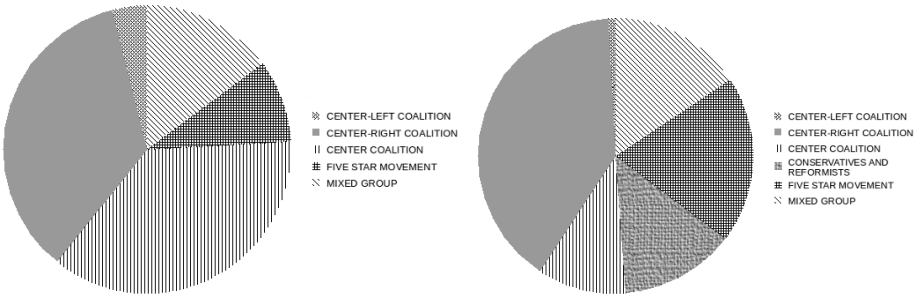

(a) (b)

FIGURE 8.5: Desertions (normalized to the final consistencies) inside the Chamber of Deputies, (a), and the Senate of the Republic, (b), during the Italian XVII Legislature (data from http://www.camera.it and http://www.senato.it, accessed on April 14th, 2016).

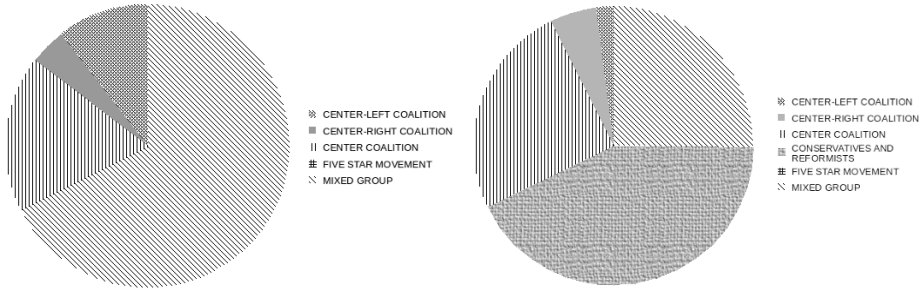

(a) (b)

FIGURE 8.6: Entries (normalized to the final consistencies) inside the Chamber of Deputies, (a), and the Senate of the Republic, (b), during the Italian XVII Legislature (data from http://www.camera.it and http://www.senato.it, accessed on April 14th, 2016).

or Mixed Group (f_5). This last compartment represents a mass of outcast politicians without any kind of internal cohesion or ideological identity.

A graphical representation of the possible political interactions among these actors is shown in fig. 8.4.

The Italian political system has been sadly characterized, especially in recent years, by a tendency of the government to attempt to hold on to power by forming coalitions to prevent the formation of any credible opposition. Phenomena such as opportunism and easy acceptance of turncoats within the various parties have strongly influenced the XVII Italian Legislature, reaching even paroxysmal levels during the first thirty months of this term (see figs. 8.5 and 8.6 for a display of the uniform disloyalty, practically exhibited by all political groups, in both the two houses of the Italian Parliament). The time series of the numerical consistencies of the parties within the Chamber of Deputies and the Senate of the Republic during the period under consideration are shown in fig. 8.7. By observing the trends that emerge from the official data about the changes of side, it springs to mind to interpret such evolutions as strongly driven by the lack of scruples. This

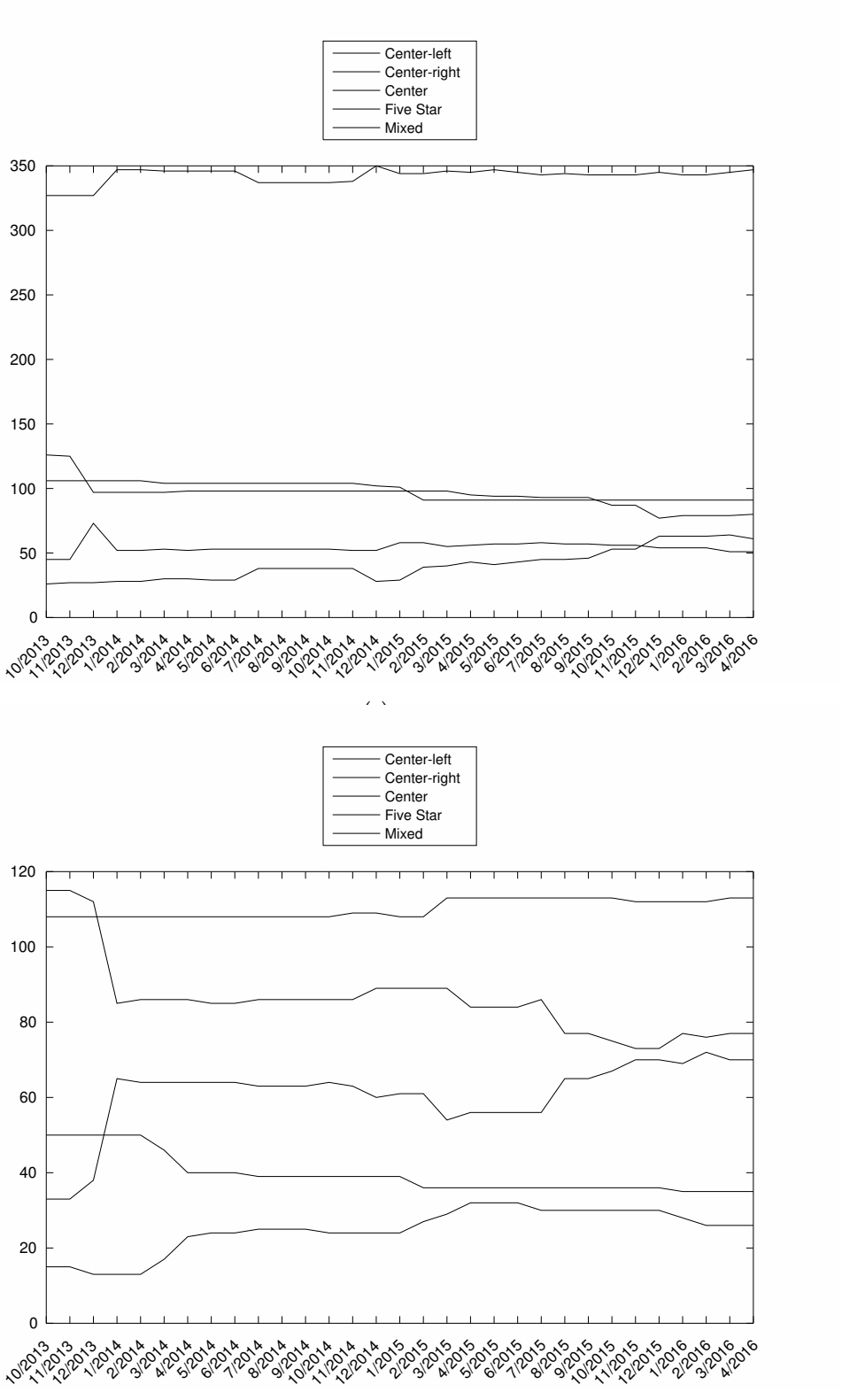

(b)

FIGURE 8.7: Time series of the numerical consistency of the political groups within the Chamber of Deputies, (a), and within the Senate of the Republic, (b), during the Italian XVII Legislature.

key translates into the possibility of using the turncoat model presented in this paper (with a specific rule ρ_P taking into account the dynamics within the Italian Parliament) in order to attempt to fit the actual data extracted from the Institutional web sites.

The various subgroups of the political parties are described by fermionic operators and their evolution is ruled by a quadratic Hamiltonian operator in the Heisenberg representation. On the basis of the observed behavior of the various parties, we describe the political interactions by means of the following Hamiltonian:

$$\begin{cases} H = H_0 + H_I, \qquad \text{with} \\ H_0 = \sum_{i,j=1}^{4} \omega_{ij}\, P_{ij}^\dagger\, P_{ij} + \omega_5 P_5^\dagger\, P_5, \\ H_I = \sum_{\substack{i,j=1 \\ j\neq i}}^{4} \lambda_i^{(j)} \left(P_{ii} P_{ij}^\dagger + P_{ij} P_{ii}^\dagger \right) + \sum_{1\leq i<j\leq 4} \mu_{ij} \left(P_{ij} P_{ji}^\dagger + P_{ji} P_{ij}^\dagger \right) \\ \quad + \sum_{i,j=1}^{4} \nu_{ij} \left(P_{ij} P_5^\dagger + P_5 P_{ij}^\dagger \right). \end{cases} \tag{8.5}$$

The equations of motion look similar to those obtained in (4.3), say

$$\begin{aligned}
\dot{P}_{11} &= i\left(-\omega_{11}P_{11} + \lambda_1^{(2)}P_{12} + \lambda_1^{(3)}P_{13} + \lambda_1^{(4)}P_{14} + \nu_{11}P_5\right), \\
\dot{P}_{12} &= i\left(-\omega_{12}P_{12} + \lambda_1^{(2)}P_{11} + \mu_{12}P_{21} + \nu_{12}P_5\right), \\
\dot{P}_{13} &= i\left(-\omega_{13}P_{13} + \lambda_1^{(3)}P_{11} + \mu_{13}P_{31} + \nu_{13}P_5\right), \\
\dot{P}_{14} &= i\left(-\omega_{14}P_{14} + \lambda_1^{(4)}P_{11} + \mu_{14}P_{41} + \nu_{14}P_5\right), \\
\dot{P}_{21} &= i\left(-\omega_{21}P_{21} + \lambda_2^{(1)}P_{22} + \mu_{12}P_{12} + \nu_{21}P_5\right), \\
\dot{P}_{22} &= i\left(-\omega_{22}P_{22} + \lambda_2^{(1)}P_{21} + \lambda_2^{(3)}P_{23} + \lambda_2^{(4)}P_{24} + \nu_{22}P_5\right), \\
\dot{P}_{23} &= i\left(-\omega_{23}P_{23} + \lambda_2^{(3)}P_{22} + \mu_{23}P_{32} + \nu_{23}P_5\right), \\
\dot{P}_{24} &= i\left(-\omega_{24}P_{24} + \lambda_2^{(4)}P_{22} + \mu_{24}P_{42} + \nu_{24}P_5\right), \\
\dot{P}_{31} &= i\left(-\omega_{31}P_{31} + \lambda_3^{(1)}P_{33} + \mu_{13}P_{13} + \nu_{31}P_5\right), \\
\dot{P}_{32} &= i\left(-\omega_{32}P_{32} + \lambda_3^{(2)}P_{33} + \mu_{23}P_{23} + \nu_{32}P_5\right), \\
\dot{P}_{33} &= i\left(-\omega_{33}P_{33} + \lambda_3^{(1)}P_{31} + \lambda_3^{(2)}P_{32} + \lambda_3^{(4)}P_{34} + \nu_{33}P_5\right), \\
\dot{P}_{34} &= i\left(-\omega_{34}P_{34} + \lambda_3^{(4)}P_{33} + \mu_{34}P_{43} + \nu_{34}P_5\right), \\
\dot{P}_{41} &= i\left(-\omega_{41}P_{41} + \lambda_4^{(1)}P_{44} + \mu_{14}P_{14} + \nu_{41}P_5\right), \\
\dot{P}_{42} &= i\left(-\omega_{42}P_{42} + \lambda_4^{(2)}P_{44} + \mu_{24}P_{24} + \nu_{42}P_5\right), \\
\dot{P}_{43} &= i\left(-\omega_{43}P_{43} + \lambda_4^{(3)}P_{44} + \mu_{34}P_{34} + \nu_{43}P_5\right), \\
\dot{P}_{44} &= i\left(-\omega_{44}P_{44} + \lambda_4^{(1)}P_{41} + \lambda_4^{(2)}P_{42} + \lambda_4^{(3)}P_{43} + \nu_{44}P_5\right),
\end{aligned}$$

$$\begin{aligned}\dot{P}_5 = i\,(&-\omega_5 P_5 + \nu_{11}P_{11} + \nu_{12}P_{12} + \nu_{13}P_{13} + \nu_{14}P_{14} + \nu_{21}P_{21}\\ &+\nu_{22}P_{22} + \nu_{23}P_{23} + \nu_{24}P_{24} + \nu_{31}P_{31} + \nu_{32}P_{32} + \nu_{33}P_{33}\\ &+\nu_{34}P_{34} + \nu_{41}P_{41} + \nu_{42}P_{42} + \nu_{43}P_{43} + \nu_{44}P_{44})\,.\end{aligned}$$

The values of the parameter involved in the model are initially selected as

$$\begin{aligned}&\omega_{11} = 0.7, \quad \omega_{12} = 0.65, \quad \omega_{13} = 0.65, \quad \omega_{14} = 0.65,\\ &\omega_{22} = 0.45, \quad \omega_{21} = 0.4, \quad \omega_{23} = 0.4, \quad \omega_{24} = 0.4,\\ &\omega_{33} = 0.65, \quad \omega_{31} = 0.6, \quad \omega_{32} = 0.6, \quad \omega_{34} = 0.6,\\ &\omega_{44} = 0.9, \quad \omega_{41} = 0.85, \quad \omega_{42} = 0.85, \quad \omega_{43} = 0.85,\\ &\omega_5 = 0.2,\\ &\lambda_1^{(2)} = 0.3, \quad \lambda_1^{(3)} = 0.35, \quad \lambda_1^{(4)} = 0.35,\\ &\lambda_2^{(1)} = 0.45, \quad \lambda_2^{(3)} = 0.5, \quad \lambda_2^{(4)} = 0.5,\\ &\lambda_3^{(1)} = 0.35, \quad \lambda_3^{(2)} = 0.3, \quad \lambda_3^{(4)} = 0.35,\\ &\lambda_4^{(1)} = 0.15, \quad \lambda_4^{(2)} = 0.2, \quad \lambda_4^{(3)} = 0.15,\\ &\mu_{12} = 0.1, \quad \mu_{13} = 0.15, \quad \mu_{14} = 0.15,\\ &\mu_{23} = 0.2, \quad \mu_{24} = 0.25, \quad \mu_{34} = 0.1,\\ &\nu_{11} = \nu_{22} = \nu_{33} = \nu_{44} = 0.1,\\ &\nu_{12} = \nu_{13} = \nu_{14} = \nu_{21} = \nu_{23} = \nu_{24} = \nu_{31} = \nu_{32} = \nu_{34} = \nu_{41} = \nu_{42} = \nu_{43} = 0.\end{aligned} \tag{8.6}$$

These values are then modified during the evolution of the system (after any time interval of length $\tau = 1$) on the basis of the variations of the densities of the various compartments associated to the parties inside the Parliament:

$$D_j = f_j(k\tau) - f_j((k-1)\tau), \qquad k \geq 1,\ j = 1,\ldots,5 \tag{8.7}$$

according to the rule ρ_P, acting as

$$\begin{cases} \rho_P(\omega_{11}) = \omega_{11}(1 + D_1/100),\\ \rho_P(\omega_{22}) = \omega_{22}(1 - (D_1 + D_3)/10),\\ \rho_P(\omega_{33}) = \omega_{33}(1 + (D_1 + D_2)/10),\\ \rho_P(\omega_{44}) = \omega_{44}(1 - (D_4 + D_5)/10),\\ \rho_P(\omega_5) = \omega_5(1 + (D_4 + D_5)/10). \end{cases} \tag{8.8}$$

The rule ρ_P, which resembles the rule ρ_1 defined in (8.2), has to be intended as a means to adjust the model to the observed phenomena in order to reasonably mimic the actual trends, as the evolutions in fig. 8.8 show.

The more realistic variant of the model described in this Section is thus able to provide satisfactory results in terms of fitting with the official data extracted from the Institutional web pages of the Italian Parliament.

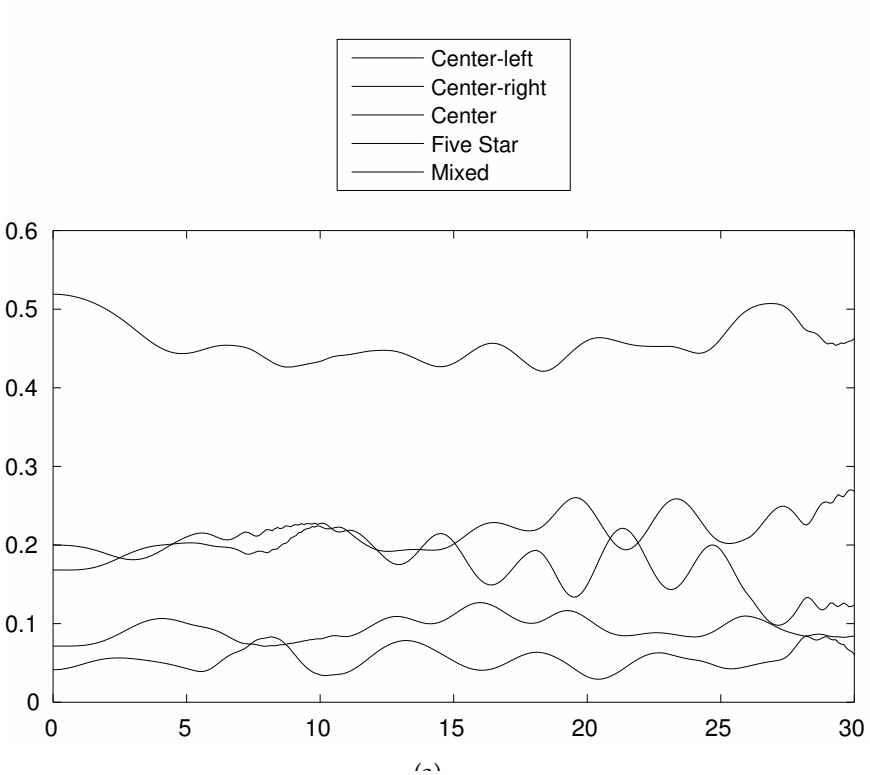

(a)

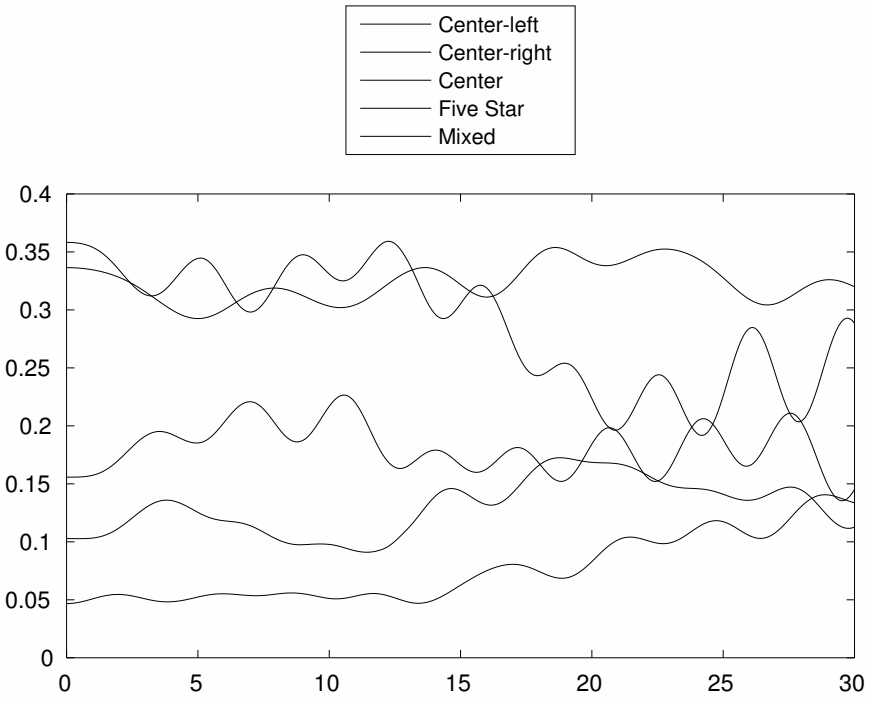

(b)

FIGURE 8.8: Time evolution of the political system according to the stepwise model with rule ρ_P and $\tau = 1$: the numerical simulations exhibit a good likeness to the actual data in both the case of the Chamber of Deputies, (a), and of the Senate of the Republic, (b). The x–axis is scaled to the number of months in the period under study; the y–axis is scaled to the fractions of the overall seats.

8.3 The interplay between politicians' turncoat habits: facets into the central government and the public opinion

In this Section, we deal with a more sophisticated approach suitable to describe the effects deriving from the mutual interactions inside the central government and the influence of the political dynamics affected by turncoat behaviors on the opinions of the voters and the abstainers (Di Salvo, Gorgone, and Oliveri, 2016a).

8.3.1 The dynamics inside the Parliament

We consider here for both the two houses of Italian Parliament the same model illustrated in fig. 4.1, and we assume that the dynamics of the compartments internal to these two subsystems making up the central government is driven by similar Hamiltonian operators having the same functional form defined in (4.2), but different sets of parameters and different initial conditions. The interplay between the political behaviors of the various actors is therefore expressed by the action of specific rules taking into account the internal events and their external implications.

Specifically, the parameters for the Chamber of Deputies and for the Senate have been chosen as

$$\begin{array}{llllll}
\omega^c_{11}=1.9, & \omega^c_{12}=0.6, & \omega^c_{13}=0.5, & \omega^s_{11}=1.7, & \omega^s_{12}=0.55, & \omega^s_{13}=0.45,\\
\omega^c_{21}=0.5, & \omega^c_{22}=1, & \omega^c_{23}=0.7, & \omega^s_{21}=0.45, & \omega^s_{22}=0.9, & \omega^s_{23}=0.65,\\
\omega^c_{31}=0.7, & \omega^c_{32}=0.9, & \omega^c_{33}=1.3, & \omega^s_{31}=0.65, & \omega^s_{32}=0.85, & \omega^s_{33}=1.1,\\
\lambda^c_{12}=0.5, & \lambda^c_{13}=0.6, & \lambda^c_{21}=0.5, & \lambda^s_{12}=0.45, & \lambda^s_{13}=0.56, & \lambda^s_{21}=0.45,\\
\lambda^c_{23}=0.2, & \lambda^c_{31}=0.6, & \lambda^c_{32}=0.2, & \lambda^s_{23}=0.15, & \lambda^s_{31}=0.55, & \lambda^s_{32}=0.15,\\
\mu^c_{12}=0.1, & \mu^c_{13}=0.15, & \mu^c_{23}=0.05, & \mu^s_{12}=0.1, & \mu^s_{13}=0.15, & \mu^s_{23}=0.05,
\end{array}$$

and the initial conditions set, on the basis of the actual data, equal to

$$p^c(0)=[0.9,0,0,0,0.4,0,0,0,0.45]\,,\qquad p^s(0)=[0.9,0,0,0,0.5,0,0,0,0.6]\,,$$

respectively. The global dynamics of the political system of the central government is shown in fig. 8.9; moreover, a zoom inside each faction is performed in figs. 8.10 and 8.11 so as to have a look at the single evolutions of the internal parties composing the faction itself. The time evolution of the numerical estimate of the possession of the seats for each faction is visible in figs. 8.12 and 8.13.

Several possible groups of conditions modifying some or all the parameters involved in the models describing the evolution of the systems which represent the Chamber of Deputies and the Senate of the Republic may be considered, and their resulting effects are consequently less or more immediate and marked on the political dynamics.

In particular, let

$$\begin{array}{ll}
\delta^c_1=f^c_1(k\tau)-f^c_1(0), & \delta^s_1=f^s_1(k\tau)-f^s_1(0),\\
\delta^c_2=f^c_2(k\tau)-f^c_2(0), & \delta^s_2=f^s_2(k\tau)-f^s_2(0).
\end{array}\tag{8.9}$$

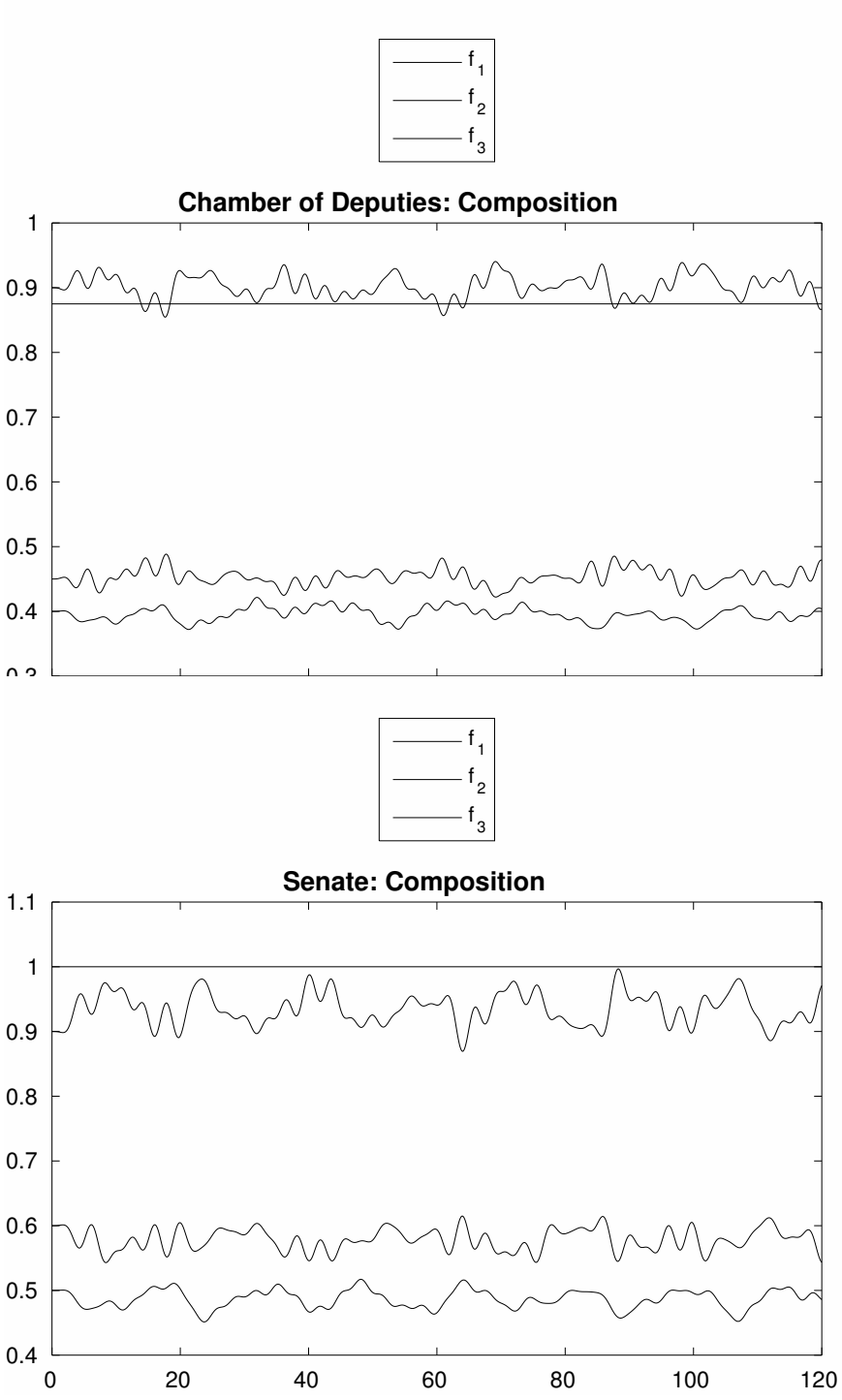

FIGURE 8.9: Linear model: time evolution of the composition of the Chamber of Deputies (on the left) and the Senate of the Republic (on the right) up to $t = 120$. The solid line represents the seat majority threshold. The x–axis is scaled to half the number of weeks in the period under study, so each step on the scale corresponds to fifteen days.

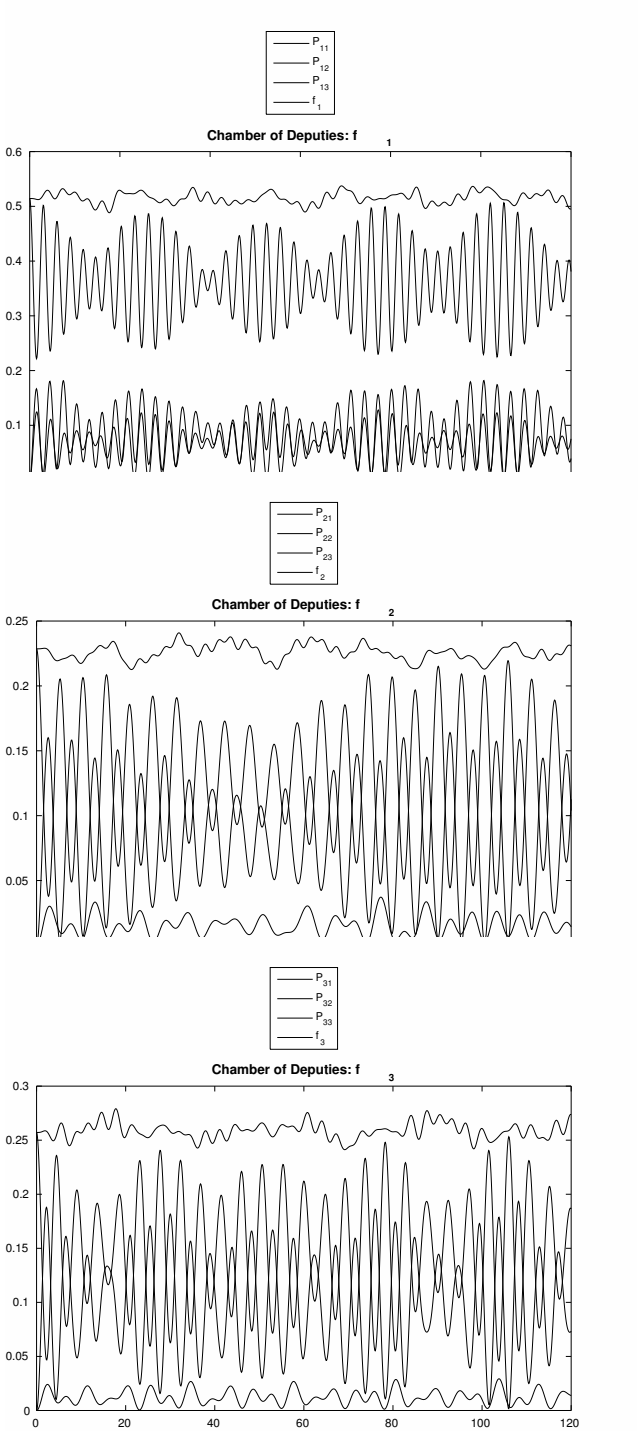

FIGURE 8.10: Linear model: zoom into the time evolution of the factions inside the Chamber of Deputies. The x–axis is scaled to half the number of weeks in the period under study, so each step on the scale corresponds to fifteen days.

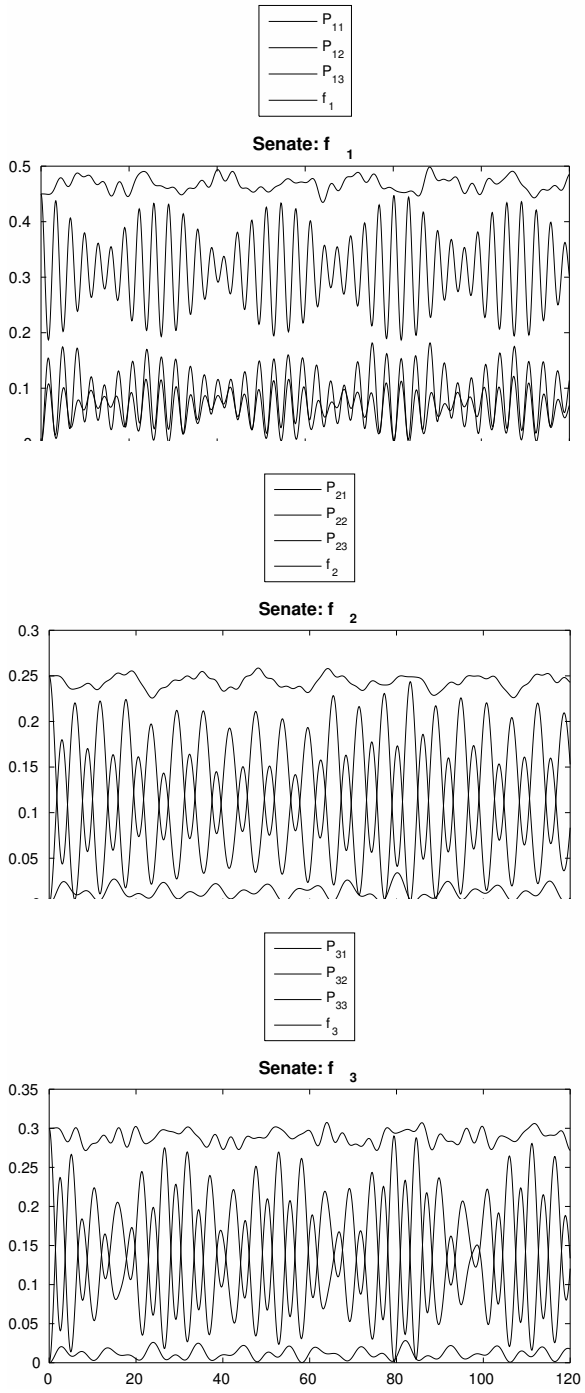

FIGURE 8.11: Linear model: zoom into the time evolution of the factions inside the Senate of the Republic. The x–axis is scaled to half the number of weeks in the period under study, so each step on the scale corresponds to fifteen days.

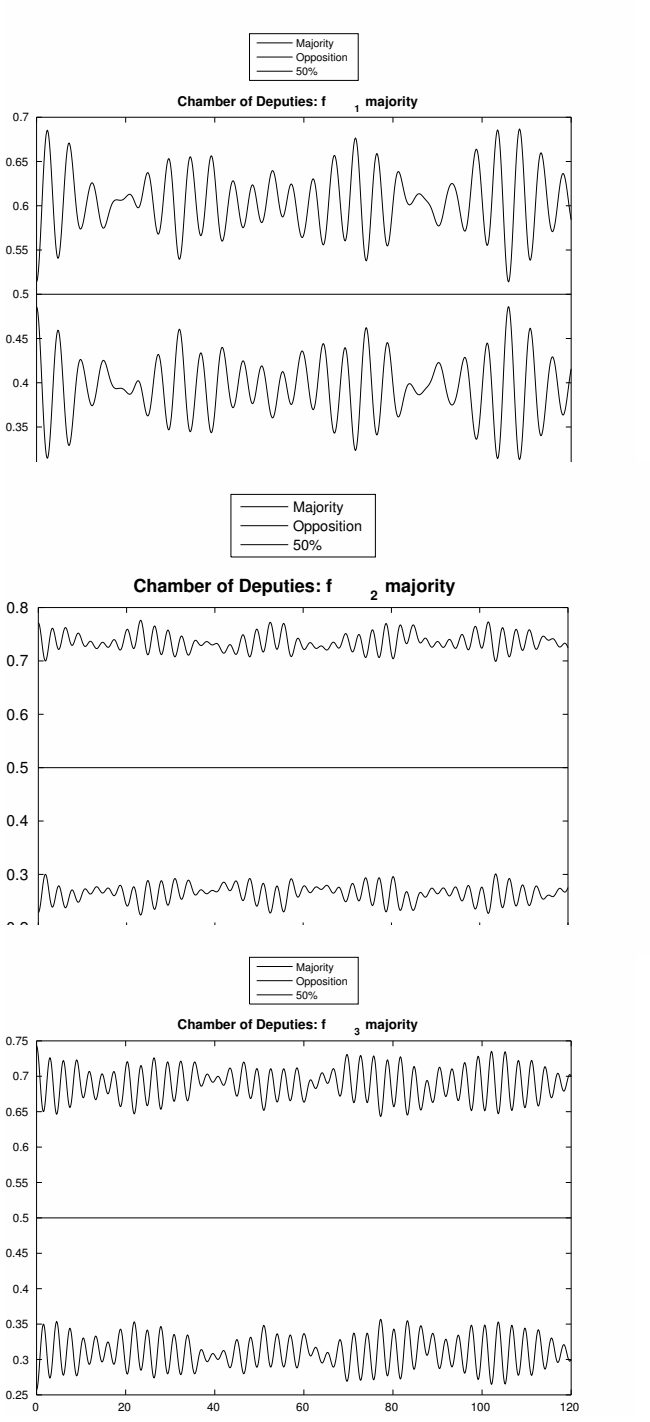

FIGURE 8.12: Linear model: time evolution of the consistencies of majority and opposition inside the Chamber of Deputies. The x–axis is scaled to half the number of weeks in the period under study, so each step on the scale corresponds to fifteen days.

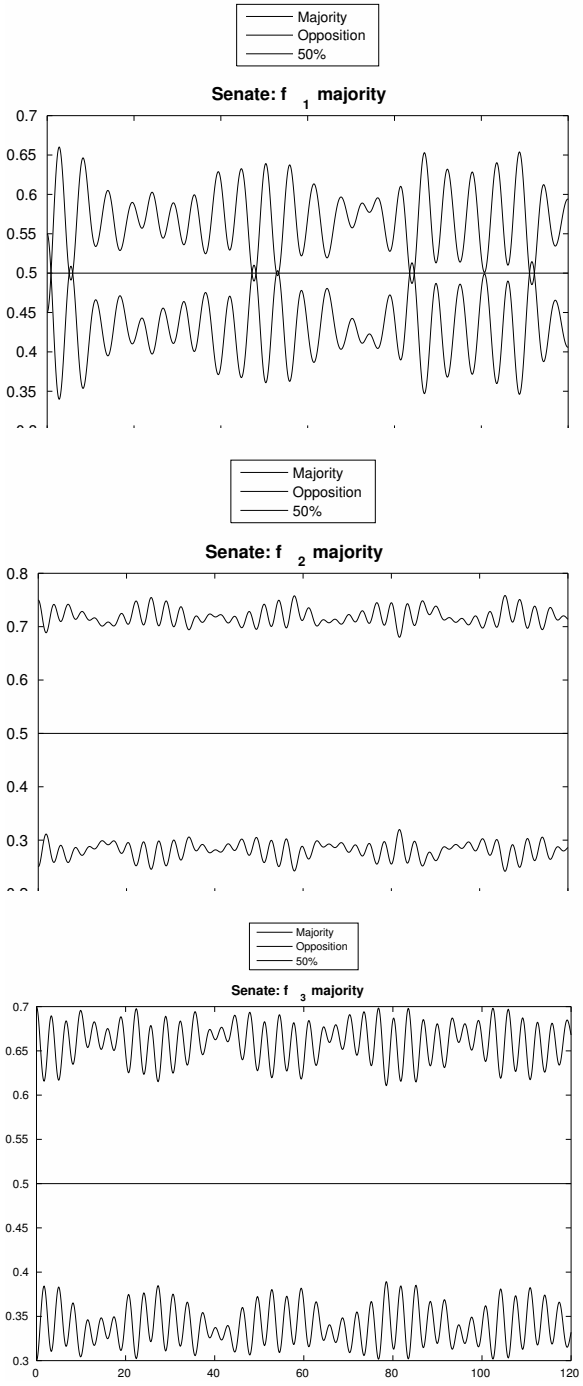

FIGURE 8.13: Linear model: time evolution of the consistencies of majority and opposition inside the Senate of the Republic. The x–axis is scaled to half the number of weeks in the period under study, so each step on the scale corresponds to fifteen days.

A way to improve the description of the dynamics of the central government by taking into account the mutual interactions between the two houses of the Parliament is achievable by computing the stepwise evolutions (according to the approach described in Chapter 5) of the two systems for the Chamber of Deputies and the Senate of the Republic with the rule ρ_G consisting in changing the inertia parameters of the compartments associated to the factions f_1 and f_2 as follows:

$$\begin{cases} \rho_G(\omega_{11}^c) = \omega_{11}^c(1+\delta_1^s), \\ \rho_G(\omega_{12}^c) = \omega_{12}^c(1+\delta_1^s), \\ \rho_G(\omega_{13}^c) = \omega_{13}^c(1+\delta_1^s), \\ \rho_G(\omega_{21}^c) = \omega_{21}^c(1-\delta_2^s), \\ \rho_G(\omega_{22}^c) = \omega_{22}^c(1+\delta_2^s), \\ \rho_G(\omega_{23}^c) = \omega_{23}^c(1-\delta_2^s), \end{cases} \qquad \begin{cases} \rho_G(\omega_{11}^s) = \omega_{11}^s(1+\delta_1^c), \\ \rho_G(\omega_{12}^s) = \omega_{12}^s(1+\delta_1^c), \\ \rho_G(\omega_{13}^s) = \omega_{13}^s(1+\delta_1^c), \\ \rho_G(\omega_{21}^s) = \omega_{21}^s(1-\delta_2^c), \\ \rho_G(\omega_{22}^s) = \omega_{22}^s(1+\delta_2^c), \\ \rho_G(\omega_{23}^s) = \omega_{23}^s(1-\delta_2^c). \end{cases} \tag{8.10}$$

The evolution of the political system of the central government and the internal dynamics obtained by combining the action of the Hamiltonian with the rule ρ_G are shown in figs. 8.14 and 8.16. Furthermore, the effect of repeatedly imposing the conditions (8.10) on the parameters of the model so far as concerns the possession of the seats for each faction is visible in figs. 8.17 and 8.18.

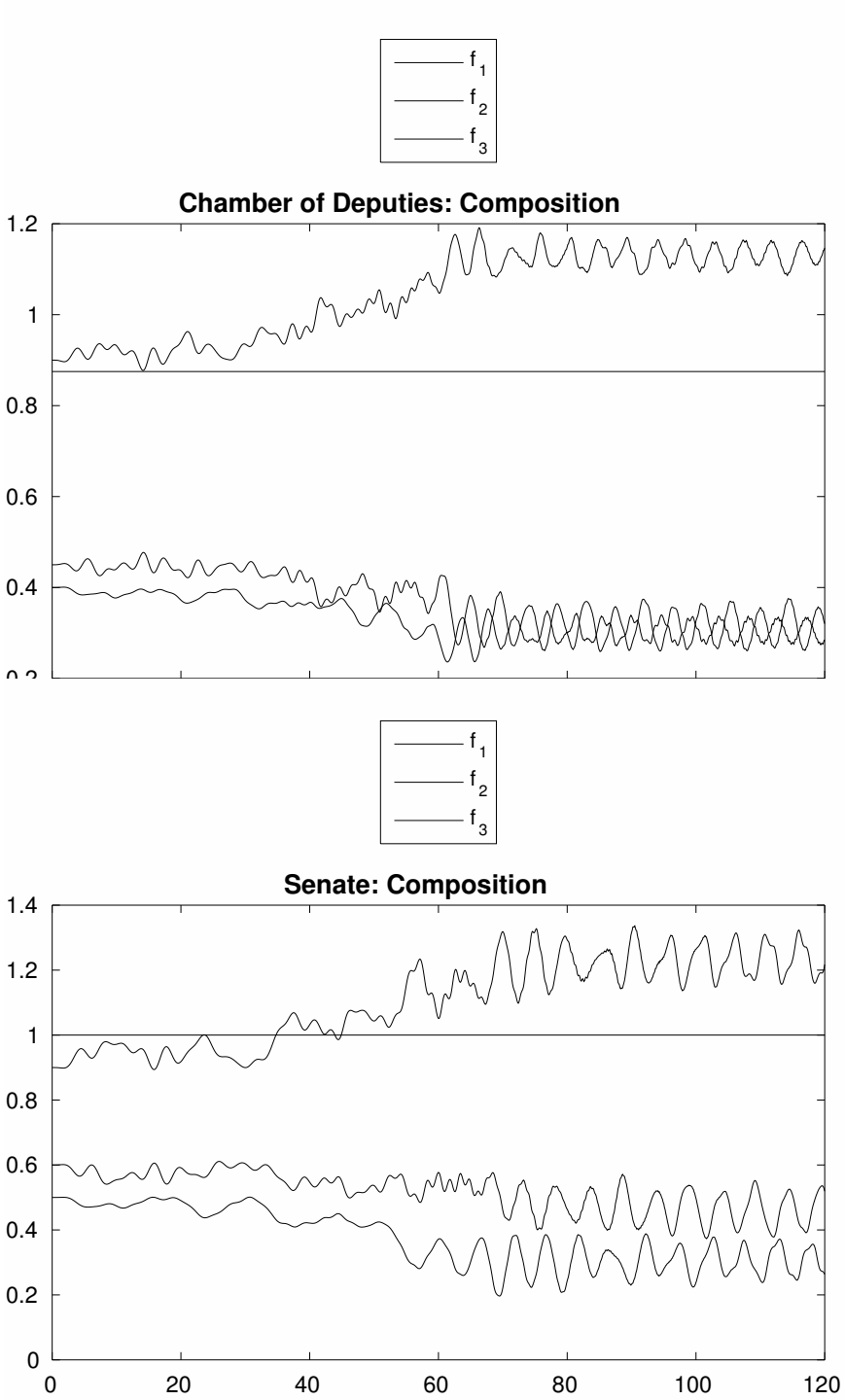

FIGURE 8.14: Stepwise linear model using the rule ρ_G with $\tau = 2$: time evolution of the composition of the Chamber of Deputies (on the left) and the Senate of the Republic (on the right) up to $t = 120$. The solid line represents the seat majority threshold. The x–axis is scaled to half the number of weeks in the period under study, so each step on the scale corresponds to fifteen days.

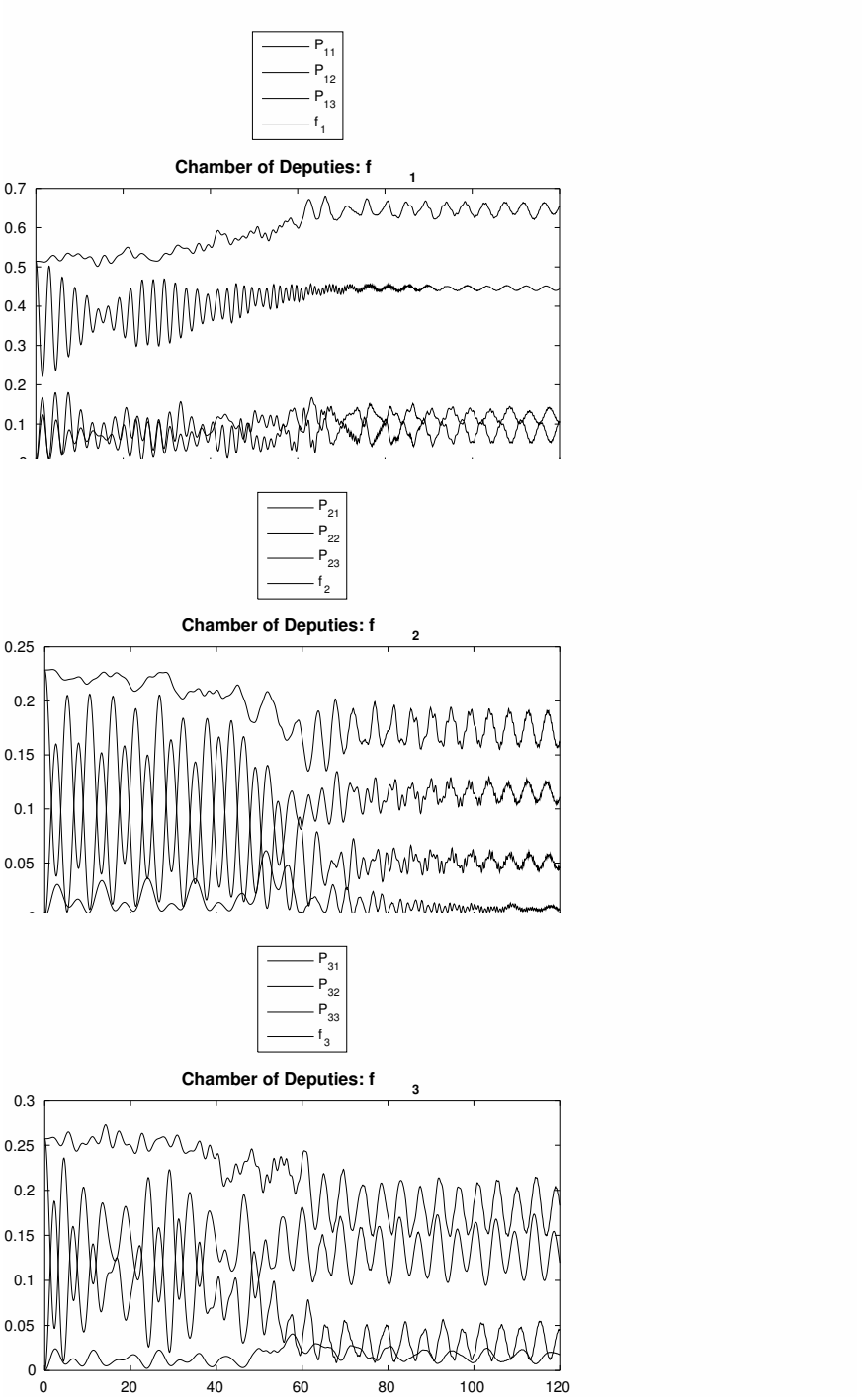

FIGURE 8.15: Stepwise linear model using the rule ρ_G with $\tau = 2$: zoom into the time evolution of the factions inside the Chamber of Deputies. The x–axis is scaled to half the number of weeks in the period under study, so each step on the scale corresponds to fifteen days.

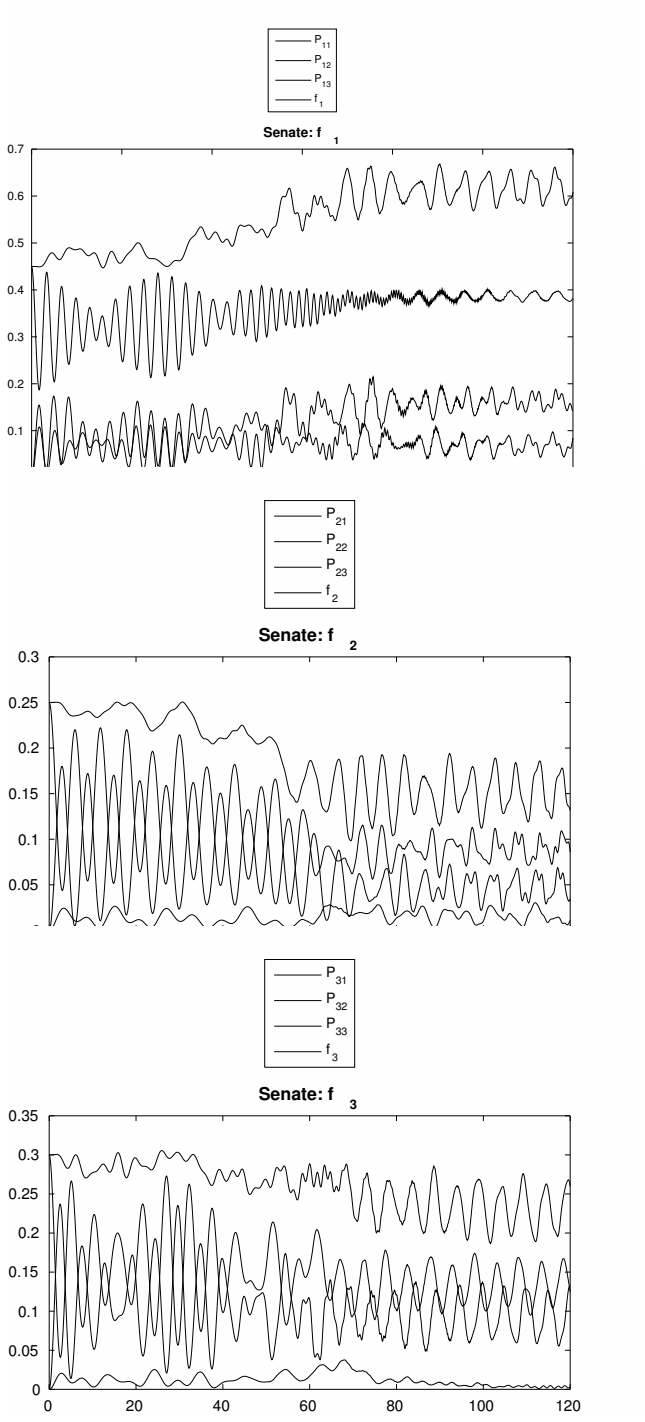

FIGURE 8.16: Stepwise linear model using the rule ρ_G with $\tau = 2$: zoom into the time evolution of the factions inside the Senate of the Republic. The x–axis is scaled to half the number of weeks in the period under study, so each step on the scale corresponds to fifteen days.

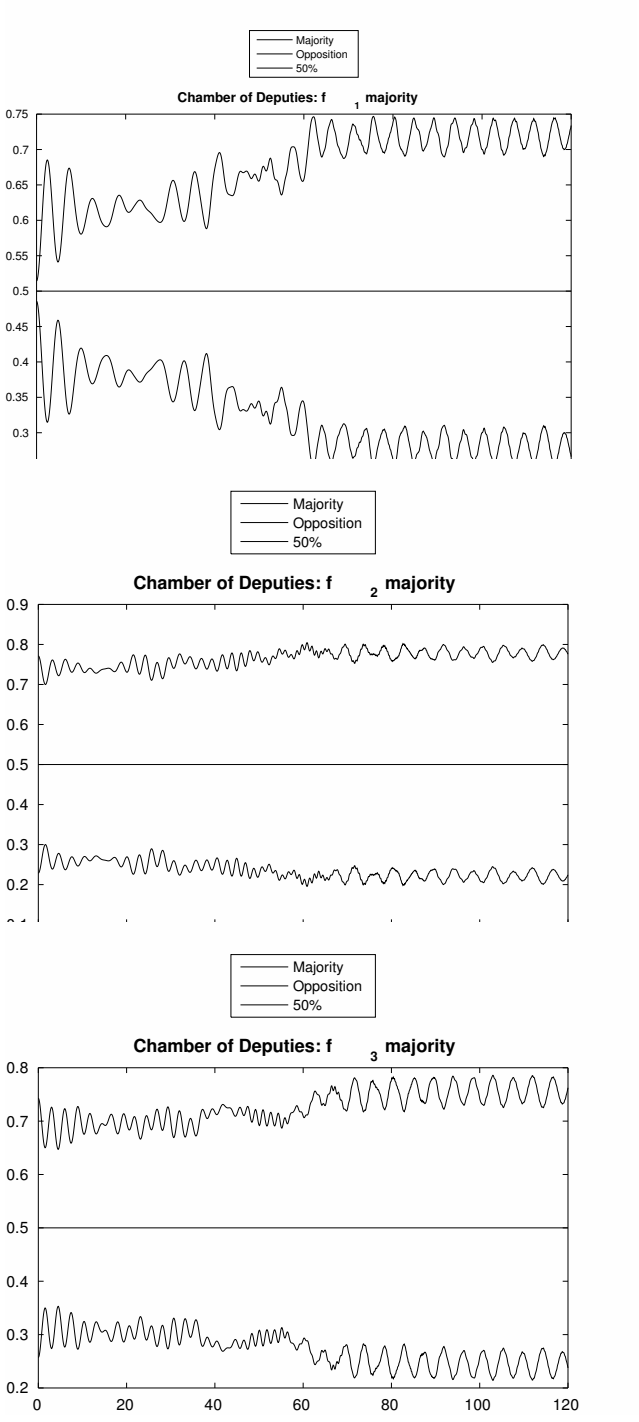

FIGURE 8.17: Stepwise linear model using the rule ρ_G with $\tau = 2$: time evolution of the consistencies of majority and opposition inside the Chamber of Deputies. The x–axis is scaled to half the number of weeks in the period under study, so each step on the scale corresponds to fifteen days.

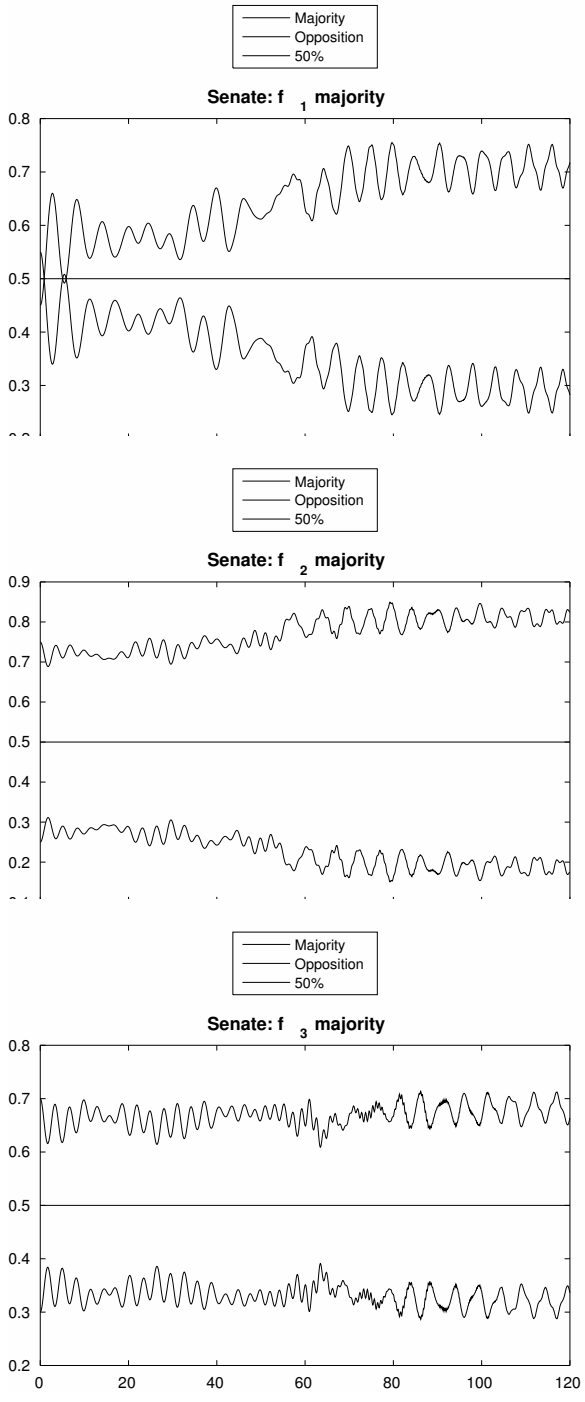

FIGURE 8.18: Stepwise linear model using the rule ρ_G with $\tau = 2$: time evolution of the consistencies of majority and opposition inside the Senate of the Republic. The x–axis is scaled to half the number of weeks in the period under study, so each step on the scale corresponds to fifteen days.

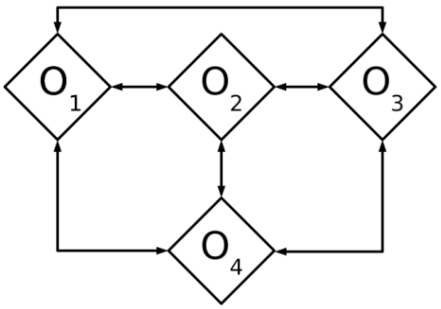

FIGURE 8.19: Diagram of the model for the opinion of voters and abstainers.

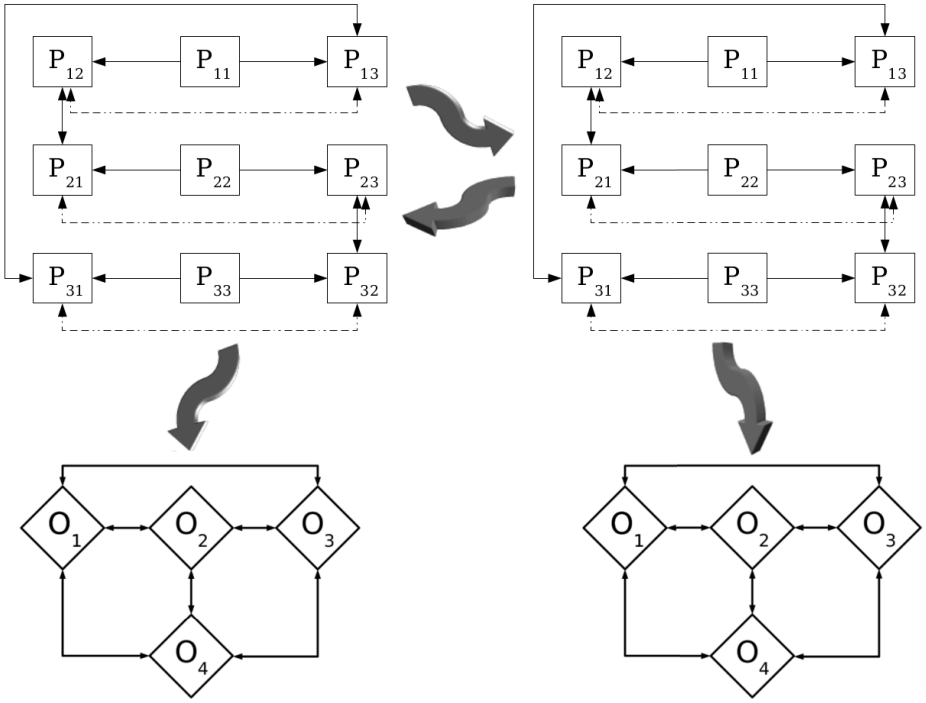

FIGURE 8.20: A schematic view to the general context.

8.3.2 The dynamics of voters' opinions

We now focus on the outcomes of the turncoat habits on the dynamics of the change of opinion of the electorate.

Consider the four–compartment linear model for the description of the interactions between voters and abstainers schematized in fig. 8.19. The actors O_j $(j = 1, \ldots, 4)$ of this secondary model are again fermionic operators, whose mean values refer to the amounts of the j–th party supporters for $j = 1, 2, 3$, and of the persons who choose not to vote for $j = 4$, respectively. The time evolution of the densities described by the number operators $O_j^\dagger O_j$ $(j = 1, \ldots, 4)$ thus offers a view on the trends of support (or dissatisfaction) of the various voters shown at the polls.

Since we are interested in the effects caused by turncoats working inside the central government, we take into consideration two similar sets

of operators (whose meaning and interchanges are those stated just above) representing the voters' opinion systems subtended to the two houses of the Italian Parliament. The overall situation we are referring to is illustrated in fig. 8.20. In both cases, the dynamics of the change of opinion of the electorate is defined by means of the self–adjoint quadratic Hamiltonian operator

$$H^o = \sum_{i=1}^{4} \omega_i^o O_i^\dagger O_i + \sum_{\substack{i,j=1 \\ i \neq j}}^{4} \nu_{ij}^o (O_i^\dagger O_j + O_j^\dagger O_i) \tag{8.11}$$

in the rule–induced formulation using the rule ρ_O, which consists in the set of conditions on the inertia parameters

$$\rho_O(\omega_i^o) = \omega_i^o (1 + S^\star n_i^o)(1 + f_i^\star), \quad i = 1, \ldots, 4, \tag{8.12}$$

where

$$S^\star = \text{sign}(f_1^\star f_2^\star f_3^\star) \tag{8.13}$$

and the superscript * may assume the values "c" or "s" depending on whether we are referring to the voters' opinion system related to the Chamber of Deputies or the one related to the Senate of the Republic. If we combine the results for the evolution of the political system of the central government obtained in Subsection 8.3.1 with the rule–induced dynamics of the voters' opinion system here defined, we get the polls of voters plotted in fig. 8.21, from which we can observe a general trend of surge and decline in support over time, with an alarming increase and consolidation of the number of electors who refuse to vote.

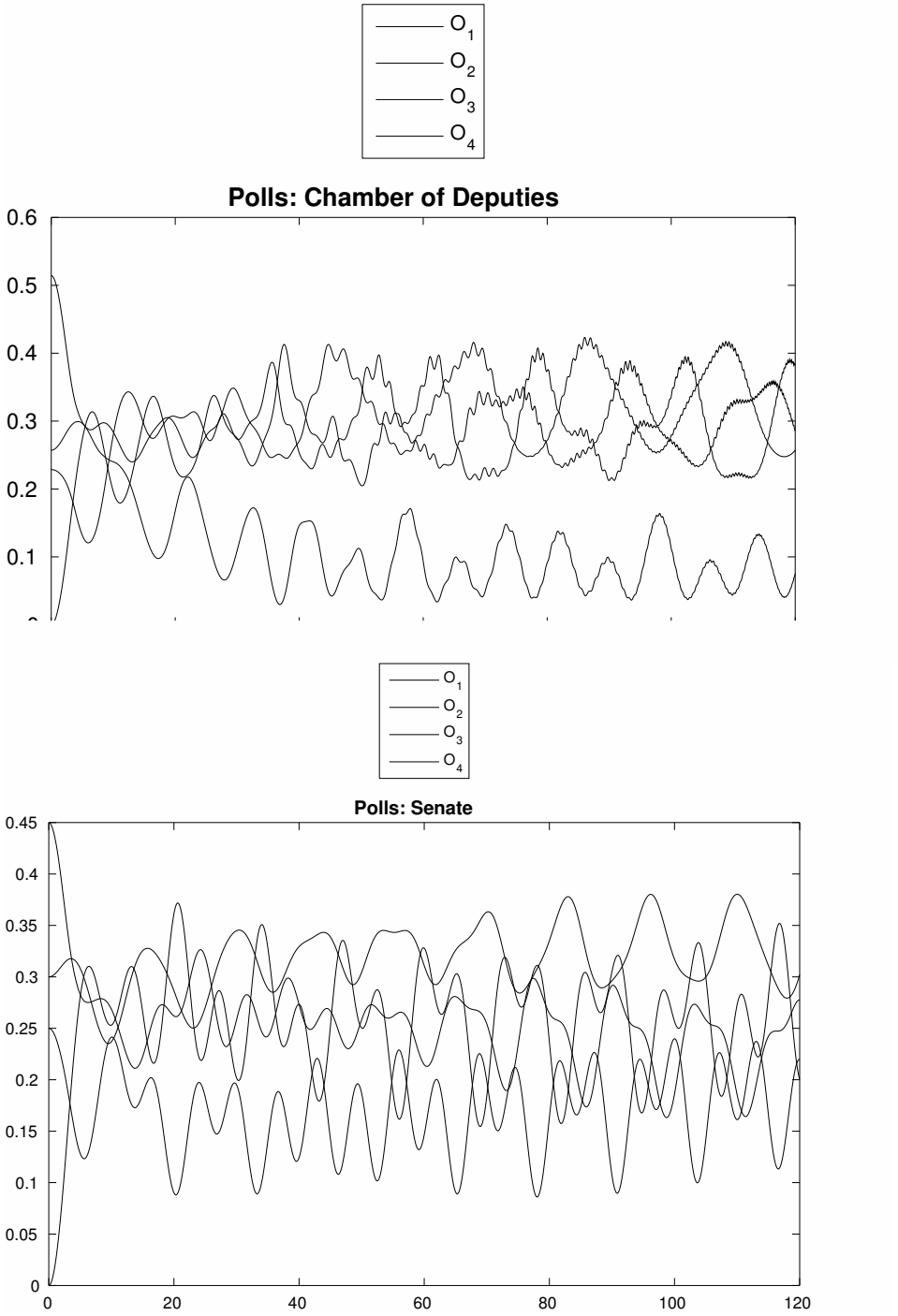

FIGURE 8.21: Time evolution of the voters' opinion obtained with the stepwise linear model using the rule ρ_O after each time step of length $\tau = 2$. The polls show the support or dissatisfaction of the voters related to the behavior of politicians inside the Chamber of Deputies (on the left) and the Senate of the Republic (on the right). The x–axis is scaled to half the number of weeks in the period under study, so each step on the scale corresponds to fifteen days.

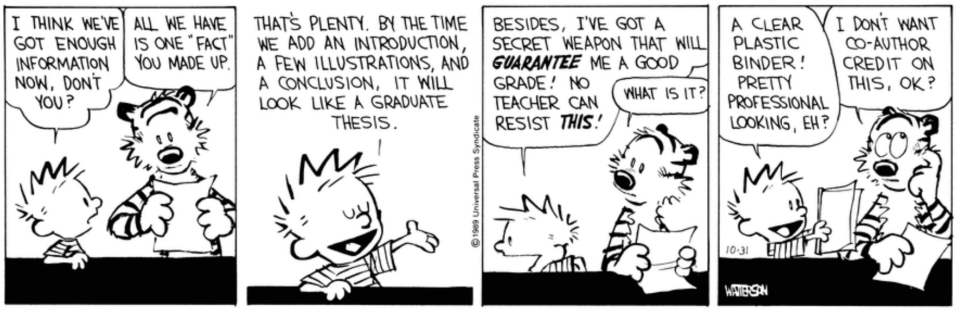
I THINK WE'VE GOT ENOUGH INFORMATION NOW, DON'T YOU?
ALL WE HAVE IS ONE "FACT" YOU MADE UP.
THAT'S PLENTY. BY THE TIME WE ADD AN INTRODUCTION, A FEW ILLUSTRATIONS, AND A CONCLUSION, IT WILL LOOK LIKE A GRADUATE THESIS.
BESIDES, I'VE GOT A SECRET WEAPON THAT WILL GUARANTEE ME A GOOD GRADE! NO TEACHER CAN RESIST THIS!
WHAT IS IT?
A CLEAR PLASTIC BINDER! PRETTY PROFESSIONAL LOOKING, EH?
I DON'T WANT CO-AUTHOR CREDIT ON THIS, OK?
© 1989 Universal Press Syndicate
10-31
WATTERSON

Bibliography

Bagarello, F. (2007). "Stock markets and quantum dynamics: a second quantized description". In: *Physica A* 386, pp. 283–302. DOI: 10.1016/j.physa.2007.08.031.

— (2012). *Quantum Dynamics for Classical Systems: with Applications of the Number Operator*. Wiley. ISBN: 978-1-118-37068-1.

— (2014). "Matrix Computations for the Dynamics of Fermionic Systems". In: *International Journal of Theoretical Physics* 53.2, pp. 555–565. DOI: 10.1007/s10773-013-1839-1.

— (2015). "An Operator View on Alliances in Politics". In: *SIAM Journal on Applied Mathematics* 75, pp. 564–584. DOI: 10.1137/140990747.

— (2016). "An improved model of alliances between political parties". In: *ArXiv e-prints*. arXiv: 1603.09658 [physics.soc-ph].

Bagarello, F., A. M. Cherubini, and F. Oliveri (2016). "An operatorial description of desertification". In: *SIAM Journal on Applied Mathematics* 76, pp. 479–499. DOI: 10.1137/15M1016515.

Bagarello, F., R. Di Salvo, F. Gargano, and F. Oliveri (2016). "(H,ρ)–induced dynamics and large time behaviors". Submitted.

— (2017). "(H,ρ)-induced dynamics and the quantum game of life". In: *Applied Mathematical Modelling* 43, pp. 15–32. DOI: 10.1016/j.apm.2016.10.043.

Bagarello, F. and F. Gargano (2016a). "Modeling interactions between political parties and electors". Submitted.

— (2016b). "The role of nonlinear interactions in modeling political alliances". In press in Accademia Peloritana dei Pericolanti.

Bagarello, F., F. Gargano, and F. Oliveri (2015). "A phenomenological operator description of dynamics of crowds: escape strategies". In: *Applied Mathematical Modelling* 39, pp. 2276–2294. DOI: 10.1016/j.apm.2014.10.038.

Bagarello, F. and E. Haven (2014). "The role of information in a two-traders market". In: *Physica A: Statistical Mechanics and its Applications* 404.C, pp. 224–233.

— (2015). "Toward a formalization of a two traders market with information exchange". In: *Physica Scripta* 90. DOI: 10.1088/0031-8949/90/1/015203.

— (2016). "First results on applying a non-linear effect formalism to alliances between political parties and buy and sell dynamics". In: *Physica A: Statistical Mechanics and its Applications* 444, pp. 403–414. DOI: http://dx.doi.org/10.1016/j.physa.2015.10.022.

Bagarello, F. and F. Oliveri (2010). "An operator-like description of love affairs". In: *SIAM Journal on Applied Mathematics* 70, pp. 3235–3251. DOI: 10.1137/10079985X.

— (2013). "An operator description of interactions between populations with applications to migration". In: *Mathematical Models and Methods in Applied Sciences* 23, pp. 471–492. DOI: 10.1142/S0218202512500534.

— (2014). "Dynamics of closed ecosystems described by operators". In: *Ecological Modelling* 275, pp. 89–99. DOI: 10.1016/j.ecolmodel.2013.12.008.

Barnett, S.M. and P.M. Radmore (1997). *Methods in Theoretical Quantum Optics*. Clarendon Press. ISBN: 9780198563624.

Ben-Aryeh, Y., A. Mann, and I. Yaakov (2004). "Rabi oscillations in a two-level atomic system with a pseudo-hermitian Hamiltonian". In: *Journal of Physics A: Mathematical and General* 37, pp. 12059–12066. DOI: 10.1088/0305-4470/37/50/008.

Birkhoff, G. and J. von Neumann (1936). "The Logic of Quantum Mechanics". In: *Annals of Mathematics* 37, pp. 823–843.

Bleh, D., T. Calarco, and S. Montangero (2012). "Quantum Game of Life". In: *EPL (Europhysics Letters)* 97.2, p. 20012.

Breuer, H.P. and F. Petruccione (2007). *The Theory of Open Quantum Systems*. OUP Oxford. ISBN: 9780199213900.

Buhler, O. (2006). *A Brief Introduction to Classical, Statistical, and Quantum Mechanics*. American Mathematical Society. ISBN: 978-0-821-84232-4.

Carnazza, S., S. Guglielmino, M. Nicolò, F. Santoro, and F. Oliveri (2008). "A paradox in life thermodynamics: the long-term survival of bacterial populations". In: *Proceedings "WASCOM 2007", 14th Conference on Waves ans Stability in Continuous Media*. Ed. by N. Manganaro, R. Monaco, and S. Rionero. World Scientific, pp. 135–140.

Chapman, A. G., L. Fall, and D. E. Atkinson (1971). "Adenylate charge in Escherichia coli during growth and starvation". In: *Journal of Bacteriology* 108, pp. 1072–1086.

Cherbal, O., M. Drir, M. Maamache, and D. A. Trifonov (2007). "Fermionic coherent states for pseudo-Hermitian two-level systems". In: *Journal of Physics A: Mathematical and Theoretical* 40, pp. 1835–1844. DOI: 10.1088/1751-8113/40/8/010.

Deutsch, D. (1985). "Quantum Theory, the Church-Turing Principle and the Universal Quantum Computer". In: *Proceedings of the Royal Society of London A: Mathematical, Physical and Engineering Sciences* 400.1818, pp. 97–117. DOI: 10.1098/rspa.1985.0070.

Di Salvo, R., M. Gorgone, and F. Oliveri (2016a). "(H, ρ)–induced political dynamics: facets of the disloyal attitudes into the public opinion". Submitted.

— (2016b). "Political dynamics affected by turncoats". Submitted.

Di Salvo, R. and F. Oliveri (2016a). "An operatorial model for complex political system dynamics". Submitted.

— (2016b). "An operatorial model for long-term survival of bacterial populations". In: *Ricerche di Matematica*, pp. 1–13. DOI: 10.1007/s11587-016-0266-z.

— (2016c). "On fermionic models of a closed ecosystem with application to bacterial populations". In: *Atti della Accademia Peloritana dei Pericolanti - Classe di Scienze Fisiche, Matematiche e Naturali* 94.2. DOI: 10.1478/AAPP.942A5.

Duck, I. and E. C. G. Sudarshan (1998). *Pauli and the Spin–Statistics Theorem*. World Scientific. ISBN: 978-981-02-3114-9.

Feynman, R. and P. W. Shor (1982). "Simulating Physics with Computers". In: *SIAM Journal on Computing* 26, pp. 1484–1509.

Flitney, A. P. and D. Abbott (2010). "Towards a Quantum Game of Life". In: *Game of Life Cellular Automata*. Ed. by A. Adamatzky. Springer London, pp. 465–486. ISBN: 978-1-84996-217-9. DOI: 10.1007/978-1-84996-217-9_23.

Gargano, F. (2014). "Dynamics of Confined Crowd Modelled Using Fermionic Operators". In: *International Journal of Theoretical Physics* 53.8, pp. 2727–2738. DOI: 10.1007/s10773-014-2068-y.

Gillespie, D. T. (1974). *A Quantum Mechanics Primer*. Wiley. ISBN: 978-0-700-22290-2.

Givskov, E., L. Eberl, and S. Molin (1994). "Responses to nutrient starvation in Pseudomonas putida KT2442: two-dimensional electrophoretic analysis of starvation- and stress-induced proteins". In: *Journal of Bacteriology* 176, pp. 4816–4824.

Grössing, G. and A. Zeilinger (1988). "Structures in quantum cellular automata". In: *Physica B+C* 151.1, pp. 366–369. DOI: http://dx.doi.org/10.1016/0378-4363(88)90196-9.

Huang, X. L., X. X. Yi, C. Wu, X. L. Feng, S. X. Yu, and C. H. Oh (2008). "Effective Hamiltonian approach to open systems and its applications". In: *Phys. Rev. A* 78, p. 062114. DOI: 10.1103/PhysRevA.78.062114.

Larson, C. S. (2015). "Primacy of Quantum Logic in the Natural World". In: *Cosmos and History: The Journal of Natural and Social Philosophy* 11.2, pp. 326–340.

Lee, J., S. Adachi, F. Peper, and K. Morita (2004). "Asynchronous game of life". In: *Physica D Nonlinear Phenomena* 194, pp. 369–384. DOI: 10.1016/j.physd.2004.03.007.

Lindeberg, T. (1994). *Scale–Space Theory in Computer Vision*. Springer US. ISBN: 978-1-4757-6465-9.

Merzbacher, E. (1998). *Quantum Mechanics*. John Wiley and Sons. ISBN: 978-0-471-88702-7.

Moler, C. and C. Van Loan (2003). "Nineteen Dubious Ways to Compute the Exponential of a Matrix, Twenty–Five Years Later". In: *SIAM Rev.* 45.1, pp. 3–49. DOI: 10.1137/S00361445024180.

Ninagawa, S. (2008). "Power Spectral Analysis of Elementary Cellular Automata". In: *Complex Systems* 17, pp. 399–411.

Ninagawa, S., M. Yoneda, and S. Hirose (1998). "$1/f$ fluctuation in the 'Game of Life'". In: *Physica D Nonlinear Phenomena* 118, pp. 49–52. DOI: 10.1016/S0167-2789(98)00025-6.

Paar, H. (2010). *An Introduction to Advanced Quantum Physics*. Wiley. ISBN: 978-0-470-68675-1.

Reeve, C. A., P. S. Amy, and A. Matin (1984). "Role of protein synthesis in the survival of carbon-starved Escherichia coli K-12". In: *Journal of Bacteriology* 160, pp. 1041–1046.

Roman, P. (1965). *Advanced Quantum Theory: An Outline of the Fundamental Ideas*. Addison-Wesley. ISBN: 978-0-201-06495-7.

Sabbatucci, G. (1998). *Trasformismo*, in *Enciclopedia delle scienze sociali*. Istituto della Enciclopedia Italiana.

Thirring, W. (1997). *Classical Mathematical Physics*. Springer New York. ISBN: 978-0-387-40615-2.

Van Overbeek, L. S., L. Eberl, M. Givskov, S. Molin, and J. D. Van Elsas (1995). "Survival of, and induced stress resistance in, carbon-starved

Pseudomonas fluorescens cells residing in soil". In: *Applied and Environmental Microbiology* 61, pp. 4202–4208.